ENGINEERING

CORNELL QUARTERLY

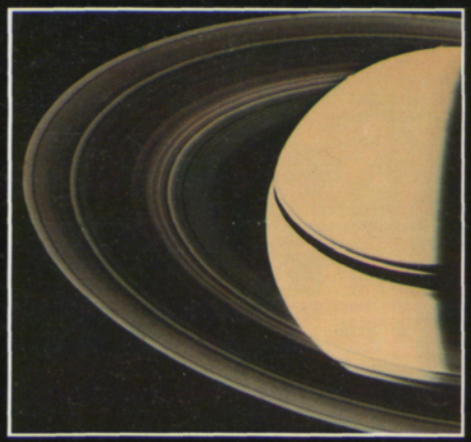

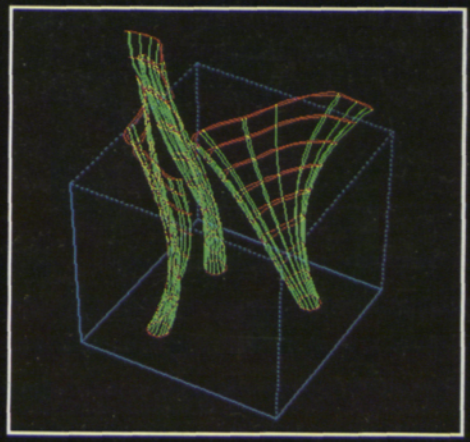

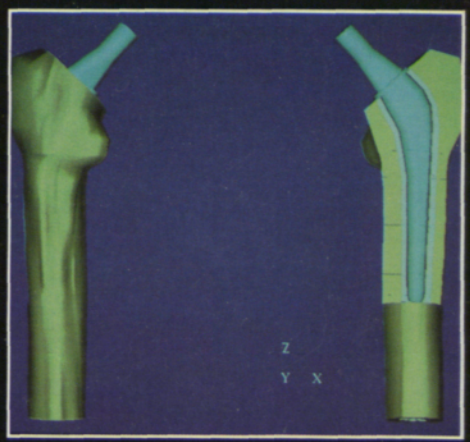

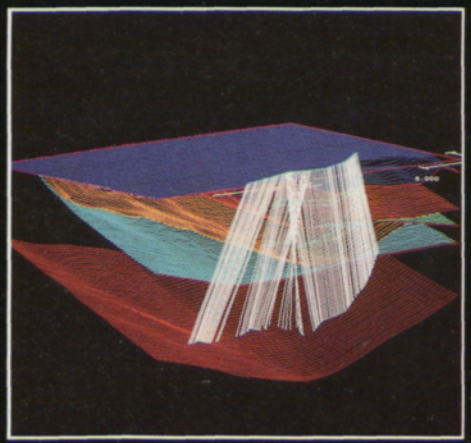

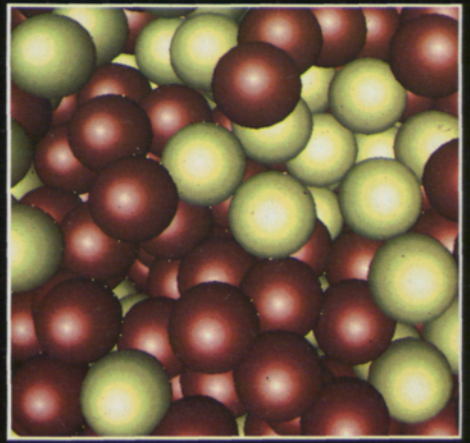

VOLUME 25
NUMBERS 2/3
SPRING 1991

SUPERCOMPUTING IN ENGINEERING RESEARCH

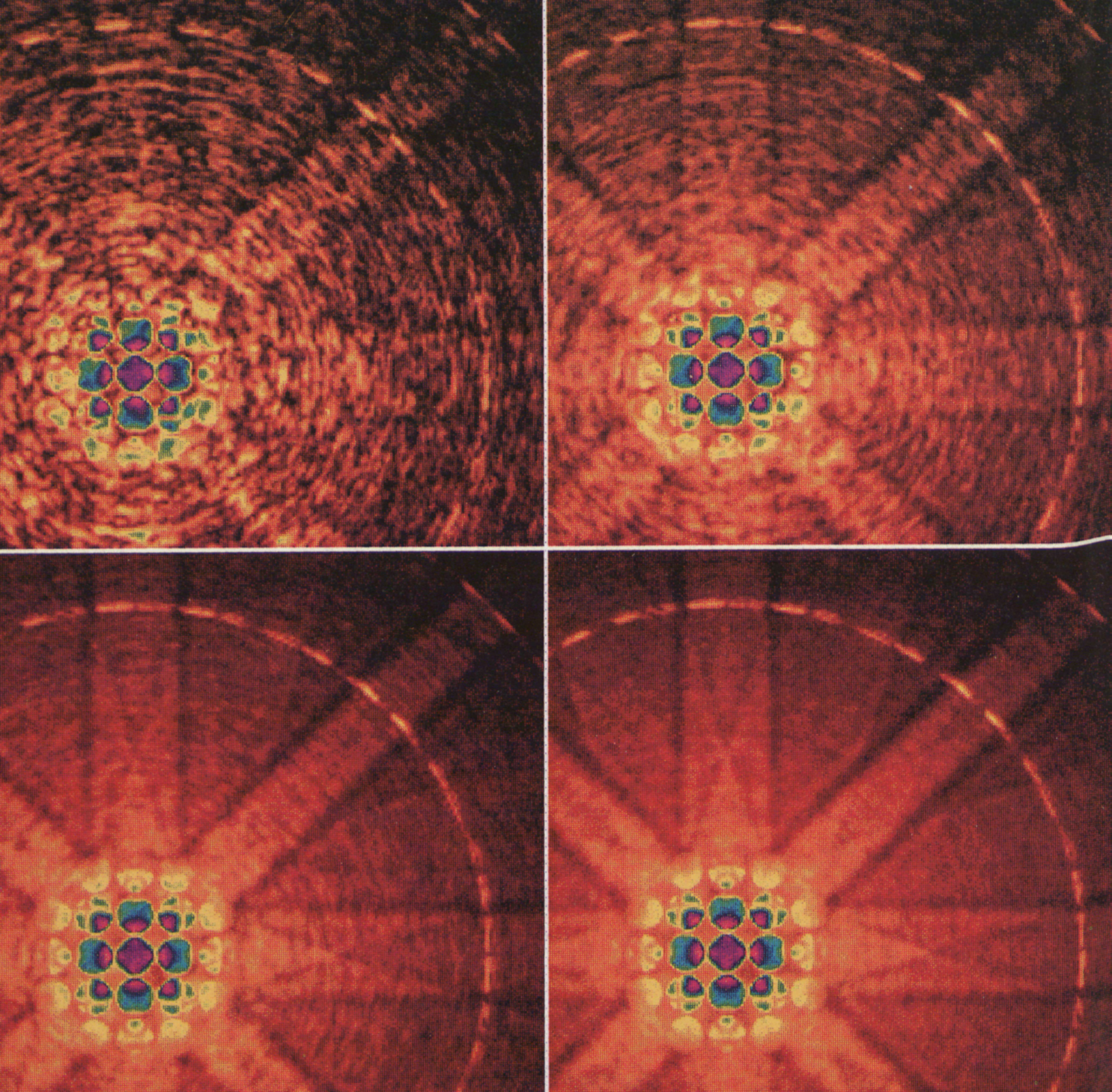

IN THIS ISSUE

Engineering: Cornell Quarterly, Vol. 25, Nos. 2/3, Spring 1991.
Published by the College of Engineering, Cornell University, Campus Road, Ithaca, New York 14853–2201.
Subscription rates: $6.00 per year or $9.00 outside the United States.

Cover illustrations, clockwise from upper left: A view of Saturn and its rings as seen by Voyager 1 (see page 9); a simulation of magnetic field lines in the solar corona (page 18); computer images showing a femoral implant (page 32); a "snapshot" of a hydrogen-bonding fluid studied with Monte Carlo simulation (page 38); a three-dimensional model of seismic reflectors in the Alps (page 27).

Opposite: Simulated scanning transmission electron microscope diffraction patterns showing the effect of increasing the number of displacement configurations from one to sixty-four (see page 52). The progression is from the top row (left to right) to the bottom row (left to right).

Burns

Kolvoord

Sudan and Longcope

Brown

Bartel

Walsh and Gubbins

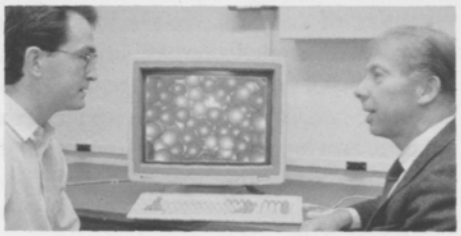

Shuler

Silcox

Pope

SUPERCOMPUTING IN ENGINEERING RESEARCH AT CORNELL

From cosmology to microstructure, and from theoretical science to practical applications, the subjects of Cornell engineering research involving supercomputing have an astonishing diversity, as the eight articles in this issue demonstrate. The topics include the solar corona, planetary moons, the deep structure of the earth, the phenomenon of turbulence, the prediction of fluid properties, the design of bone implants, genetic engineering, and the imaging of atomic-level structures at magnifications up to 10 million times their actual size.

These topics are far from giving a complete picture of Cornell engineering research on supercomputers, however. Almost seventy projects headed by engineering faculty members are currently underway at the supercomputing facility operated by the Cornell Theory Center. (A listing appears on pages 4 and 5). Work in other fields brings the total number of Cornell projects to about one hundred sixty. Overall, more than five hundred projects—in areas including social sciences and economics, as well as the various physical, biological, and mathematical sciences—are underway at the Theory Center.

Most of these projects are part of comprehensive research programs. In some cases supercomputing capability facilitates the lengthy computations that are required for an investigation, or is necessary to accomplish the job at all. In other cases supercomputing is an intrinsic part of experimental study. And across the fields of science and technology, supercomputing has opened up new methods of investigation, such as visual simulation.

WHAT SUPERCOMPUTING CAN ACCOMPLISH

Malvin H. Kalos, director of the Cornell Theory Center, has aptly summarized the significance of supercomputing capability. "High-performance computing has become an essential element in modern science and engineering," he said. "Contemporary high-energy physics and the study of materials by synchrotron radiation, to name just two fields, depend completely on computation at almost every stage of work.

"Much of this computational work requires very large resources, either of sheer arithmetic power, of memory, or of ancillary data storage. For this reason, supercomputers, by definition the most powerful computing resources available at any one time, have become a universal tool for science and engineering. The National Science Foundation's creation of the National Supercomputing Centers was an important recognition of that fact."

SUPERCOMPUTING AND ITS SIGNIFICANCE IN ENGINEERING

William B. Streett, dean of the Cornell University College of Engineering, has pointed out the "natural affinity" between engineering and supercomputing.

"Supercomputing has enormous potential for revolutionizing the practice and teaching of engineering and expanding the frontiers of engineering research," he said. "Some of the most challenging problems that are being studied with the supercomputer are real problems in engineering and technology."

The parallel development of enormously powerful computers and computer graphics techniques has proved to be a very powerful combination, Streett said. Supercomputers can handle equations too complex to be solved analytically, he explained; moreover, these equations can be solved for extremes of physical conditions that can be attained in the laboratory only with great difficulty or not at all. Computer graphics techniques

increase the effectiveness of such computations by allowing researchers to "see" the behavior of a system on a computer screen.

The resources of supercomputer centers such as Cornell's enable engineering researchers to attack problems that have an impact on technology, Streett said. This is consistent, he pointed out, with the goals of promoting university-industry interaction and of improving the nation's productivity and economic competitiveness.

ORGANIZATION AND FACILITIES OF THE NATIONAL CENTER

The Cornell Theory Center was established in 1984 with physics professor Kenneth G. Wilson as the founding director. Engineering faculty members have been instrumental in the center's development; for example, R. N. Sudan, the IBM Professor of Engineering, served as deputy director during the early years, and David A. Caughey, professor of mechanical and aerospace engineering, was acting director after Wilson's departure and until Kalos' appointment. The largest group of users and technology developers are from the College of Engineering.

In 1985 the Theory Center was designated by the National Science Foundation as a National Advanced Scientific Computing Center (there are currently four). It began operations with major funding from NSF (a three-year grant of $21.9 million) and $30 million in equipment and services from IBM. NSF has renewed its support with a $79-million grant that will run through 1995, and IBM continues to provide staff assistance and equipment. (The value of IBM contributions has reached a total of about $125 million.) Funding has been provided also by other corporations, by New York State, and by Cornell.

As a national center, the Cornell facility is available to users throughout the country.

The new $35.2 million Engineering and Theory Center Building houses the Cornell Theory Center and the Program of Computer Graphics on the upper four floors, and facilities of the College of Engineering—including offices and specialized laboratories—on the lower three floors and basement. The building is 210,000 square feet (gross) in size. The towers are stairwells.

Situated near the southeast corner of the Joseph N. Pew, Jr. Engineering Quadrangle, the building is connected to Upson Hall on three levels. Part of the building, facing Hoy Field, follows the curve of Hoy Road.

The building was designed by Gwathmey Siegel and Associates of New York and built by the Turner Construction Company. Construction manager was James Kemp, a 1961 Cornell graduate in civil engineering.

Capital funds for the building are being provided through grants and loans from New York State and contributions from corporate and private sources.

Currently, more than two thousand researchers access the facility over high-speed networks. All the projects are approved by the National Allocations Committee.

The center's resources include two IBM ES/3090 600 J supercomputers, each with six processors and vector facilities. They are capable of 64 billion calculations per second, and as the technology advances, much greater speeds can be anticipated.

The provision of supercomputing services to users is the responsibility of the Cornell National Supercomputer Facility (CNSF), an arm of the Theory Center. The development of new technology is coordinated by the center's Advanced Computing Research Institute.

PLANS FOR IMPROVED FACILITIES AND SERVICE AT THE CENTER

A major focus of the Advanced Computing Research Institute is the development of massively parallel systems. (Parallelism allows simultaneous computation of different parts of a calculation.) Twelve-way parallel processing is now available at the center, and a 64-processor capability is planned for implementation in 1994.

Theory Center staff members are also working to develop mass data-storage systems capable of efficiently storing and retrieving terabits of information. (A terabit is one trillion bits, approximately the equivalent of a thousand Encyclopaedia Britannicas.)

Service to users will be improved by implementing the UNIX operating system throughout the Theory Center facilities, and by improving the high-speed networks so that they will be able to transmit 45 million bits of information per second.

Network communication would be greatly expanded by the proposed National

(continued on page 6)

Shoemaker

Two Cornell engineering professors, Christine Shoemaker and Paul R. Dawson, are currently designated by the Theory Center as "Strategic Users"—those whose work involves parallel processing requiring a large amount of staff support. To qualify for the Strategic User Program, the work must show promise for near-term scientific accomplishments or contribute to the advancement of supercomputing in the course of scientific research.

Shoemaker is a specialist in numerical optimal control and its application to environmental problems. Dawson conducts research in the modeling of the deformation of materials and of joining processes.

Dawson

Cornell Engineering Research Projects Currently Active at the Theory Center

Most of the principal investigators listed are faculty members. Often other researchers, such as postdoctoral associates and graduate students, work on the projects.

Agricultural and Biological Engineering
Albright, L. D. *Computations of Recirculating Flows in Slot-Ventilated Livestock Buildings*
Datta, A. K. *Estimation of Thermokinetic Changes in Convective Heating of Liquid Food Systems*

Applied and Engineering Physics
Rhodin, T. N. *Electronic and Atomic Structure of Interfaces*
Webb, W W. *Dynamical Measures in Fluctuation Processes*
___. *Protein Interactions and Self-Diffusion on Membranes*

Chemical Engineering
Clancy, P. *Non-Equilibrium Molecular Dynamics Studies of Rapid Solidification*
Gubbins, K. E. *Associating Fluid and Fluid Mixtures*
___. *Fluid Phase Transitions in Narrow Capillary Pores*
___. *Mixtures of Polar and Associating Liquids*
___. *Theory and Simulation of Fluids of Associating Chain Molecules*
___. *Thermodynamics and Transport Properties of Fluids in Pores*
Panagiotopoulos, T. *Simulations on Micellar and Protein Systems*
Shuler, M. L. *Models for Genetically Modified Cells*
Steen, P. H. *Approximate Inertial Manifolds for a Bénard Convection System*

Civil and Environmental Engineering
Hover, K. C. *Effect of Air-Entraining on the Frost Resistance of Concrete*
Jirka, G. *Mixing in Turbulent Free Shear Flows Constrained in a Shallow Fluid Layer*
Liggett, J. A. *Transport and Free Surface Flows*
Liu, P. L.-F. *Three-Dimensional Operator-Splitting Methods for Coupled Transport Phenomena*
___. *Mass Transport in Water Waves*
Philpot, W. D. *Characterization of Texture in Remotely Sensed Imagery*
Shoemaker, C. A. *Application of Dynamic Optimization Algorithms to Problems Arising in Agricultural and Environmental Management*
Stedinger, J. R. *Optimization and Simulation of Stochastic Hydropower Systems*

Computer Science
Salton, G. *Automatic Indexing with Complex Content Indicators*

Electrical Engineering
Krusius, J. P. *Education Project*
MacDonald, N. C. *Monte Carlo Simulation of Electron Energy Loss in Nanostructures*
Pollock, C. R. *Simulation of Ultrashort Optical Pulses Generated in a Coupled Cavity Laser*
Seyler, C. E. *Theory and Simulation of Ionospheric Irregularities*
Sudan, R. N. *Dynamical Behavior in Two-Dimensional Magnetohydrodyamic Compressible Convection*
___. *Large-Scale Turbulence in the Equatorial Electrojet*
___. *Mechanisms for Solar Coronal Heating*
___. *Two-Dimensional Electron Flow in High-Power Magnetically Insulated Transmission Lines and Plasma Opening Switches*
Tang, C. L. *Semiconductor Lasers with Novel Cavity Configurations*
___. *Simulating the Mode-Locking Behavior of Diode Lasers*
Thorp, J. S. *Monitoring the Potential Energy-Boundary Surface for an Electric Power System*

Geological Sciences

Brown, L. D. *Applications of Wave-Equation Techniques to Processing Deep Seismic Data*
___. *Intracratonic Basins; COCORP Deep Seismic Research*
___. *Reprocessing of Deep Seismic Reflection Data from Brazil*
Cathles, L. M., III. *Basin Resource Modeling*
Hauser, E. C. *Interactive Processing of Large Sets of Industry Seismic Data in the Central U.S.*
Jordan, T., and D. L. Turcotte. *Forward Modeling of Facies and Stratigraphic Sequences in Foreland Basins*

Materials Science and Engineering

Dieckmann, R. *Nonstoichiometry of Binary Oxides and Kinetics of Spinel Formation Reactions*

Mechanical and Aerospace Engineering

Avedisian, C. T. *Numerical Analysis of Film Boiling of Spherical Droplets and Horizontal Surfaces*
Bartel, D. L., and D. Taylor. *Bone Morphology and Remodeling As a Problem in Optimal Structural Design*
Boyce, D. *Cornell Computational Optimization Project*
Caughey, D. A. *Computation of Transonic Aerodynamic Flows Past Complex Aircraft Configurations*
___. *Large-Scale CFD by Finite Element Methods*
___. *Multigrid Calculations of Three-Dimensional Turbomachinery Flows*
Dawson, P. R. *Modeling Elastoviscoplastic Steady-State Forming Processes*
___. *Modeling Texture Development in Bulk Forming Processes*
deBoer, P. C. T. *Numerical Simulation of a Strongly Heated, Enclosed Binary Gas Mixture*
George, A. R. *Class Project on Automobile Frame Design*
Gouldin, F. C. *Simulation of Flow and Combustion in Mass Burn Incinerators*
Gouldin, F. C., and G. J. Wolga. *Spectroscopic Inversion Procedures for Smart Sensor-Based Process Control*
Leibovich, S., and J. Lumley. *Generation of Coherent Vorticity in a Rotating Tank*
Leibovich, S., and J. Lumley; P. Holmes and J. Guckenheimer (Theoretical and Applied Mechanics). *Coherent Structures at the Air-Sea Interface and in Turbulent Wall Layers*
Lumley, J. L. *Surface Mixed Layer Studies*
Moore, F. K. *Compression-System Dynamics*
Pope, S. B. *Numerical Investigation of Turbulent Flame Sheets*
Shen, S.-f. *Unsteady Separation over Three-Dimensional Maneuvering Bodies—Theory and Simulation*
Taylor, D. L. *Nonlinear Dynamics of Geometrically Imperfect Journal Bearings*
Torrance, K. E. *Droplet Ejection Using Boundary Element Methods*
___. *Two-Phase Thermal Convection*
Wang, K.-K. *Integration of CAD/CAM for Injection Molded Plastic Parts*

Operations Research and Industrial Engineering

Muckstadt, J. A. *Analysis of Allocation Rules of a Multi-Echelon Distribution System*
Schruben, L. W. *Response Surface Analysis for Computer Simulation Models*

Theoretical and Applied Mechanics

Burns, J. A. *Narrow Planetary Rings: Simulation and Animation*
Hart, E. W. *A Search for Non-Singular Crack-Tip Fields in Inelastic Media*
Holmes, P. J. *Numerical Computation of Fine Structure*
Mukherjee, S. *Analysis of Inelastic Deformation in Metals by the Boundary Element Method*

Cornell Theory Center Administrators

Malvin H. Kalos, Professor of Physics, *Director*
Peter M. Siegel, *Director, Cornell National Supercomputer Facility*
Linda Callahan, *Associate Director, Cornell Theory Center, and Director, Corporate and External Relations*
Tom Coleman, *Director, Advanced Computing Research Institute*
Jay Blaire, *Executive Director*

Available Publications

■ Descriptions of more than three hundred research projects now underway at the Cornell Theory Center are given in the 1990 *Abstracts*. The book also includes listings of publications by the researchers, and a keyword index. The work represents a wide range of disciplines in the physical, mathematical, agricultural, and social sciences, as well as all aspects of engineering. The volume is available from the Cornell Theory Center, Cornell University, ETC Building, Ithaca, NY 14853–3801.

■ More information about the research at the Cornell College of Engineering is given in *Research in Engineering and Applied Science at Cornell*. Included are descriptions of the programs of individual faculty members, along with biographical information and publications listings, and summaries of research programs in the various schools and departments. The recently published third edition of this 356-page book is available from the College of Engineering.

Research and Education Network, which is to be voted on by Congress this year. The Cornell Theory Center is to be part of this network. According to the Federal Office of Science and Technology Policy, the network would expand and enhance the United States portion of the existing worldwide infrastructure of interconnected computer networks, called Internet.

CORNELL LEADERSHIP IN COMPUTER GRAPHICS

One of the areas of advanced computer technology in which Cornell has been a leader is computer graphics and scientific visualization.

The Program of Computer Graphics, an independent interdisciplinary center located in the Engineering and Theory Center Building, conducts research in three principal areas—computer graphics, structural engineering mechanics, and visualization for scientific computing—and receives funding from NSF and industry. It is headed by Donald Greenberg, the Jacob Gould Sherman Professor of Computer Graphics.

A very recent development is the award by NSF and the Defense Advanced Research Projects Agency of a five-year grant of $14.68 million for a new effort in computer graphics and scientific visualization. The program will be based at five universities, including Cornell, and will be directed by Greenberg. The participating institutions in addition to Cornell are Brown University, the California Institute of Technology, the University of North Carolina at Chapel Hill, and the University of Utah.

Researchers at the five centers will develop interactive computer-graphics tools for basic research and commercial applications. Initial work will focus on cancer therapy, brain research, and the design of parts for airplanes, automobiles, and microchips. The grant is expected to be augmented by funding or gifts of equipment from industry, universities, and state governments.

THE THEORY CENTER'S EDUCATIONAL SERVICES

The Cornell Theory Center has an educational as well as a scientific and technological role. In addition to providing and advancing hardware and software and providing computing time, it sponsors conferences, lecture series, workshops, and training programs.

For example, the center offers summer classes for undergraduates who are taking courses in various fields at participating institutions. Research projects begun in the summer are continued during the academic year with access to the supercomputers via the high-speed networks.

A similar program for high school students, SuperQuest, is supported by IBM and NSF. Four teams chosen on a competitive basis come to Cornell with their teachers for several weeks during the summer; they learn how to use the supercomputer and begin projects that are continued back at school with use of workstations donated by IBM.

New this spring at the Theory Center are "SuperSaturdays"—workshops for middle-school and high-school students and their teachers. Each of three workshops meets on two consecutive Saturday mornings for lectures, discussions, and work on both high-performance and Macintosh computers. The series is a project of a recently formed National Engineering Education Coalition of eight universities headed by Cornell. The coalition is sponsored by NSF.

CORPORATE PARTICIPATION IN THE CENTER AND ITS PROGRAMS

In addition to contributing equipment and funds for the new Engineering and Theory Center Building, companies are involved with the Cornell Theory Center through special institutes and programs.

The Corporate Research Institute, which facilitates the collaboration of scientists at Cornell and in industry, now has thirteen members and is continually expanding. Members include IBM, Corning Incorporated, and Xerox. This institute also sponsors a program for small-business affiliates and coordinates the corporate affiliates program of the recently formed Global Basins Research Network (GBRN).

Researchers from both industry and universities are participants in the GBRN, which is studying the coupled physical and chemical processes that control the movement of oil and gas in sedimentary basins. The organization is headed by Lawrence M. Cathles, III, a Cornell professor of geological sciences. Members include ten major oil companies and eight academic institutions.

Also closely connected with the Theory Center is the Design Research Institute, which was formed in 1990 by Xerox and Cornell and is expected to enroll additional corporations. The purpose is to focus modern computer science and the processing power of supercomputers on the design and engineering of high-technology products. The institute makes use of the combined resources of the participants.

SUPERCOMPUTING AS A COOPERATURE VENTURE

As the articles in this issue demonstrate, supercomputing is a powerful tool for research in all aspects of science and technology. And as the success of the Cornell Theory Center demonstrates, state-of-the-art facilities can be made widely available through cooperative ventures involving universities, government, and industry.—GMcC

SUPERCOMPUTER AS OBSERVATORY?

A Search for Moons in Planetary Rings Using the Cornell National Supercomputer Facility

by Joseph A. Burns and Robert A. Kolvoord

Discoveries over the past fifteen years have revolutionized our understanding of planetary rings. Until recently, the only known ring system was Saturn's elaborate one, first spied by Galileo in 1610, but in 1977 rings were detected about Uranus. Shortly after that, rings were found about Jupiter (1979) and Neptune (1984), demonstrating that all of the giant planets are adorned by these elegant structures.

While each of the ring systems is distinctive, they share certain common traits: every one contains innumerable particles, ranging in size from dust specks to large boulders, which orbit their planets in flattened disks that extend from somewhat beyond the planet's cloud tops to distances of a few planetary radii. The mechanics and origin of these rings are intriguing subjects for research.

Our group at Cornell is contributing to the study of planetary rings by investigating the presence and effects of small satellites in the ring regions. We have been able to find embedded moonlets—which had become the Holy Grail of planetary ring research—using supercomputer-based modeling and images obtained from Voyager spacecraft observations.

MODELING THE COMPLEX PHYSICS OF PLANETARY RING SYSTEMS

Many complicated physical processes, acting over eons, are thought to sculpt the intricate forms visible in the rings. For example, particles orbit at different rates according to their distance from the planet, and so collisions among members of dense rings are unavoidable. Because of these frequent impacts, sharp boundaries are less likely. Furthermore, particles may agglomerate or be destroyed in such impacts, and so over time individual bodies may not retain their integrity.

Throughout their orbital motions, the ring particles in an ensemble feel gentle gravitational tugs from satellites that lie beyond the ring system; these forces have been shown to be capable of producing clumps, waves, and even gaps at discrete places in the rings. Simultaneously, mutual gravitational attractions between the largest of the ring particles will cause them to scatter off one another; these random impulses may thereby scramble organized structures.

In addition, ring particles are bombarded by interplanetary meteoroids and energetic cosmic radiation; these processes can move particles about, alter their physical characteristics, or even cause their entire disintegration.

Successful modeling of the details of this complex of interactions requires the computational power provided by today's supercomputers. Such theoretical studies are especially meaningful when they can be supplemented by searches of spacecraft images to see what actually has occurred.

CLUES TO THE FORMATION OF THE SOLAR SYSTEM

Planetary rings are useful laboratories in which to investigate this sort of physics. But there is another aspect of ring systems that intrigues many researchers: the putative close connection between the origin of the planetary rings and the formation of the solar system itself.

The conventional wisdom is that rings developed as part of an imperfectly understood scheme whereby planets accumulated in the solar nebula—the swarm of gas and dust that is believed to have surrounded the proto-Sun as it grew. All of this would have occurred some four and one-half billion years ago, during the gravitational collapse of an interstellar gas cloud.

"We have been able to find embedded moonlets—which had become the Holy Grail of planetary ring research—using supercomputer-based modeling and images obtained from Voyager spacecraft observations."

As the planets accumulated, they would have been orbited by their own flattened disks of gas and dust, much like the solar nebula itself. In regions far from the planet, pairs of particles in the disks would have accreted into larger objects whenever their mutual gravitational attraction or surface stickiness could overwhelm the planet's tidal force; in this way, satellites would gradually grow in much the same fashion as the planets. But close to the planet, within some ill-defined distance known as the Roche limit, circumplanetary materials would be unable to agglomerate into sizable solid objects. In this region, material would remain dispersed as centimeter-to-meter-sized particles in a primordial disk that may have endured to produce the planetary rings visible today.

While many scientists have a philosophical bias toward the view that rings are ancient, as the above model postulates, some recent evidence has suggested that planetary rings may be comparatively young, perhaps only a few hundred million years old. If this new information is being interpreted correctly, the extant rings must have developed more recently than had been thought, perhaps after the original ones had eroded away under the bombardment of interplanetary projectiles. According to this revisionist model, the rings arose when nearby satellites were catastrophically disrupted by cometary impacts, or when an errant comet or a satellite was torn asunder by strong planetary tides after it ventured too near. These close-in satellites may have formed earlier at greater distances from the planet by the mechanism previously described, but then gradually spiralled inward because of drags exerted by the surrounding nebula.

A clear discriminator between these two models of ring origin is the presence of moonlets in the rings. If a ring system is the remnant of a primordial circumplanetary nebula, its particles should be generally small, since, owing to planetary tides, large objects cannot accrete in today's ring region. On the other hand, if rings were produced in catastrophic disruption events, there should be some moonlet-sized objects: simulations of such collisions indicate that large fragments would be generated and would not subsequently be ground down.

WHAT VOYAGER IMAGES REVEAL ABOUT THE RINGS

Although planetary rings can be studied—with difficulty—from ground-based telescopes, much more detailed observations were obtained by the Voyager spacecraft. During the decade starting in 1979, this engineering marvel made rapid flybys of the distant planets Jupiter, Saturn, Uranus, and Neptune, making close-up surveys.

To partially address the question of ring origin, images returned from Voyager have been scrutinized for moons embedded within the rings. A few craggy shards, mostly small (ten to many tens of kilometers in mean radius) have been located, generally toward the outskirts of the ring systems. In particular, Voyager discovered a pair of moons close to the outer edge of Jupiter's main wispy ring; they are believed to be the largest of a group of parent bodies that are gradually being broken apart to generate the much smaller Jovian ring particles that are seen in the images.

In the Saturn system (Figures 1 and 2), two small "shepherd" satellites were found to orbit alongside the clumpy narrow F ring, the outermost of the planet's primary rings. According to a theory developed at the California Institute of Technology by Peter Goldreich (who studied at Cornell for a 1960 B.S. degree in engineering physics and a 1963 Ph.D.) and Scott Tremaine, satellites can, over time, gravitationally repulse a nearby disk of orbiting matter. This would mean that two moonlets could herd particles together, causing them to form a ringlet instead of spreading apart as a result of collisions.

Another pair of shepherds seems to confine Uranus's epsilon ring, and it is postulated that many others imprison the remaining eight slender but dense strands that encircle the planet.

A tiny moonlet skirts the inner edge of each of the two threadlike Neptune rings that were discovered in August 1989 by Voyager. Many other embedded moonlets are suspected to exist, because each planet's retinue contains some rings that have radially abrupt density discontinuities and other rings that are punctuated by lanes apparently cleared of all material. Such features were not expected. It was thought

Figure 1

Figure 1. Saturn as seen by Voyager 1 from 1.57 million kilometers above and behind the planet. Visible through the rings is the planet's bright overexposed limb.

The C ring (closest to the planet) is relatively faint as it crosses the planet's limb. The material in parts of the B ring is so closely packed that it entirely screens the planet in places. The A ring comprises the outer third of the ring system, between the Cassini Division (the dark band curving through the center of the image) and the black background of space. The F ring, as narrow and variable as a pencil line, sits about 4,000 kilometers off the outer perimeter of the A ring. The Encke Gap is the dark line located at about an equal distance radially inward from the A ring's edge as the F ring is outward. Some have suggested that the "record groove" appearance of Saturn's rings might be due to small embedded moonlets.

Figure 2a

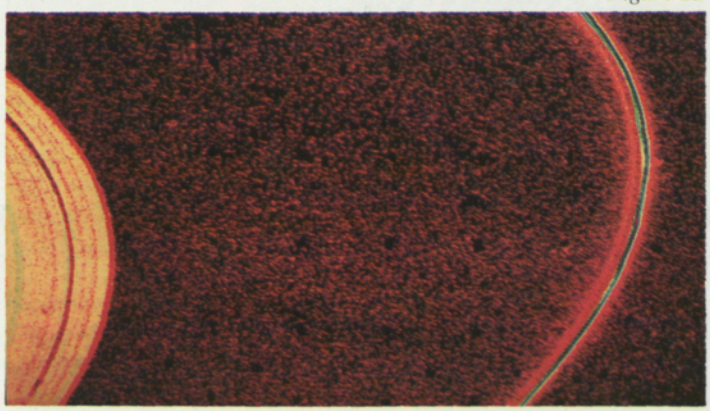

Figure 2b

that particles should rapidly diffuse across density boundaries because of the jostling that would occur in mutual collisions.

Although the Voyager observations have provided invaluable data on the presence of embedded moonlets, as well as on the basic morphology of the rings and the properties of their constituents, they are quite limited because the flybys were so brief. Many things could not be scrutinized at all, and those that were viewed could not be studied long enough to ascertain how—or even if—they changed with time. Under such circumstances, theoretical and numerical studies are important because they allow results to be extrapolated; investigations that connect the few available observations to theory are especially valuable.

LARGE-SCALE COMPUTATION IN STUDIES OF PLANETARY RINGS

Some large computational efforts have been mounted to study the long-term history of planetary rings.

Among the earliest was an investigation by André Brahic at the Paris Observatory, begun in the mid-seventies on an IBM 360-65 and carried on more recently on a Cray 1 Supercomputer. In this simulation, about one hundred particles were followed as they orbited a massive planet while occasionally colliding with one another. Brahic found that the system swiftly collapsed to a thick disk so that all the particles circled the planet nearly in its equatorial

Figure 2. The F ring of Saturn. This narrow and enigmatic ring can appear either like a smooth and featureless ribbon or, as in 2a, like a set of knotted and braided strands. This clumpy appearance is generally ascribed to the action of the shepherding satellites Prometheus and Pandora (2b) discovered by Voyager, and perhaps to other as yet unseen bodies as well.

plane (Figure 3). Subsequent collisions, which took place owing to the relative drift of orbiting particles, occurred at a much slower rate and caused the ring to gradually spread inward and outward.

More recent computational codes have been used to watch the radial and vertical evolution of systems in which particles of many different sizes bang into one another while being gravitationally forced by adjacent satellites.

ONGOING RESEARCH USING THE CORNELL SUPERCOMPUTER

In our research at the Cornell National Supercomputer Facility, we have studied the perturbative effects of nearby satellites on narrow rings.

Our original goal was to understand how certain structures—clumps, kinks, and braids—observed in Saturn's F ring could form (see Figures 1 and 2). We first duplicated the results for a two-dimensional problem that Mark Showalter, a recent Cornell Ph.D., and Burns had analytically simplified and then numerically integrated. In this case the ring particles and the shepherd satellites lie on nearby, slightly elliptical orbits that are all in Saturn's equatorial plane (Figure 4).

Our extension to the problem was to solve it in three dimensions by direct numerical integration of the equations of motion. Since many of the Voyager images were taken at very shallow viewing angles, we wished to determine whether slight out-of-plane tugs introduced by continguous satellites on inclined orbits might produce some of the odd structures seen. We actually noticed very little difference (Figure 5).

We then animated the results and produced our own movies on a Macintosh personal computer. Not surprisingly, we quickly learned that dynamically evolving structures can be most easily understood when they are watched *dynamically*.

Finally, we simulated mutual collisions between ring members through a simple Monte Carlo routine that caused random jumps in particle velocities similar to those that would occur during impacts with other ring particles. As expected, these "collisions" caused the organized structures to disappear at a rate that depended on the frequency and severity of the impacts (Figure 6).

With use of the supercomputer we could incorporate all these effects and still be able to follow enough particles (7,200) to actually see interesting forms as they developed. We are now in the process of trying to apply our understanding of this problem to the accumulation of planetary-sized bodies in the solar nebula.

Through computer visualizations and associated theoretical studies, we now understand that satellite perturbations on a narrow elliptic ring will produce clumps and kinks with a characteristic spacing of $3\pi\delta a$, where δa is the radial separation between the ring and the satellite.

Our numerical results have also called into question a previous explanation for the braiding of a ring: our results demonstrated that collisions will "erase" any structure that is imposed on a narrow ring by a satellite embedded within that ring. However, we have not yet formed our own hypothesis concerning the formation of the braids, despite our hope that the three-dimensional simulation would give us some clues.

While developing our models, we simultaneously analyzed some Voyager images of the F ring (Figure 2). Through investigation of the variations in brightness of the ring using Fourier techniques, we were able to demonstrate that the $3\pi\delta a$ signature of Prometheus, the inner shepherd satellite, was present in the ring's fluctuations measured by the Voyager cameras. Several other periodic signals were identified as well, and we associate at least one of these with an as yet unseen satellite

Figure 3

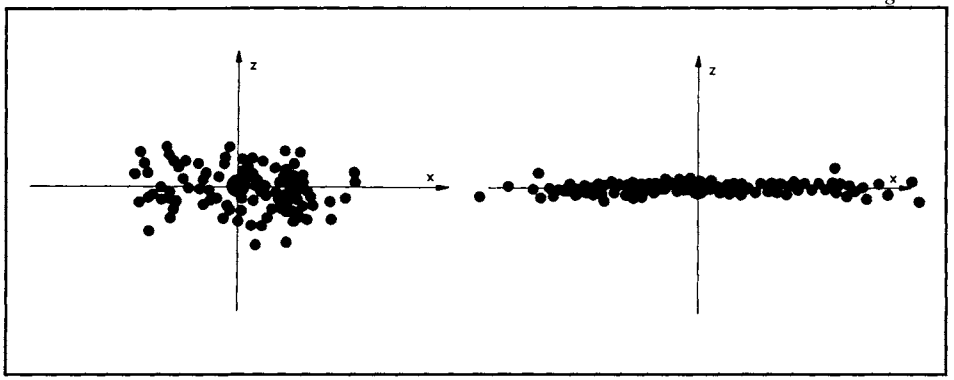

Figure 3. A simulation of a system containing about one hundred orbiting particles, as projected onto a plane parallel to the initial angular momentum vector.

The diagram on the left shows the initial distribution and the diagram on the right displays the particles some time later, after each particle has experienced fifty collisions on average.

After the flattening stage shown here, the simulation indicates that collisions produce ring spreading, with a few particles escaping altogether and others falling onto the planet.

Figure 4

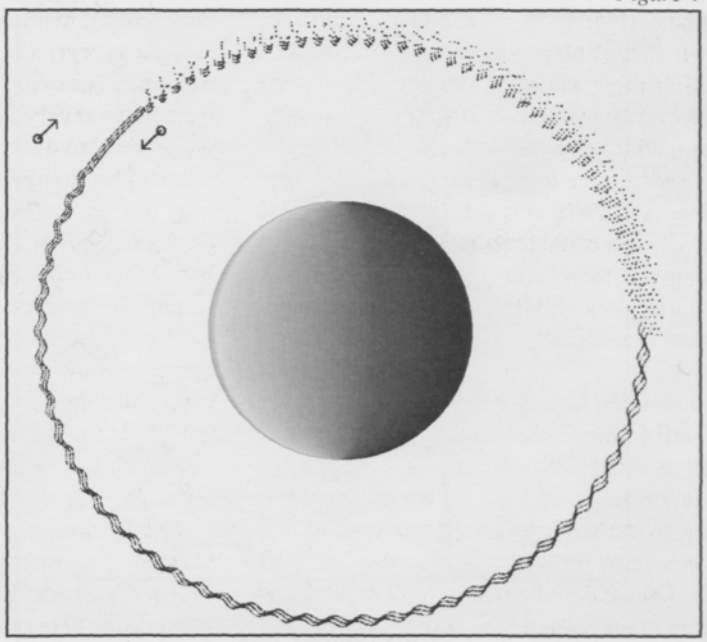

Figure 4. A computer simulation showing how moons could perturb an initially circular ring of particles orbiting around a planet.

The system consists of 2,400 particles and two shepherd satellites, an outer one moving in a circular orbit, and an inner one moving in an eccentric orbit. The reference frame is rotated at the orbital rate so that the average ring particle appears not to move, while the outer and inner satellites drift at their relative rates clockwise and counterclockwise, respectively.

The exterior moon, because it—like the unperturbed ring particles—moves on a circular path, creates a trail of smooth, sinusoidal waves. Long after the disturbance has occurred, the three sinusoidally distorted strands will overlap (for example, at 3 o'clock) as a result of the relative drift of the particles.

The inner moon, on an eccentric orbit, creates waves that contain discrete clumps and kinks (between 11 and 12 o'clock) that travel ahead of it; this clumping is produced by the variable strength of the perturbations owing to the eccentric orbit.

The spacings of some structures seen in Saturn's F ring compare favorably with those that should develop due to the shepherd satellites assumed in this model. As time goes on in the simulations, these structures are seen to shear apart (for example, at 2 or 3 o'clock).

Radial separations are magnified to clarify the image.

that is imprinting its characteristic wavelength on the ring.

In related work carried out last summer, Showalter found a moonlet during a computer-aided search through the Voyager images of the Encke Gap, a clear region in Saturn's main ring A (see Figure 1). In accordance with the shepherding argument, a satellite might have been suspected to have cleared the gap and, indeed, Jeffrey N. Cuzzi of NASA-Ames Research Center did detect waves running along the gap's edges in Voyager images. (Cuzzi is a 1967 Cornell graduate in engineering physics.) The wavelength of these oscillations, their longitude, and other characteristics allowed Showalter to pinpoint the moonlet's position, then to predict which Voyager images it should appear in, and finally to identify the object.

Figure 5

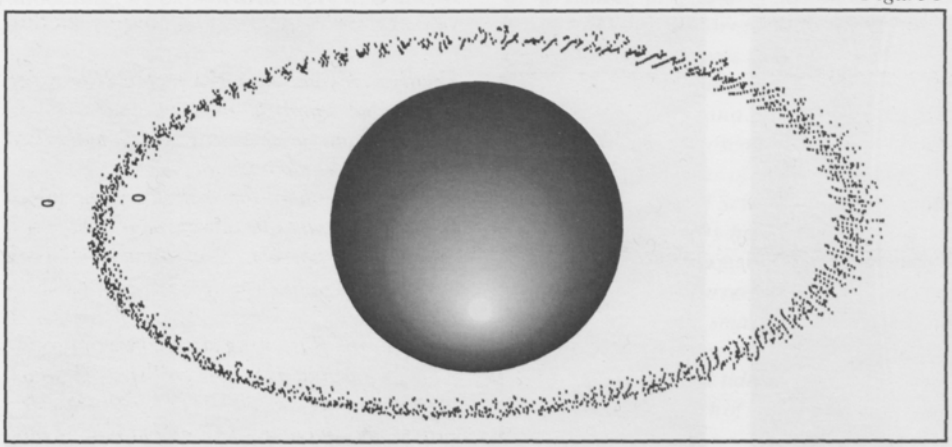

Further detailed searches of the Saturn system will have to await the arrival of the Cassini-Huygens mission, a joint venture of NASA and the European Space Agency. This mission, scheduled for launch in 1996, will observe Saturn and its companions for four years, starting in the year 2002. Burns has just been appointed as a member of the imaging team of this mission.

The success that we and others have had in finding embedded moonlets is one more

Figure 5. A supercomputer simulation of a narrow ring that has been perturbed by two small moons having orbits that are both slightly inclined and elliptic. The view is from an angle of 30 degrees from the plane of the page. The ring has gone through 120 full rotations, so that the outer moon has lapped it nearly twice and the inner moon has lapped it more than once.

Figure 6

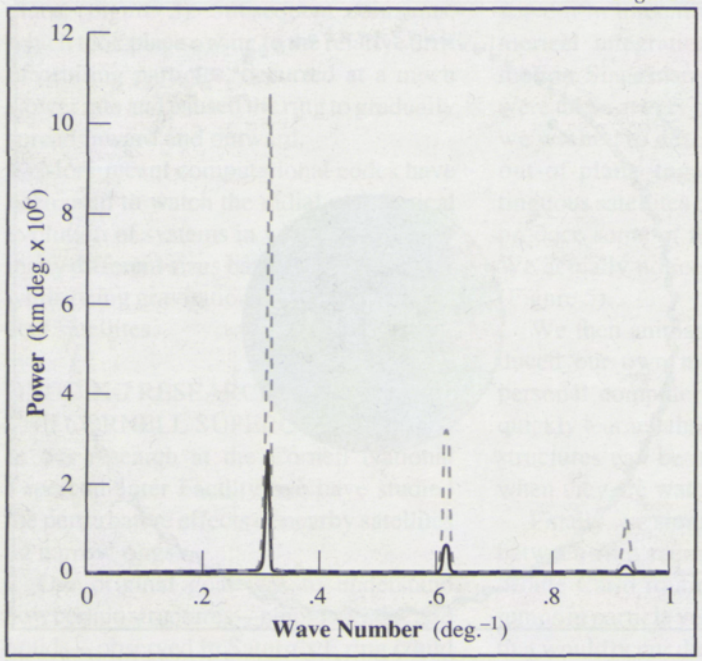

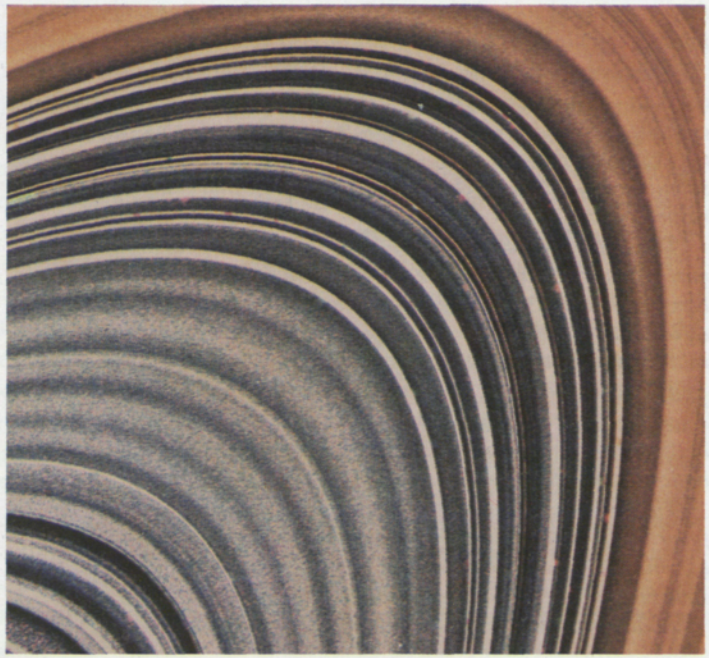

Figure 6. A plot, based on simulations, showing how collisions destroy any organized structure in the ring.

The plot shows the amount of power contained in waves of various frequencies. The broken lines correspond to a low frequency of collisions and the solid lines to a frequency 10 times greater; at a frequency 100 times greater, there is almost no signal. Accordingly, the model shows that the strength of the organized signal is damped significantly as more collisions stir up the system.

The strong signal at about 0.3 degree^{-1} is, as expected, from a shepherd satellite placed at the distance at which the actual shepherd is positioned. The signals at multiples of this primary signature are thought to be caused by nonlinear coupling in this complex problem.

Above and below: Computer-processed Voyager 1 images of Saturn's rings obtained at distances from one to several million kilometers. These images resolved previously unimaginable architecture and revealed much about the size, shape, and distribution of particles in the system. Saturn's rings are much more elaborate and complex than those of any of the other planetary systems.

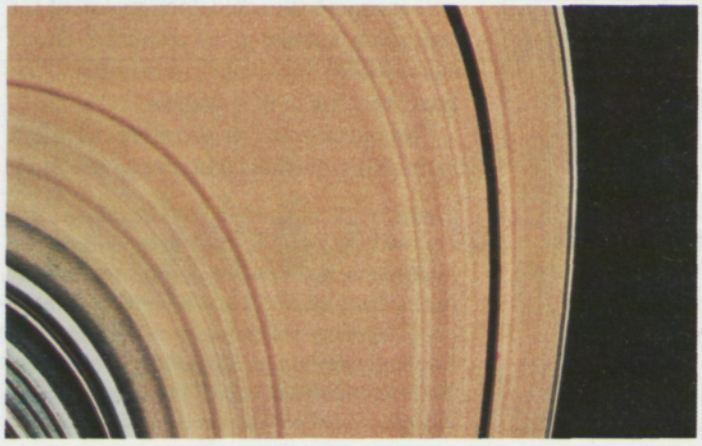

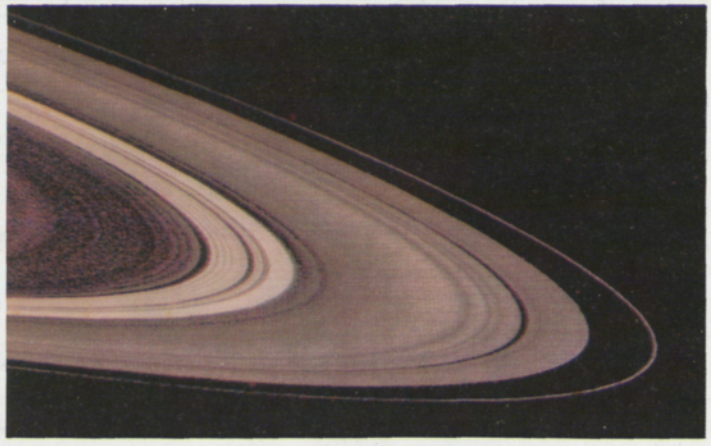

indication that the rings seen today are not primordial.

STUDIES MADE POSSIBLE BY SUPERCOMPUTERS

Supercomputers have proven to be invaluable in studies of the myriad interactions that influence ring particles. They have also contributed fundamentally to our current understanding of the long-term evolution of the solar system.

The simple question of whether the orbits of the nine extant planets and their satellites have always been qualitatively the same cannot be answered analytically, but may yield to numerical investigation. Several recent studies, principally by Jack Wisdom at M.I.T., Stanley F. Dermott and Renu Malhotra (then at Cornell), and Andrea Milani (a visiting professor at Cornell in 1988–89) have demonstrated that various real solar-system orbits are chaotic. We are now trying to understand what this means. Does chaos have a kind of order, in accordance with recent theories? Does it give clues—or erase them—about the conditions when the planets were born?

With the powerful combination of spacecraft imaging and supercomputer modeling, we expect to achieve new understanding of our planetary neighborhood.

Joseph A. Burns is a professor and chairman of Cornell's Department of Theoretical and Applied Mechanics, and also a professor of astronomy. Robert A. Kolvoord worked with Burns as a graduate student; he received his Ph.D. in the summer of 1990 and is currently a research associate in the Lunar and Planetary Laboratory at the University of Arizona.

Burns

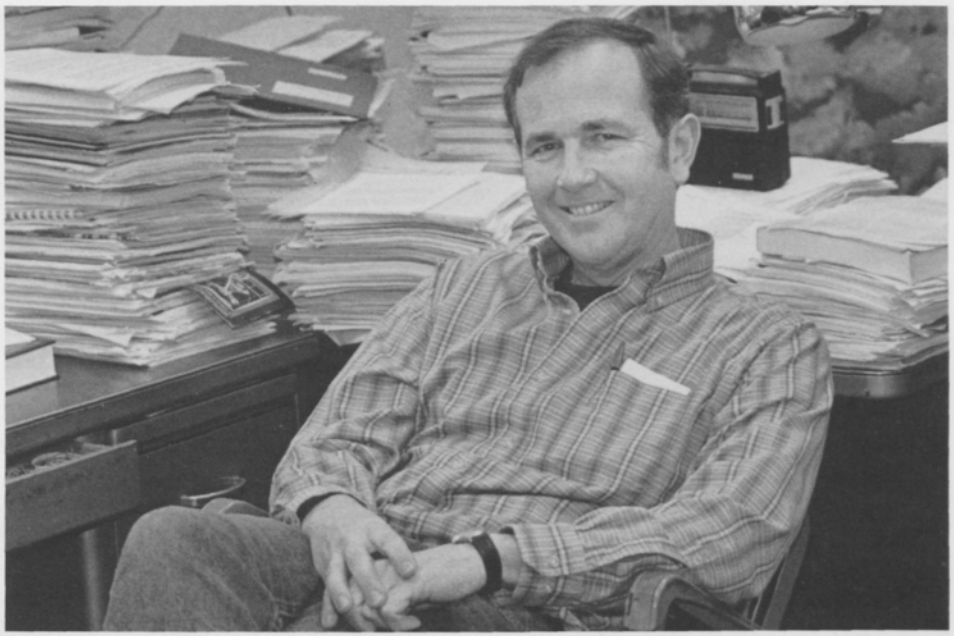

Burns did his undergraduate work at the Webb Institute of Naval Architecture, earned a Cornell doctorate in 1966, and then joined the Cornell faculty as an assistant professor.

He has spent sabbatical leaves at NASA's Goddard Space Flight Center on a National Research Council postdoctoral fellowship (1967–68) and at NASA's Ames Research Center (1975–76 and 1982–83). He has served as a visiting professor of astronomy at the University of California at Berkeley, and during 1989–90 he was a visiting scientist at the Lunar and Planetary Laboratory of the University of Arizona. He has also spent extended leaves in Moscow, Prague, and Paris.

Burns is a member of several panels of the National Academy of Sciences and NASA, and since the late 1970s he has been editor of Icarus: The International Journal of Solar System Studies. *His current research concerns planetary rings, the small bodies of the solar system (dust, satellites, comets, and asteroids), orbital evolution and tides, and the rotational dynamics and strength of satellites, planets, and asteroids.*

Kolvoord

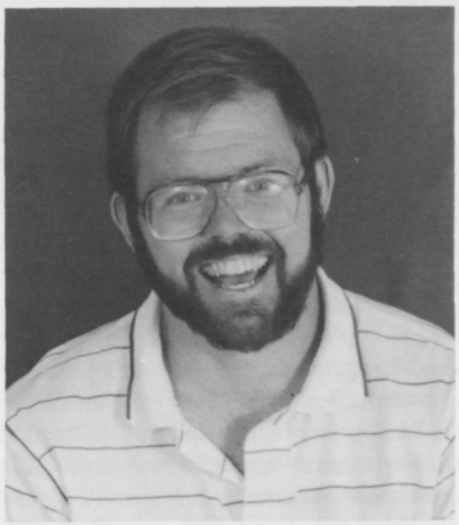

Kolvoord earned a B.A. degree in physics and an M.S. degree in materials science at the University of Virginia. His doctoral thesis at Cornell centered on the dynamics of Saturn's F ring. At the University of Arizona he is now working on problems of planetary formation.

HEATING OF THE SOLAR CORONA

by Ravi Sudan and Dana Longcope

Figure 1a

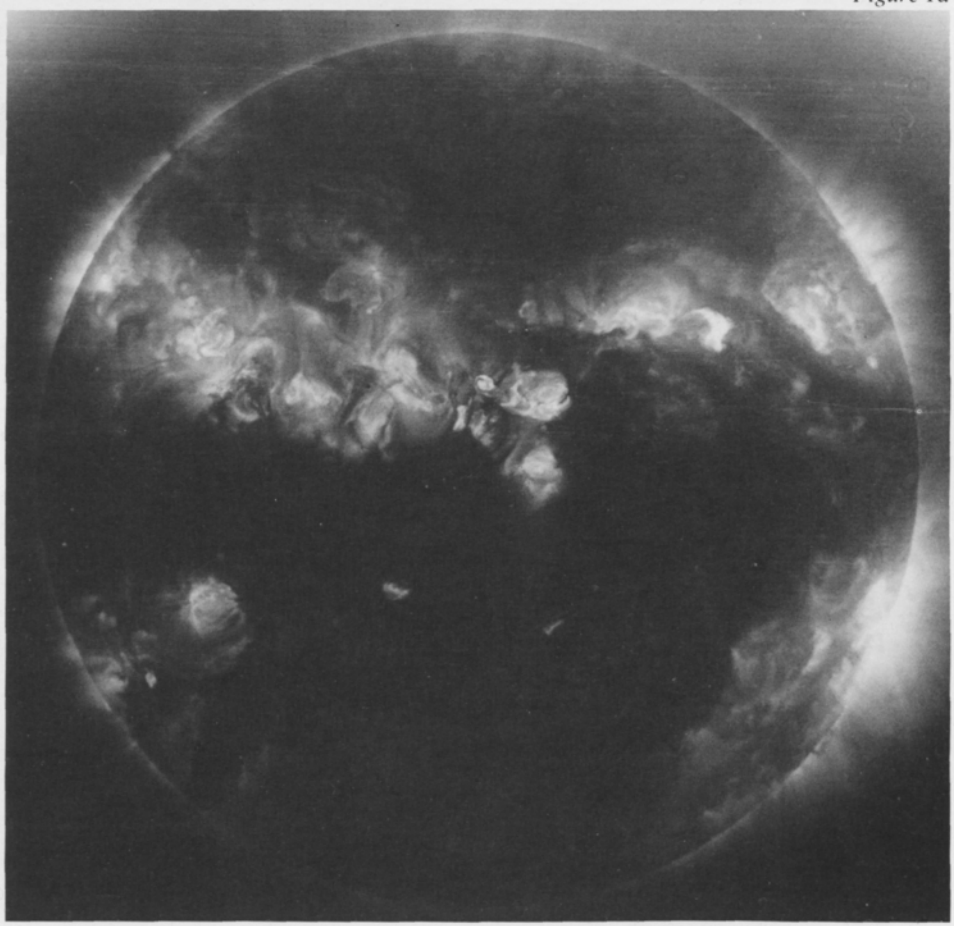

Our Sun is merely an average star, but its proximity makes it the most important celestial object to us on Earth. It is the only star we can study in some detail in a whole range of electromagnetic emissions, from microwaves to x-rays.

The visible disc of the Sun is surrounded by a very tenuous envelope of hot plasma that can be seen by the eye only during solar eclipses because it radiates most of its energy at wavelengths too short to be perceived by the retina. This radiation is in the range of soft x-rays, an indication that the coronal temperature is between one million and three million degrees Celsius—far greater than the 5,800-degree temperature at the surface, or *photosphere*. Because of this remarkably high temperature, the outer portions of the corona escape the Sun's gravitational force in the form of a solar wind that blows right through the solar system and beyond the outermost planets.

Since heat flows from regions of high temperature to those at low temperature, it came as a surprise when it was discovered, by Edlén around 1941, that the coronal temperature is far greater than that of the Sun's disc, so that heat is actually being conducted from the corona to the photosphere. It is

Figure 1b

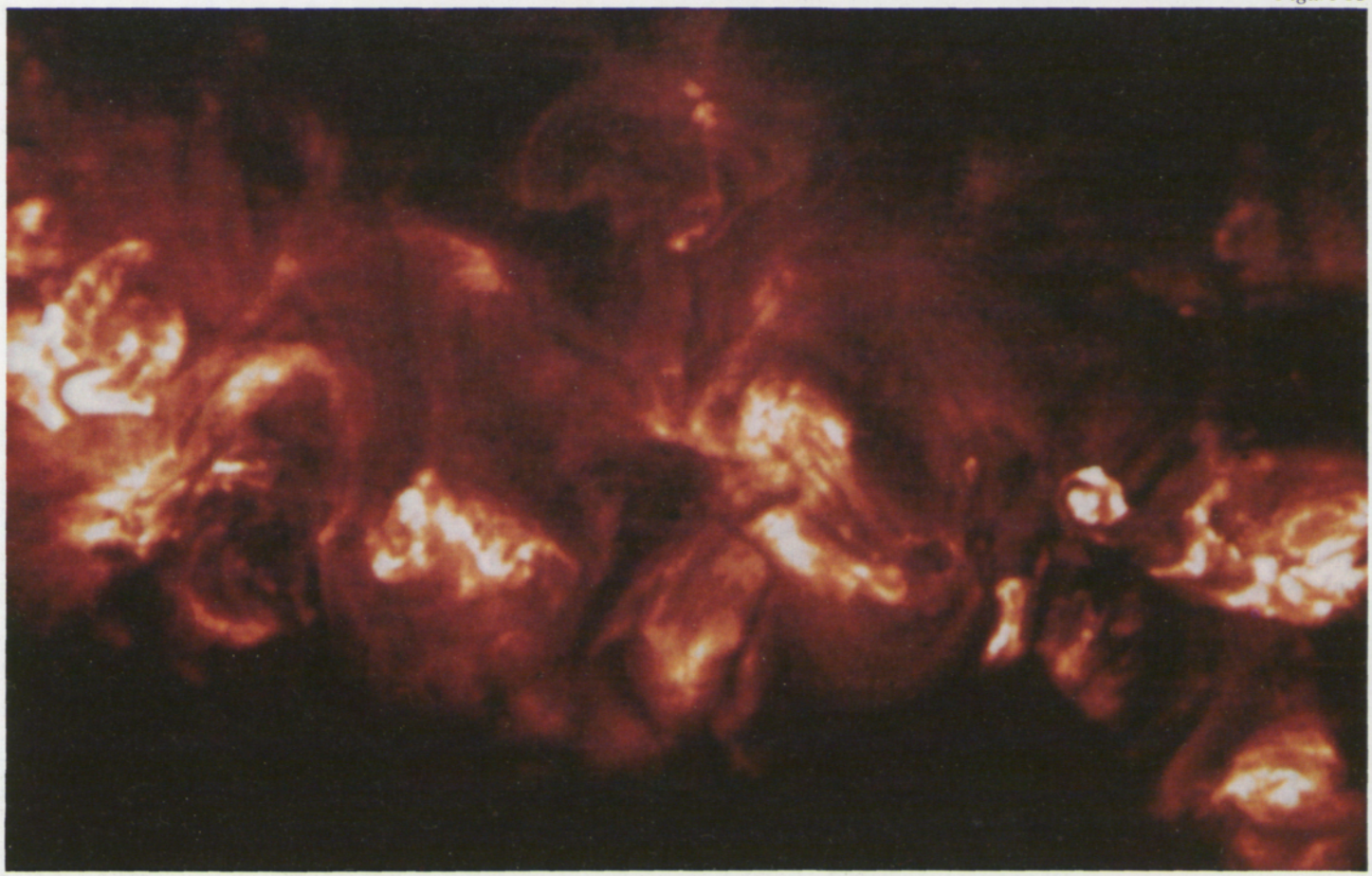

Figures 1a and 1b. High-resolution x-ray images of the Sun's corona. Figure 1b is a detail of 1a.

The photograph was taken on September 11, 1989, by the Smithsonian Astrophysical Observatory/IBM telescope aboard a NASA sounding rocket at a height of about 240 kilometers. The spatial resolution is 3/4 arc second (approximately 500 kilometers). Active regions (the bright areas) in Fe XVI line at 63.5 Å show a temperature of 2–3 million degrees Celsius. Coronal loops and a medium-sized flare can be seen.

(Courtesy of Leon Golub, Smithsonian Astrophysical Observatory, and IBM Research.)

immediately apparent, then, that the coronal temperature must be replenished by *mechanical* energy transported from the photosphere. The relatively dense photosphere is in a state of continual turbulence caused by the eddies that transport heat from the deep solar interior to the surface, just as in a boiling pot of water.

In what form the photosphere supplies this mechanical energy to the corona, and how it is transported, are matters of some debate. Our research is devoted to clarifying the physical mechanisms that are responsible for these processes.

IDEAS FOR EXPLAINING CORONAL HEATING

The earliest suggestion, offered independently by Biermann (1946) and Schwartzschild (1948), was that the heating is due to the dissipation of acoustic shock waves driven by the turbulent motion of the photosphere. The acoustic noise from a jet engine is a familiar example of such a process. Later work showed that this process is, if anything, too efficient; the acoustic energy would dissipate not far from the source in a thin layer known as *chromosphere*. No energy would penetrate far into the corona by this process.

"It is the only star we can study in some detail in a whole range of electromagnetic emissions, from microwaves to x-rays."

A more promising idea is that the Sun's magnetic field could play a role in the transport of energy. This magnetic field has complex structure and is continually evolving—waxing and waning with a period of twenty-two years. Sunspots are locations where the magnetic field is particularly strong, but there are also broad regions where the magnetic activity is high.

The magnetic field emerges through the photosphere in the form of loops that are eventually destroyed or blown away with the solar wind. It soon became evident that the magnetic field could act as a conduit for transporting energy well into the corona. The energy would come from the turbulent motion of the photosphere, and the magnetic field would transport it in the form of Alfvén waves (named after the Swedish plasma physicist and Nobel laureate). Alfvén waves are akin to waves that propagate on a taut string when it is plucked; the magnetic field plays the role of a string under tension.

Once it was realized that the magnetic field is the key to this problem, other mechanisms involving magnetic fields were proposed. We will address these hypotheses and return to Alfvén waves in our concluding remarks.

THE STRUCTURE OF THE SUN'S MAGNETIC FIELD

The photograph shown in Figure 1a and Figure 1b, taken from a rocket above Earth's atmosphere, records the Sun in soft x-rays of wavelength 63.5 angstroms (Å).

The bright loops image the magnetic-field loops because the denser plasma within the loops emits more x-rays than the surrounding matter. The loops range in length from a thousand to a few hundred thousand kilometers. The magnetic field lines of a loop are "anchored" in the much denser photospheric plasma; the places they are anchored are called *footpoints*. Because of the high electrical conductivity of the plasma, the field lines are "frozen" to the photospheric plasma and are carried around by the plasma motion.

Since the plasma motions of the two ends of a loop are uncorrelated, the field lines get twisted and untwisted. And since a twisted field line must carry a current in accordance with Ampère's law, it stores energy because of the additional magnetic field it generates.

The energy that builds up in this way in the magnetic field of the loop must eventually be dissipated. When the release is sudden, a solar flare erupts; the largest of these flares are catastrophic events that release, in a matter of minutes, 10^{25} joules of energy as x-rays, light, microwaves, and energetic subatomic particles. (This is enough energy to bring to boil a cube of water 300 kilometers on a side.) The energy dissipated over longer time scales serves to heat the corona and maintain its temperature. This dissipation can only be attributed to the ohmic resistance of the plasma to the currents flowing in the loop.

But here there is a paradox: the resistivity of the plasma decreases as the temperature increases, and it is quite small at the prevailing temperature. So how does the energy dissipate in a highly conducting inviscid plasma? The picture that emerges from the calculations (see Figure 2) is that the current flowing in the loop undergoes a filamentation process, first conjectured by van Ballegooijen (1985). In this process, strands of smaller and smaller cross section are formed, so that the total current flows in a small fraction of the area available to it. Thus the local current density may exceed the average current density by orders of magnitude, and this results in locally intense regions of dissipation.

The filamentation of the current also leads to a random fine structure in the mag-

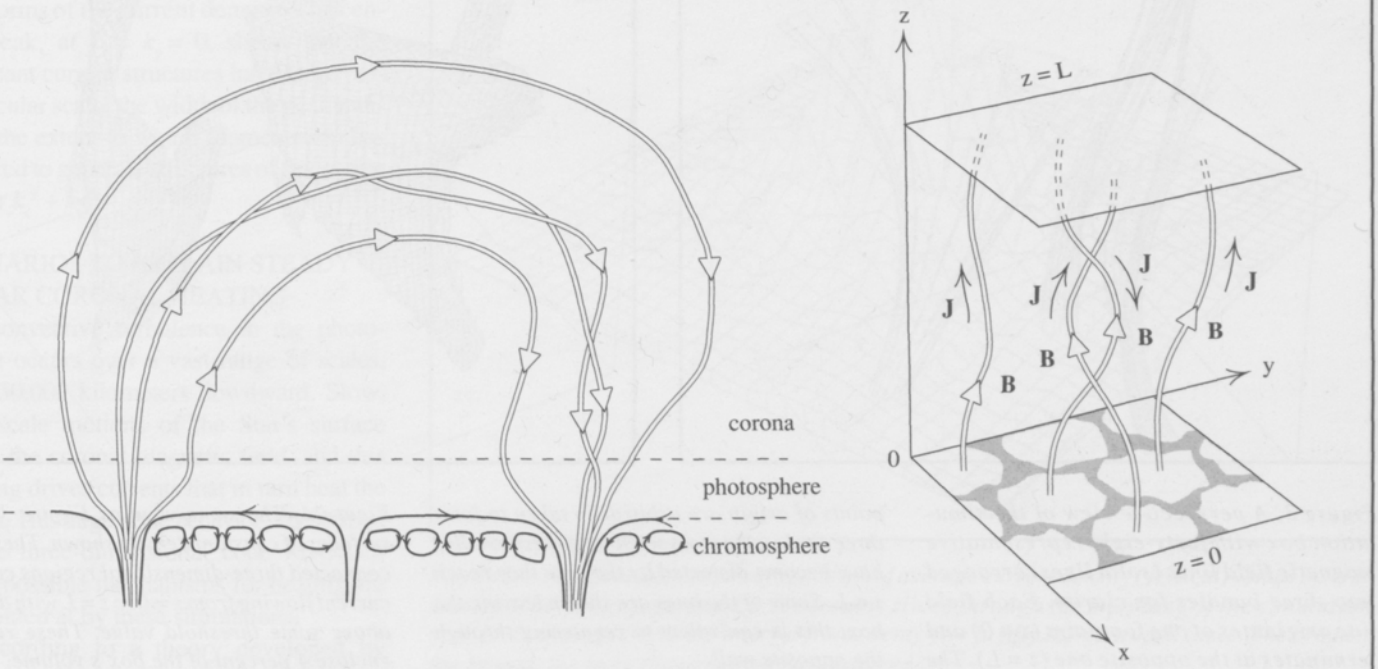

Figure 2. The simulation of coronal loop dynamics.

The schematic diagram at left (not to scale) pictures the twisted magnetic field lines of a solar coronal loop. The field lines have been twisted by convective turbulent motion in the photosphere. The small circular lines represent eddies.

The diagram at right illustrates the model actually used in the numerical modeling. It consists of a uniform magnetic field bounded by two planes at z = 0 and z = L, representing the ends of the loop anchored in the photosphere. Random motions are imposed externally at the bounding planes; these have specified perpendicular correlation length l and correlation time t to correspond to the eddy size and eddy turnover time of the turbulent photospheric motions. **J** *and* **B** *are current density and magnetic field lines, respectively.*

The evolution of the magnetic field between the planes is determined by the equations of magnetohydrodynamics (MHD):

$$\rho_0 \frac{d}{dt} \mathbf{v} = \mathbf{J} \times \mathbf{B} ,$$

$$\mathbf{J} = (1 / 4\pi) \nabla \times \mathbf{B} = \sigma (\mathbf{E} + \mathbf{v} \times \mathbf{B}) ,$$

where **v** *is the plasma velocity, ρ_0 is the density (taken as constant for simplicity),* **J** *is the current density,* **E** *and* **B** *are the electric and magnetic fields, and σ is the electrical conductivity. Pressure has been neglected.*

These fields are represented on a discrete grid of 30,000 or more points inside a box bounded by conducting photosphere at z = 0 and z = L and periodic in the other directions (x and y). The equations of MHD (actually a modified version known as reduced MHD) then give a prescription for advancing the quantities on each grid-point; this is done in steps using a second-order Runge-Kutta time integrator.

On the supercomputer, the fully vectorized code, MARLO, takes ten seconds per time step to advance a 64 x 64 x 32 grid, and since there are three thousand steps in a typical run, the CPU time required is about ten hours. Doubling the resolution in all three dimensions would require a run time of 160 hours.

Figure 3

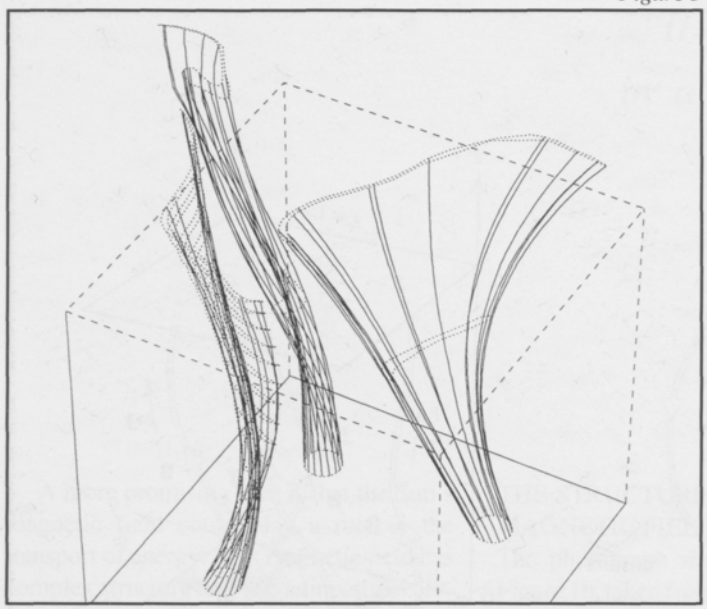

Figure 4

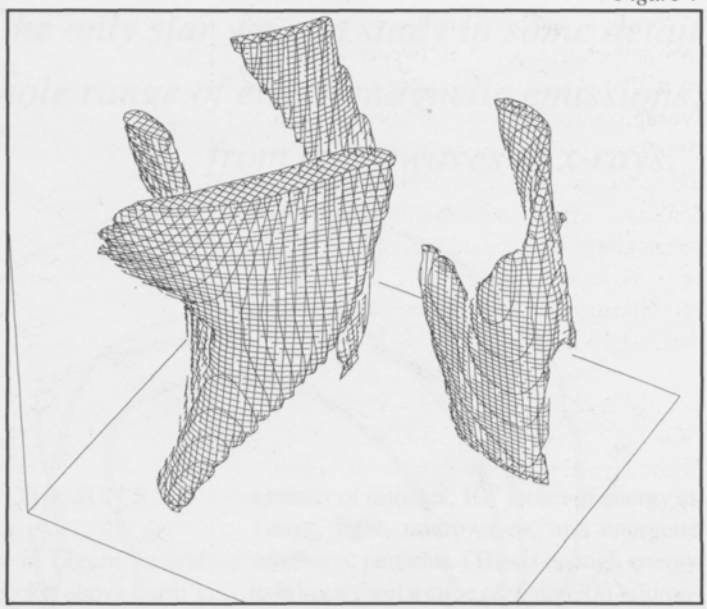

Figure 3. A perspective view of the simulation box with forty-eight representative magnetic field lines (solid lines) arranged into three bundles for clarity. Each field line originates at one footpoint ($z = 0$) and terminates at the opposite one ($z = L$). The points of origin are arbitrarily taken to form three circles; the cross sections of these bundles have become distorted by the time they reach $z = L$. Some of the lines are shown leaving the box; this is equivalent to reentering through the opposite wall.

Figure 4. The same view as Figure 3, with surfaces of constant density shown. These disconnected three-dimensional regions contain current flowing from $z = 0$ to $z = L$ with density above some threshold value. These regions enclose 4 percent of the box's volume.

netic field. Field lines that are close together at one footpoint diverge rapidly with height, as shown in Figure 3. More detailed studies indicate that some field lines are actually stochastic. It is our prediction that as greater and greater resolution is achieved in images of the solar corona, more and more structural complexity will be revealed for the magnetic field in the loops. The structure may even turn out to have a "fractal" nature.

NUMERICAL SIMULATION OF CORONAL LOOP DYNAMICS

A schematic diagram of a coronal loop is shown in Figure 2. The loop itself is modeled by the much simpler geometry shown in the sketch at the right in the figure.

The evolution of the magnetic field is calculated on the basis of the magnetohydrodynamic equations, as described in the figure caption. The computational domain is a box bounded in z by planes representing the photosphere, and periodic in x and y. A grid of points is set up and values of the electric and magnetic fields, **E** and **B**, are calculated in time steps on an IBM 3090-600J supercomputer at the Cornell Theory Center. A fully vectorized code, MARLO, is used. A typical run of three thousand time steps takes about ten hours. Doubling the resolution in every dimension would also require the number of time steps to be doubled, leading to a sixteenfold increase in the run time.

The key to the effective analysis of data churned out by a large three-dimensional code such as MARLO is proper visualization techniques. Figures 3 and 4 depict one snapshot taken after fifty time units (one time unit is the time required for an Alfvén wave to travel the length (L) of the loop.

Figure 3 shows forty-eight representative magnetic field lines arranged into three bundles for clarity. Each of these would have been a straight vertical line to begin with, but has been distorted due to the random motion of the photosphere.

Figure 4 demonstrates the filamentation and concentration of the current. The surfaces shown enclose regions in which the current density exceeds some threshold value; these regions occupy 4 percent of the volume but account for 18 percent of the ohmic dissipation.

Finally, Figure 5 was made by slicing each snapshot from the last twenty-five time units through the midplane ($z = L/2$) and averaging the two-dimensional Fourier transforms of the current density. The central peak, at $k_x = k_y = 0$, shows that the dominant current structures have large perpendicular scale; the width of the peak indicates the extent to which filamentation has occurred to generate structures of finer scale (larger $k_x^2 + k_y^2$).

SCENARIOS TO EXPLAIN STEADY SOLAR CORONAL HEATING

The convective turbulence in the photosphere occurs over a vast range of scales, from 30,000 kilometers downward. Slow, large-scale motions of the Sun's surface tangle the coronal magnetic field, and this tangling drives currents that in turn heat the corona. This large-scale behavior is described by the three-dimensional code MARLO. Other possible mechanisms for heating are also hinted at by these simulations.

According to a theory developed by Similon and Sudan, faster, finer-scale motions that are unresolved by MARLO drive Alfvén waves along the magnetic-field loops. This energy also gets dissipated, creating additional heating, but only because the magnetic structure has been made stochastic by the large-scale motion. Alfvén waves propagating along the field lines of a stochastic magnetic field have their wavefronts shredded into very fine structure by the diverging field lines, and this leads to rapid damping. The evolution of a phase front is shown in Figure 6. Without the complex magnetic structure created by the slow, large-scale motion, the Alfvén waves would be almost undamped in the volume of the loop, and their energy would be dumped back into the photosphere after resonating in the loop for a long time.

Figure 5

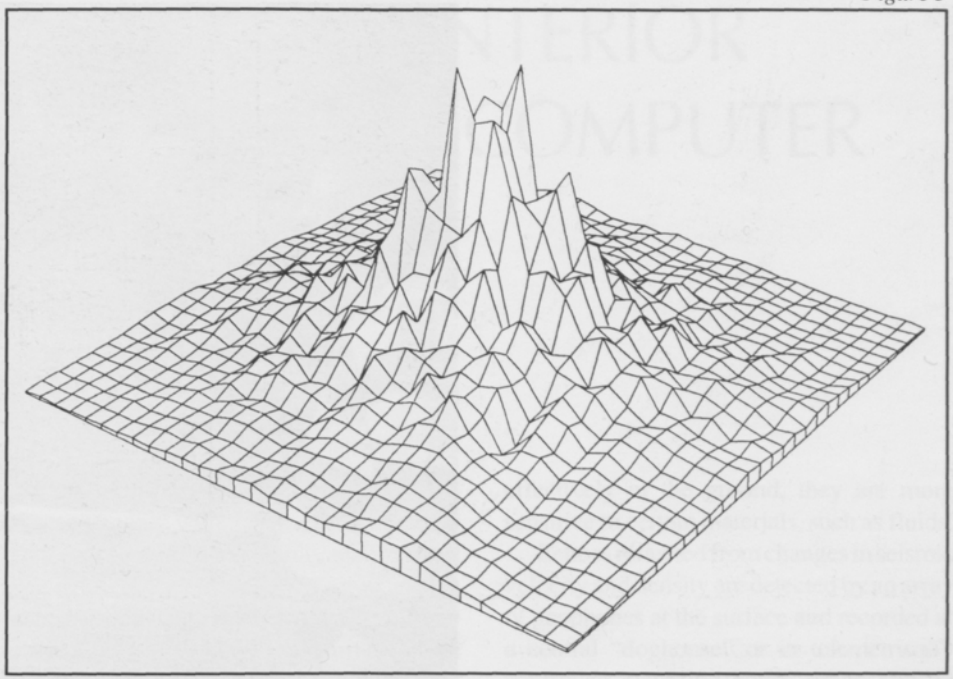

Figure 5. A two-dimensional power spectrum of average current density (vertical) versus inverse x and y scale lengths (k_x and k_y). It contains slices through the midplane of the simulation ($z = L/2$) averaged over the interval from twenty-five to fifty Alfvén transit times. The broader the spread, the more filamentation has occurred.

Figure 6. Typical stages of the wavefront of an Alfvén wave packet along a stochastic magnetic field. (From P. L. Similon and R. N. Sudan, Astrophysical Journal *336:442–53, 1989.)*

Figure 6

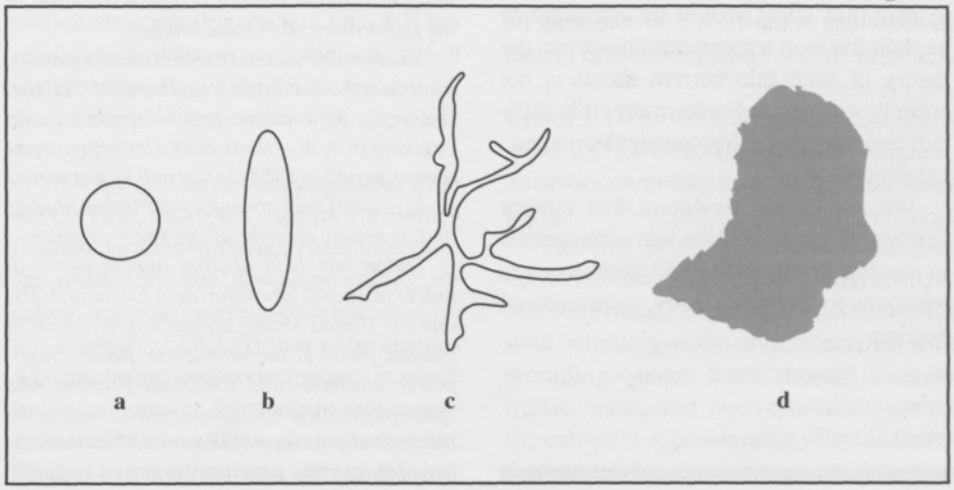

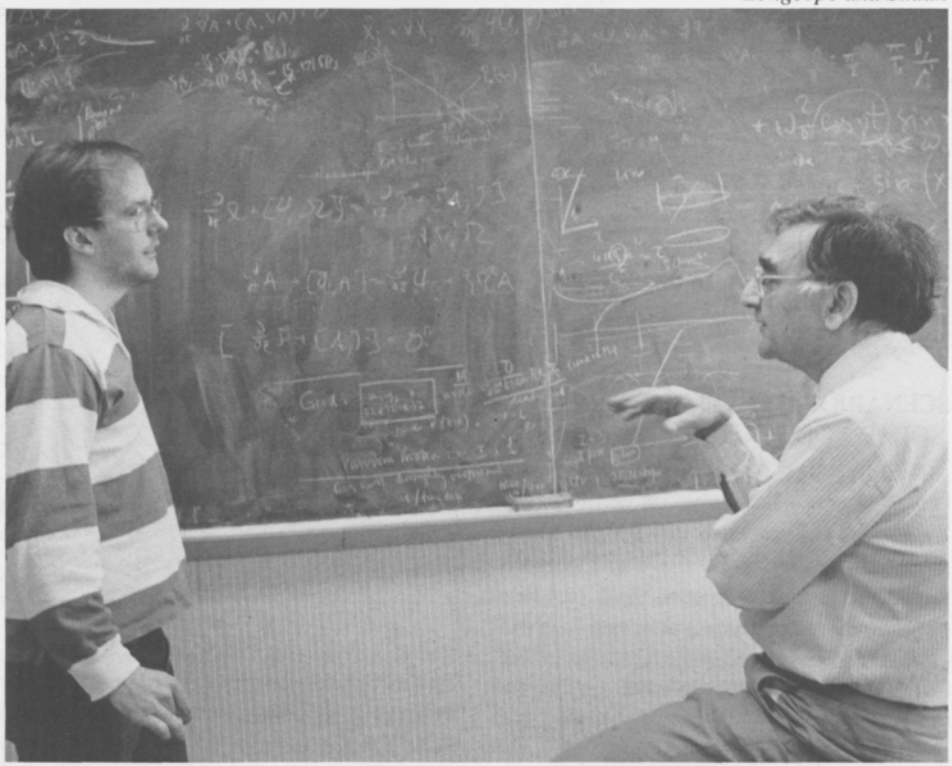

There is a third scenario, developed by Parker (1983), that postulates the formation of very thin current sheets into which almost the entire current condenses. The dissipation in this thin sheet would be adequate to explain the loop temperature; however, the theory of such thin current sheets is not entirely watertight. Furthermore, it is difficult to demonstrate this concept by numerical simulation.

We are of the viewpoint that current filamentation and Alfvén wave dissipation in stochastic magnetic-field geometry are adequate to explain steady solar coronal heating.

Ravi Sudan is the IBM Professor of Engineering in Cornell's School of Electrical Engineering and School of Applied and Engineering Physics. Dana Longcope is a Ph.D. candidate in applied physics and a research assistant in the Laboratory of Plasma Studies.

Sudan was educated in India and England—he received a doctorate from Imperial College, University of London—and he worked as an engineer in both of those countries before coming to Cornell in 1958. At *Cornell he has served as director of the Laboratory of Plasma Studies and as deputy director of the Theory Center.*

Sudan has held visiting appointments at universities and laboratories in England, Italy, and the United States, conducting research in plasma physics, thermonuclear fusion, high-power electron- and ion-beam physics, and space physics. He has also served as head of the theoretical plasma physics section at the U.S. Naval Research Laboratory and as a scientific adviser there. He is active as a consultant, has chaired several international conferences, and serves as an editor for journals and for the Handbook of Plasma Physics.

He is a fellow of the American Physical Society and of the Institute of Electrical and Electronics Engineers. He received the 1989 James Clerk Maxwell Prize of the American Physical Society.

Longcope, a 1986 Cornell graduate in applied and engineering physics, is doing his doctoral research with Sudan. He is currently studying mechanisms of magnetohydrodynamic heating in the solar corona, using both analytical and numerical approaches. He has also participated in an investigation of stochastic diffusion of electron orbits in a magnetized plasma.

After receiving his degree, Longcope plans to continue research in theoretical plasma physics.

EXPLORING THE EARTH'S INTERIOR WITH THE CORNELL SUPERCOMPUTER

by Larry D. Brown

For the past sixteen years, earth scientists at Cornell have been leading a major new initiative to understand the earth's interior. Using echo-sounding techniques originally developed by the oil-exploration industry, they have been systematically probing the subsurface to depths of 30 kilometers or more in an attempt to map the internal structure of the earth's crust.

Surveys carried out by this project—the Consortium for Continental Reflection Profiling (COCORP)—have traced extensive faults underpinning the Appalachian Mountains of the eastern United States and the Basin and Range of Utah; ancient buried basins and fauit lines in the mid-continent; mid-crustal magma chambers beneath areas of the southwest that are even now being pulled apart; and new-found complexity at the base of the crust, the "Moho". COCORP's success in revealing new aspects of continental architecture has stimulated similar programs in more than twenty countries around the world.

While only a fraction of the world's continents have yet been sampled by such geophysical surveys, the mass of data already accumulated has completely revised our view of the continents. It has also presented geoscientists seeking a comprehensive synthesis of this work with a major computational challenge: how to meaningfully analyze these vast datasets, each of which require extensive signal processing. In this article I review some aspects of COCORP's effort to use the Cornell National Supercomputer Facility to meet this challenge.

REVEALING STRUCTURE WITH SEISMIC IMAGING

Computational power is an essential ingredient in modern seismic exploration, in which elastic waves are used to "illuminate" subsurface structure (Figure 1). COCORP has used a method known as Vibroseis, which was developed by CONOCO to circumvent the problems experienced with explosive sources.

In Vibroseis, large vibrating trucks (Figure 2) emit radar-like "chirps", in which frequency varies with time. These vibrations are usually up and down, generating so-called "acoustic" waves, much like sound in air. Recently, COCORP has experimented with transverse-motion techniques in which trucks are vibrated from side to side to generate shear waves. Although shear waves are harder to produce, and propagate less effectively in the ground, they are more sensitive to certain materials, such as fluids.

Echoes reflected from changes in seismic velocity and density are detected by an array of geophones at the surface and recorded at a central "doghouse" or in telemetrically controlled recording boxes called *seismic group recorders (SGR)*. These recordings are then processed by computer to produce an image that resembles a geologic cross section.

The seismic reflection method is capable of resolving structures down to the scale of a few meters. In deep seismic work, resolution on the order of a few tens to hundreds of meters is commonplace.

COMPUTING THE DATA AND INTERPRETING THE RESULTS

Seismic computing consists of three basic parts.

The first is *signal enhancement*. The echoes from subsurface rock units are usually very weak, especially in comparison with vibratory noise that interferes with recording—noise from sources such as traffic, wind, and even animals chewing the cables(!). Considerable effort is therefore expended in using signal-detection

Figure 1

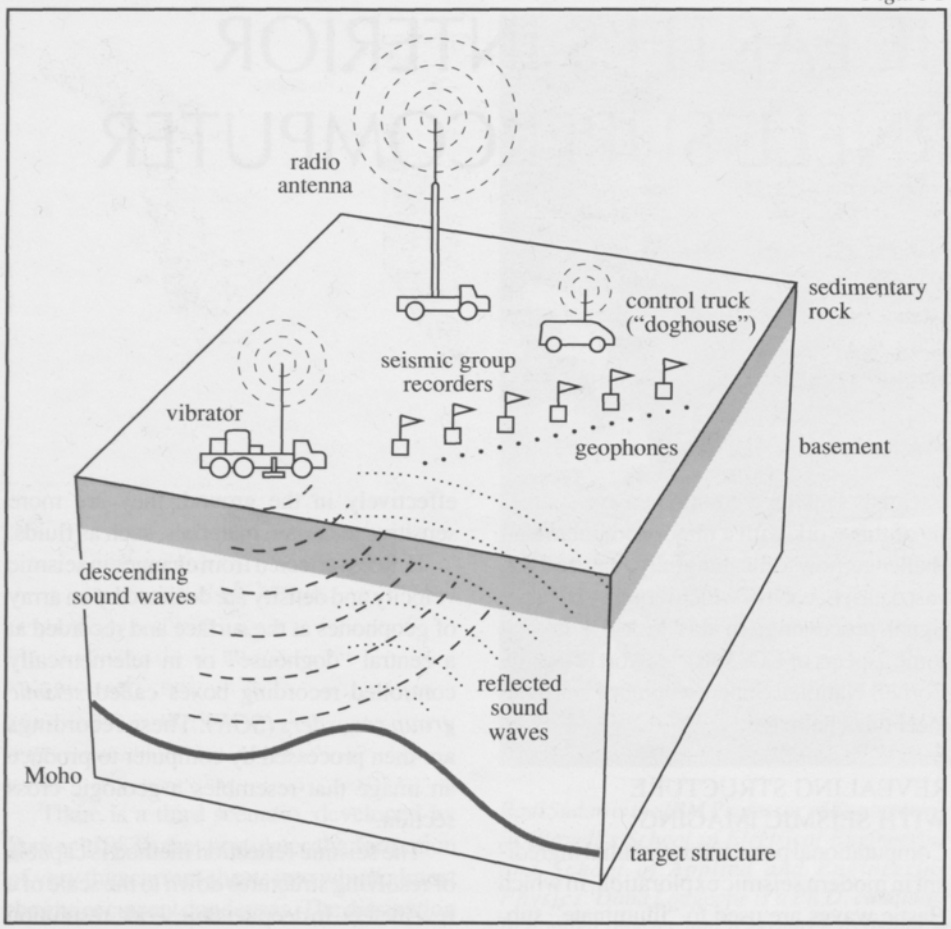

Figure 2

Figure 3

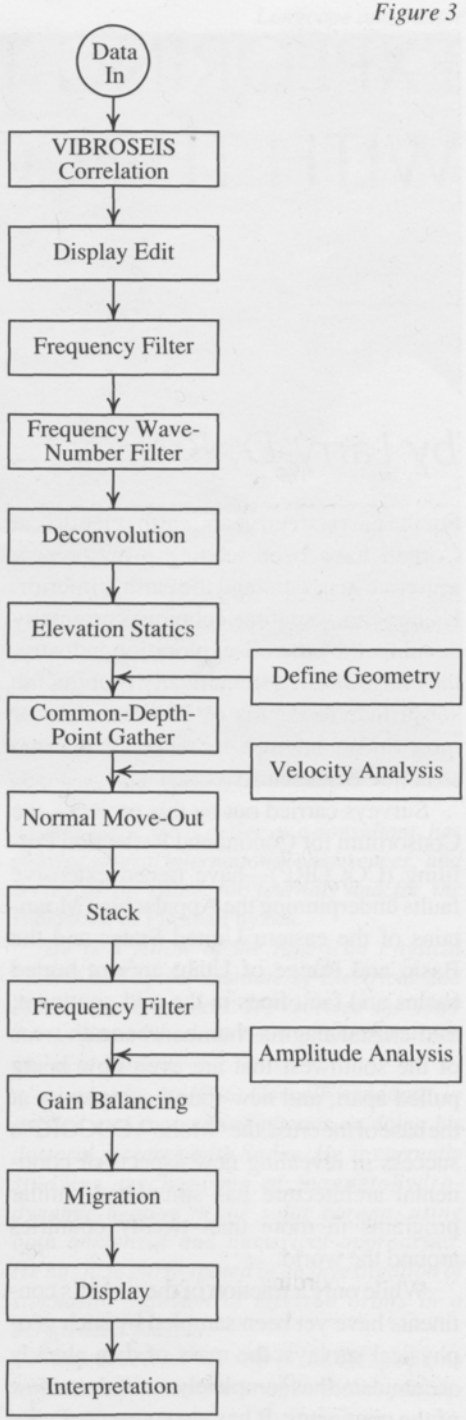

Figure 4

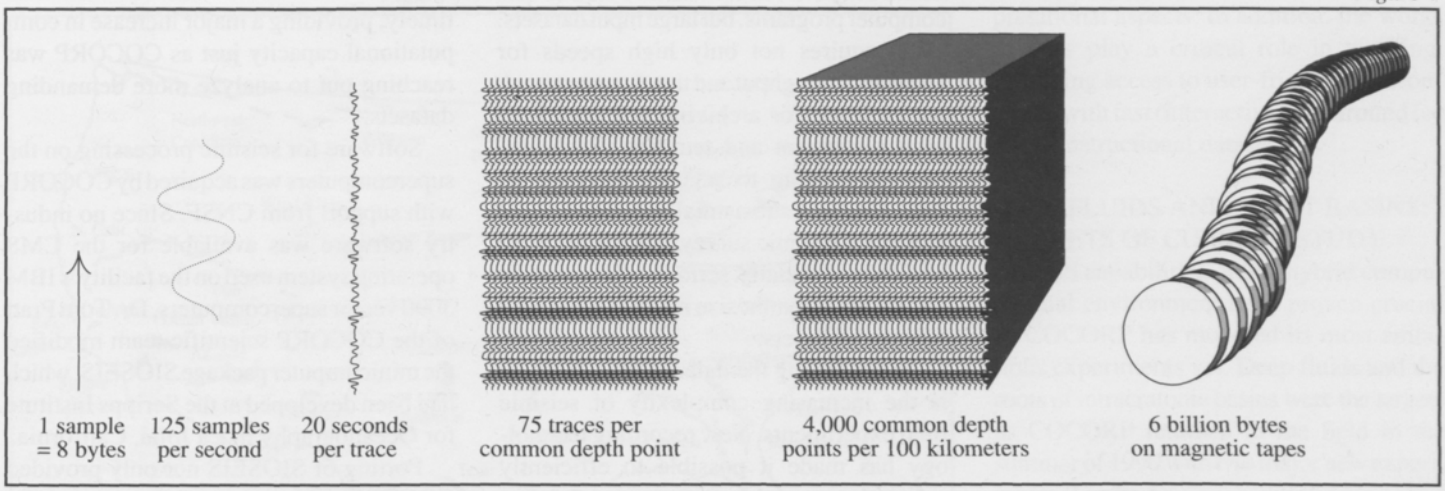

Figure 1. The seismic reflection method.

Figure 2. Vibrators in action in southeastern Georgia, searching for a deep fluid body. These vibrators were developed by AMOCO to allow both vertical and horizontal vibration. The vibrating pad has "teeth" that allow the pad to shake from side to side as well as up and down.

Figure 3. A typical processing sequence used with a supercomputer to produce seismic images.

Figure 4. An illustration of the volume of data needed to produce a typical seismic image.

algorithms to filter out noise and increase relative signal strength. Among the techniques used are *match filtering* (Vibroseis correlation), *noise spike editing, frequency and frequency-wavenumber filtering*, and *wavelet shaping* or *deconvolution*. A typical processing sequence is shown in Figure 3.

The most important tool in seismic signal enhancement is called *common-depth-point (CDP) stacking*. In this technique, multiple recordings of reflections from the same subsurface point are summed in such a way that desired signals are in phase, while various noise sources are out of phase and interfere with each other. It is in this process that the massive redundancy incorporated in seismic recording is used to isolate target reflections.

The second component of seismic computing is *imaging*, also known as *migration*, in which the signals detected in the first phase are reconstructed into an accurate geometric image of subsurface reflectors. The result is a seismic section that looks very similar to a geologic cross section. Although fewer data are usually involved in imaging than in signal enhancement, the algorithms are more complex and computer-intensive.

The last phase of seismic computing is *interpretation*, in which the geophysicist or geologist visually identifies significant reflection correlations and geometries. In the past this procedure was largely manual, with the analyst marking paper plots with colored pencils. Now such work is done on computer graphics workstations, with the analyst electronically marking significant relationships on the seismic image. Interpretation workstations have become a necessity as seismic exploration has moved from simple two-dimensional profiling to full three-dimensional imaging.

THE DATA PROBLEM: QUANTITY AND COMPLEXITY

The computational algorithms used in seismic imaging range from the very simple, such as visual editing, to the exceedingly complex, such as migration. The complex procedures are inherently time-consuming and in virtually any circumstance would make demands upon even the fastest computers, but there is a special challenge in seismic processing because of the very large volume of data.

As I have indicated, seismic signal detection is usually built around algorithms that make use of data redundancy to achieve signal-to-noise increases. Redundancy factors of 48 to several hundred are typical *for each data point* in a seismic image. As each image may contain thousands of data points, the algorithms may operate on several gigabytes for each interpretable image (Figure 4). Since there is still as much art as science in such processing, frequently these procedures are applied in an interactive fashion, with use of multiple passes in which varying parameters are tried.

Thus the computational challenge for seismologists involves not only complex

computer programs, but large input datasets. This requires not only high speeds for adequate throughput and timely turnaround, but facilities for archiving and retrieving both permanent and temporary datasets, each amounting to several gigabytes in size. This is a substantial requirement for any given seismic survey, but the problem becomes especially serious when there is an attempt to synthesize results from many different datasets.

Exacerbating the data-volume problem is the increasing complexity of seismic field experiments. New recording technology has made it possible to efficiently collect larger and larger amounts of data corresponding to more complex field geometries and innovative seismic sources, such as the shear-wave vibrators. Managing these new datasets has led to exploitation of new recording technologies such as VHS and 8-millimeter videotape formats. (For example, a single 8-millimeter tape that can be held in the palm of the hand contains the equivalent of more than twenty standard 9-track computer tapes.)

"The establishment of the Cornell National Supercomputer Facility . . . was therefore most timely, providing a major increase in computational capacity just as COCORP was reaching out to analyze more demanding datasets."

SEISMIC SUPERCOMPUTING AT CORNELL

COCORP's seismic processing was supported for a number of years by the dedicated minicomputer system MEGASEIS, a standard oil-industry system for moderate exploration programs. For basic processing of the datasets then being collected, MEGASEIS proved reliable and adequate.

However, as the international effort to explore the continents expanded and COCORP's own experiments increased in complexity, the limitations of such a system became more and more obvious. The establishment of the Cornell National Supercomputer Facility (CNSF) at the Cornell Theory Center was therefore most timely, providing a major increase in computational capacity just as COCORP was reaching out to analyze more demanding datasets.

Software for seismic processing on the supercomputers was acquired by COCORP with support from CNSF. Since no industry software was available for the CMS operating system used on the facility's IBM 3090 vector supercomputers, Dr. Tom Pratt of the COCORP scientific team modified the minicomputer package SIOSEIS, which had been developed at the Scripps Institute for Oceanography in La Jolla, California.

Porting of SIOSEIS not only provided COCORP with a powerful new tool for basic seismic computing, it also taught us some important lessons in the exploitation of high-performance computers. One lesson was that raw computational speed is not the only means of achieving increased computational efficiency. At least as important as the computational speed-ups made possible by the vector compilers and processors of the 3090 was the machine's large memory, which allows for easy loading of large datasets. With a major portion of the dataset resident in memory, subsequent processing could proceed efficaciously without time wasted on explicit swapping of data to and from disk or tape. The extended memory of the supercomputer thus proved to be one of its most useful, though least touted, features.

With major computational speed-ups achieved by exploitation of vector and extended memory features of CNSF computers, COCORP's whole approach to processing was affected. Interactive or near-interactive seismic processing became a reality. Rather than relying on the conventional approach of feeding everything into the computer with a few trial parameters and then waiting hours for the result, ana-

Figure 5. A map of COCORP surveys in the United States.

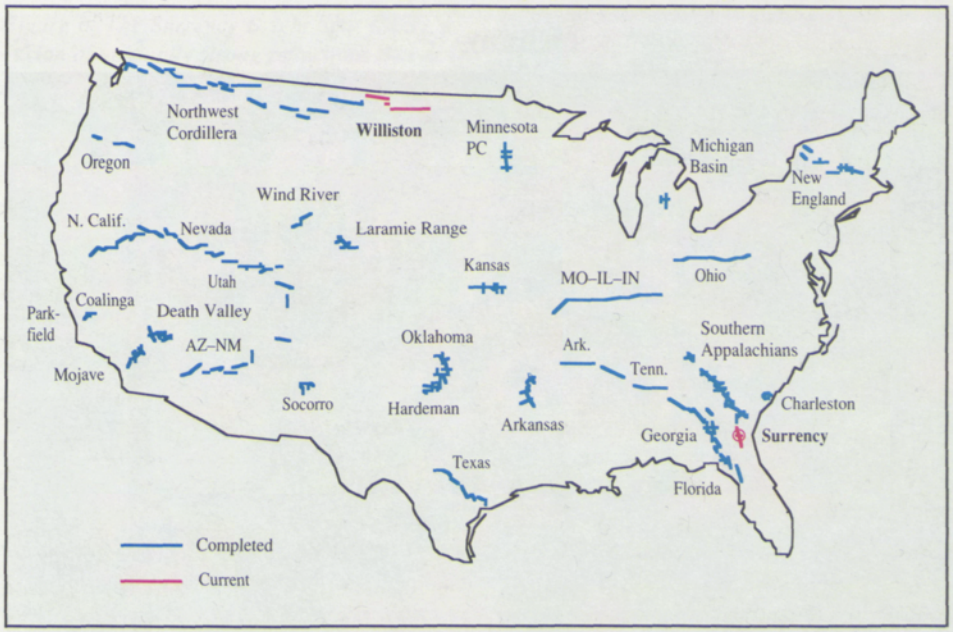

lysts could load test portions of the data and iterate processing with various parameters to see which were most effective. Because of shorter turnaround times for individual tests, the range of parameter tests could be expanded and therefore processing could proceed more quickly and accurately.

Implicit in the exploitation of CNSF for seismic imaging is the heavy use of graphics workstations to display and pick parameters from the data. COCORP programmers developed a number of display and picking tools for use on the IBM 5080 terminals linked to the supercomputer. The image datasets to be displayed require fast transfer rates from the central processing unit to the display device; thus, a key to the success of this mode of graphics was the fiber-optics link between remote terminals in Snee Hall (where the Department of Geological Sciences is located) and the central computer facility across campus.

As work with CNSF has progressed, it has also become clear that the most efficient approach to processing seismic data is to not rely on the supercomputers alone. For many of the display and some of the processing functions, the high-speed central units are unnecessary or even inappropriate. Modern graphics workstations can offload many of these functions and thus free up the supercomputers for tackling the truly intensive aspects of the seismic imaging process. Accordingly, COCORP has worked over the past six months to establish a hybrid computing environment consisting of graphics workstations, special tape support, and network links to CNSF.

Although software is still lacking to tie all of these elements together as effectively as we would like, the components are in place and contributing to our overall productivity. The CNSF mainframes are still the core workhorses for our current processing, but graphics workstations have taken over many of the display and interpretational aspects. In addition, the workstations play a critical role in teaching, providing access to user-friendly environments with fast (interactive) turnaround for small instructional datasets.

DEEP FLUIDS AND GIANT BASINS: TARGETS OF CURRENT STUDY

The full capabilities of this hybrid computational environment have proven crucial as COCORP has mounted its most ambitious experiments yet. Deep fluids and the roots of intracratonic basins were the targets as COCORP returned to the field in the summer of 1990 with two major new experiments (Figure 5).

The first, carried out in southeastern Georgia, included COCORP's first attempt to use shear waves to probe the deep crust. The objective was a bright spot that a previous COCORP transect of buried Appalachian structure had revealed fifteen kilometers beneath the Atlantic Coastal Plain (see Figures 6 and 7). It has been speculated that this feature, called the Surrency Bright Spot, represents mid-crustal fluids, perhaps emplaced by Appalachian overthrusting.

The Surrency experiment was the most complex COCORP had ever undertaken. In addition to three-component common-depth-point (CDP) profiles along the original COCORP line over the bright spot, the researchers collected a P- and S-wave expanding spread, a mini-crossline, and a sparse-grid 3-D dataset. The experiment was made possible by an arrangement with AMOCO to use their special P- and S-wave convertible vibrators, which have rotatable pads that allow them to "shake" in two perpendicular horizontal directions. Complementing these special sources was AMOCO's remote recording SGR system, which is operated by radio telemetry and

has some six hundred channels. This SGR "superchannel" system provided the flexibility needed to accommodate the complex geometries involved in the new experiments.

The AMOCO system also played a central role in COCORP's second field initiative: a regional, "ultradeep" survey across the center of the Williston Basin. This basin, a typical example of intracratonic subsidence, lies over a major Precambrian suture zone, the Trans-Hudson Orogen. The new surveys link with COCORP's previous profiles to the west to form an almost continuous traverse of the northwestern United States. It extends from the active subduction zone along the west coast of Washington and Oregon, across the craton, and into the Williston Basin of Montana and North Dakota.

A special aim in the Williston Basin experiment was to penetrate into the subcrustal lithosphere. Original plans called for the co-located use of explosives as well as Vibroseis sources. Explosives could not be used because of liability issues that arose at the last minute, but fortunately, the Vibroseis data alone revealed prominent lower-crustal and upper-mantle reflectors. The data were collected with the use of eight large vibrators (five were usually used in past COCORP surveys).

Although the main objective in the Williston survey was to obtain a regional CDP profile, the AMOCO system allowed collection of considerable auxiliary data, including mini-crosslines and widelines for 3-D control, and expanded spreads for greater velocity control at lower crustal depths. The CDP spread itself incorporates the largest offsets (15 kilometers) yet used for routine crustal profiling. The overall result was the most extensive and diverse dataset that COCORP has yet analyzed.

The design of these surveys and the use of the AMOCO system reflect a new level of technological innovation in COCORP exploration. The new computational demands of these acquisition efforts have been substantial, and they would not have been practical without the power at CNSF. For example, in the Surrency experiment, we obtained nine different seismic images—corresponding to the different shear components involved—rather than the single image usually obtained from simple acoustic waves. And in addition to conventional profiling, we were able to obtain three-dimensional imagery, providing a new view of the target structure—one that required not only the processing speed of the supercomputer, but the interpretational tools of a dedicated graphics workstation (Figure 7). The Department of Geological Sciences recently acquired such a workstation through a grant from the Landmark Corporation.

Figure 6

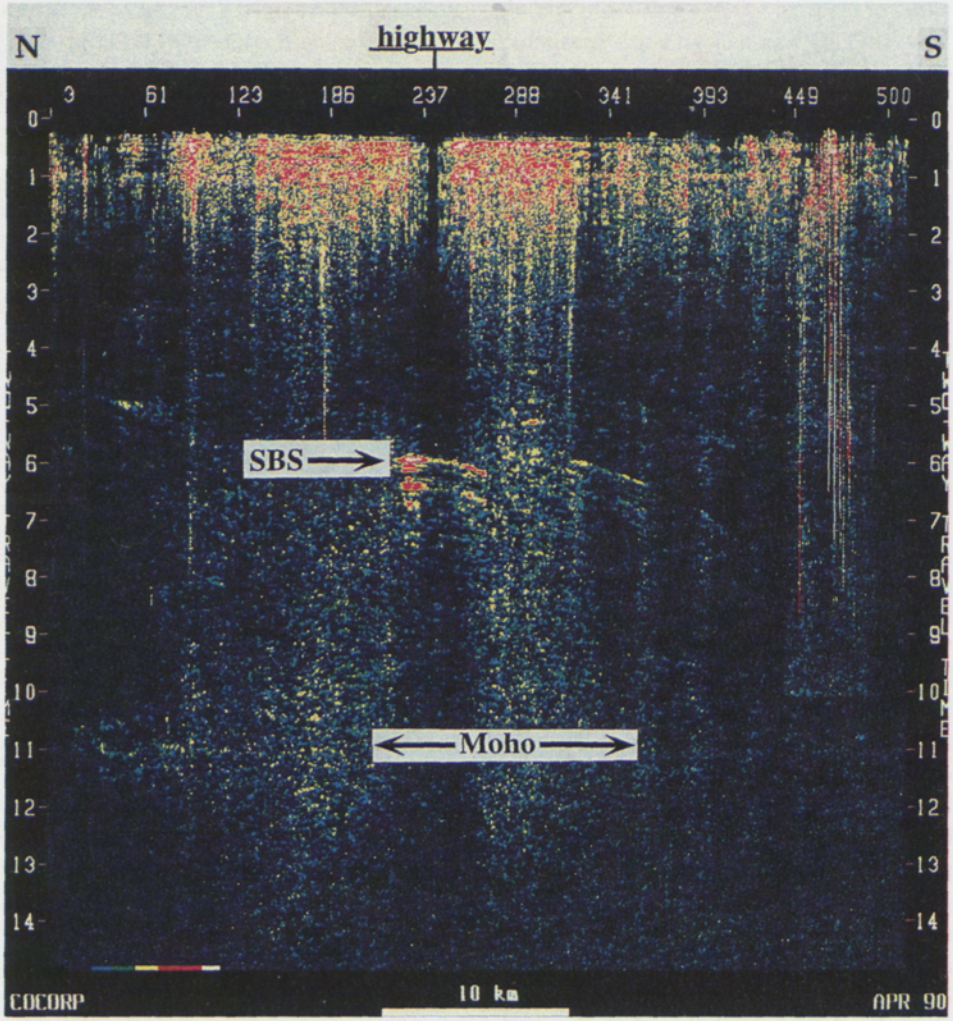

Figure 6. The Surrency Bright Spot (SBS), a region of unusually strong reflections that define a 15-kilometer-deep body thought to contain fluids. The bright spot was the target of a shear-wave and three-dimensional survey made last summer by COCORP. On this true-amplitude display, other reflections at depth are too weak to be seen. The horizontal patterns at the top correspond to the sedimentary layers of the Atlantic coastal plain. (Courtesy of Tom Pratt.)

Figure 7. An interpretation of the three-dimensional extent of the Surrency Bright Spot, executed on a Landmark Seismic Interpretation Workstation. The image, derived from analysis of seismic sections produced at the Cornell National Supercomputer Facility, was generated by graduate students Andrew Gatt and Joel Mondary.

Figure 8. A three-dimensional model of subsurface faults in the Alps. This was produced by graduate student Robert Litak using the Sierra modeling software on a graphics workstation.

Figure 7

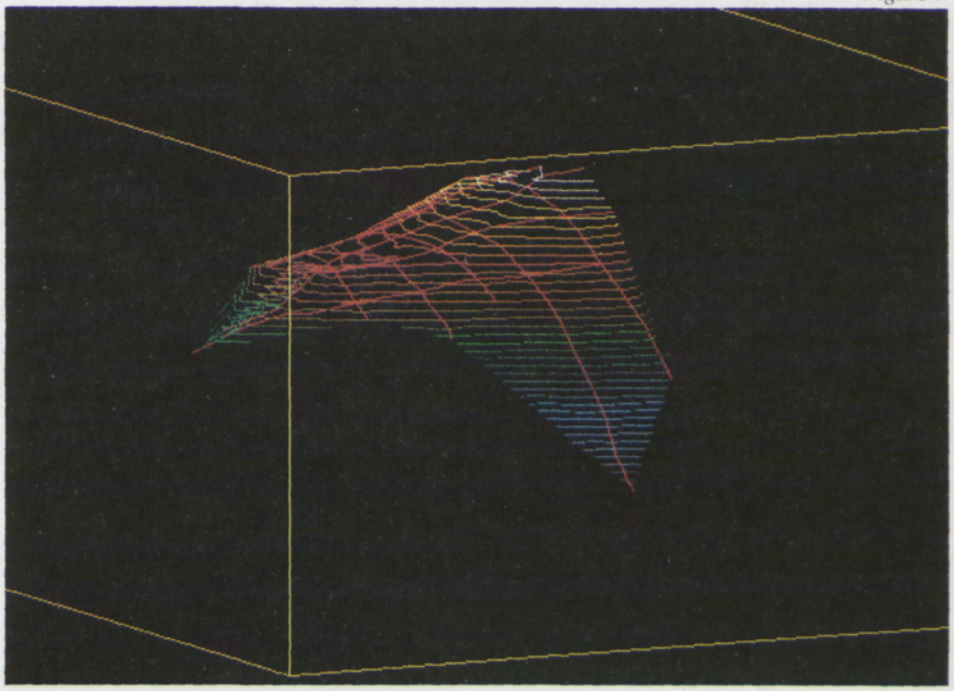

Figure 8

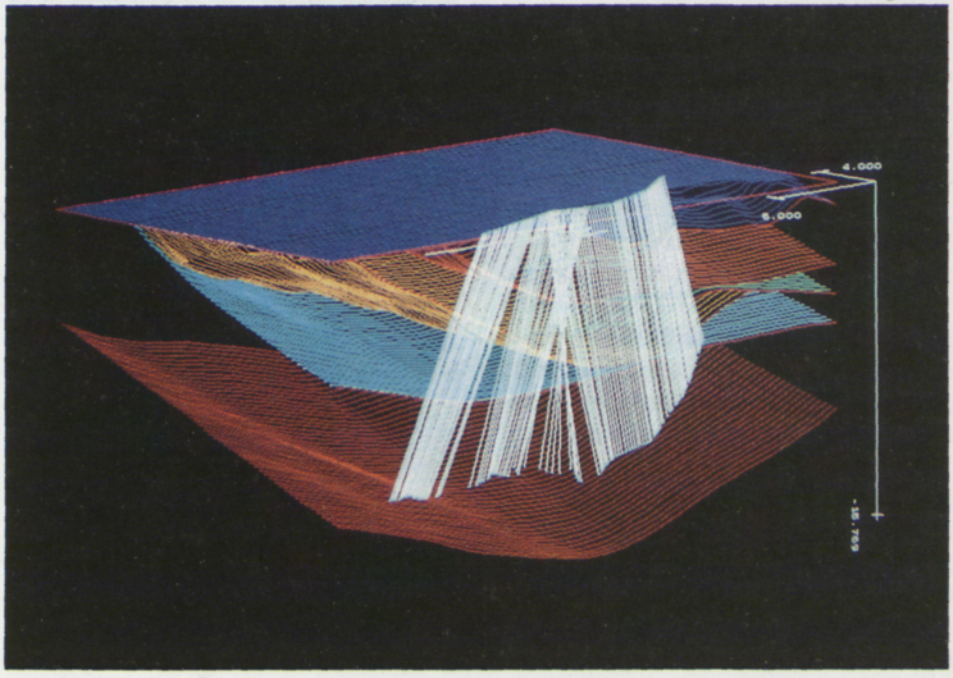

COCORP researchers are also investigating other datasets. In a joint program with the Universities of Geneva and Lausanne, COCORP is interpreting deep seismic results from the Alps and their implications for similar COCORP results in the United States. Computer modeling on a graphics workstation at Cornell (Figure 8) has proven very useful for understanding the three-dimensional structure revealed by seismic images produced at the Swiss supercomputer facility at Lausanne.

CNSF is also promoting deep seismic research in another way. A special high-speed link between CNSF and its sister supercomputer facility in Montpellier, France, has led to a new collaboration of geoscientists at these two institutions; they are involved in joint software development and analysis of results from the COCORP experiment over the bright spot.

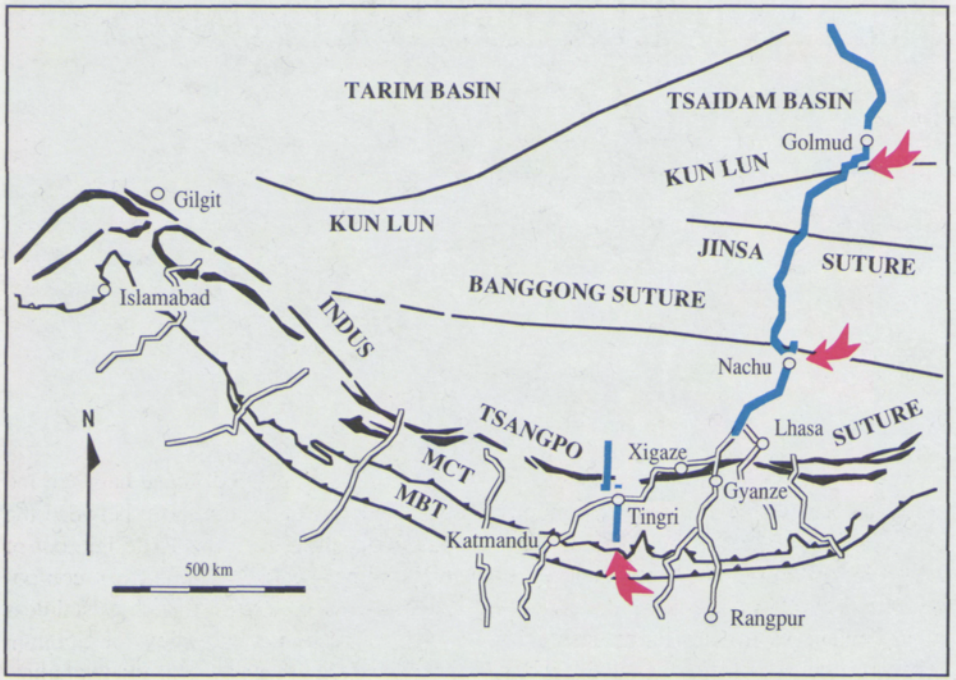

Figure 9. The location of a planned deep seismic survey (indicated by the blue lines) in Tibet. The arrows indicate possible sites for a pilot survey.

THE GLOBAL PERSPECTIVE OF COCORP RESEARCH

The international aspects of COCORP research emphasize the global nature of its purview. A quantitative synthesis of deep seismic data from around the world is needed, and toward this end COCORP has sought to assemble a comprehensive collection of deep seismic results. This collection, a major data resource, is kept in the tape library at CNSF and is available in digital form to researchers everywhere.

COCORP's global perspective is not limited, however, to mere compilation of available data from other projects in other countries. COCORP scientists are major participants in efforts to explore some of the critical geological terranes abroad. Currently, a Cornell-led consortium is mounting an effort to record a deep seismic reflection profile across the Himalayas and Tibet (Figure 9)—a region that is viewed by many geoscientists as the key to understanding continental evolution. A pilot study is planned for next year to probe the deep structure resulting from the collision and underthrusting of the Indian subcontinent beneath Tibet. If successful, this joint undertaking with Chinese scientists should lead to profiling across the entire India-Asia zone of continental collision.

Supercomputing power and special graphics workstations are critical for the analysis of data such as these, and essential for understanding the deep structure of our planet.

Larry D. Brown, a professor of geological sciences, first came to Cornell as a graduate student in 1973. He received the Ph.D. degree in 1976, continued at Cornell as a postdoctoral research associate, and joined the faculty in 1977. His undergraduate degree is from the Georgia Institute of Technology.

Brown has been a guest professor at the Institute for Geophysics at Christian Albrecht University in Kiel, Germany, and a visiting scientist at the Institute of Geophysics of the University of Lausanne, Switzerland, and at the Bureau of Mineral Resources in Canberra, Australia. In 1981 he received the ARCO Outstanding Junior Faculty Award.

He is a member of the American Geophysical Union, the Geological Society of America, the Society of Exploration Geophysicists, the European Union of Geosciences, and the European Geophysical Society.

He serves on two committees—on strategic users and on national policy—of the Cornell National Supercomputer Facility.

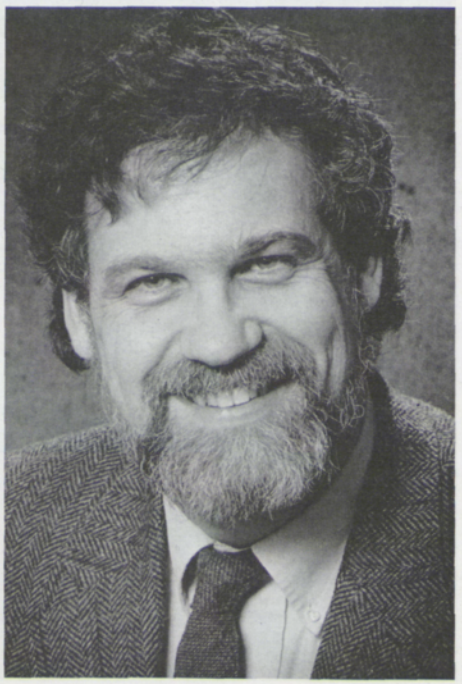

MECHANICS AND SUPERCOMPUTING IN HUMAN JOINT REPLACEMENT

by Donald L. Bartel

Damaged human joints such as hips and knees are now commonly replaced with orthopaedic structures that include both of the articulating surfaces. These replacements are remarkably successful—most of them last for the lifetime of the patient—because of advances that have been made during the past two decades through collaboration between surgeons and engineers. Our research group at Cornell has had a role in the extraordinary success of implant surgery today, and even better results are on the way.

Our program is a joint effort of researchers in mechanical engineering on the Ithaca campus, and colleagues in the Department of Biomechanics at the Hospital for Special Surgery (the orthopaedic affiliate of the Cornell Medical College) in New York City. Those at the engineering college who are active in the program include Professor Dean L. Taylor and his students.

Our work in Ithaca is mainly on the structural problems associated with joint replacement. The analysis of these structures presents formidable challenges because the problems are highly nonlinear and because accurate representations of complex geometry and material properties are required. We construct "customized" structural models using our graphics data base and special software, plus computerized tomography (CT) scans of particular joints to be replaced. Also, we use computer-based analysis to better understand and predict the behavior of bone-implant systems. For the extensive calculations that are necessary in all this work, we rely on the Cornell National Supercomputer Facility.

THE DESIGN AND IMPLANTATION OF JOINT REPLACEMENTS

In joint replacement surgery, the goals are to relieve pain and to restore the function of joints that have been damaged by disease, trauma, or long-term wear and tear. This can be achieved through design that assures proper fit of the implant and that incorporates features to make the implant do the work of missing ligaments or other joint structures. For long-lasting benefit, long-term changes in the bone-implant system need to be taken into account.

In the orthopaedic procedure, both of the articulating surfaces are replaced. For example, in a total hip replacement both the ball portion of the joint (the femoral head) on the femur and the socket (acetabulum) in the pelvis are replaced. In the knee, two pairs of surfaces are implanted: those between the tibia and the femur and those between the patella and the femur. In most designs one of the surfaces—usually the convex component—is made of a metal such as stainless steel, chromium-cobalt alloy, or titanium alloy, and the other surface is made of ultra-high-molecular-weight polyethylene. This combination was first used in total hip replacements to minimize wear and to provide low-friction contact.

Some of the prosthetic components are surface replacements and some replace an entire structure (see Figure 1). For example, hip sockets and the three components used in a total knee replacement are surface replacements; the surgical procedure is to remove a relatively thin layer of bone and replace it with the prosthetic component. But in the total hip replacement procedure, the entire femoral head is replaced; the new femoral head is attached to a metal stem that extends into the medullary cavity to fix the head to the femur. The components of most prosthetic elbow joints are also attached to bone with fixation stems. In a prosthetic shoulder joint, the humeral component is fixed with a stem, but the glenoid component (the shallow socket) is a surface replacement.

Figure 1

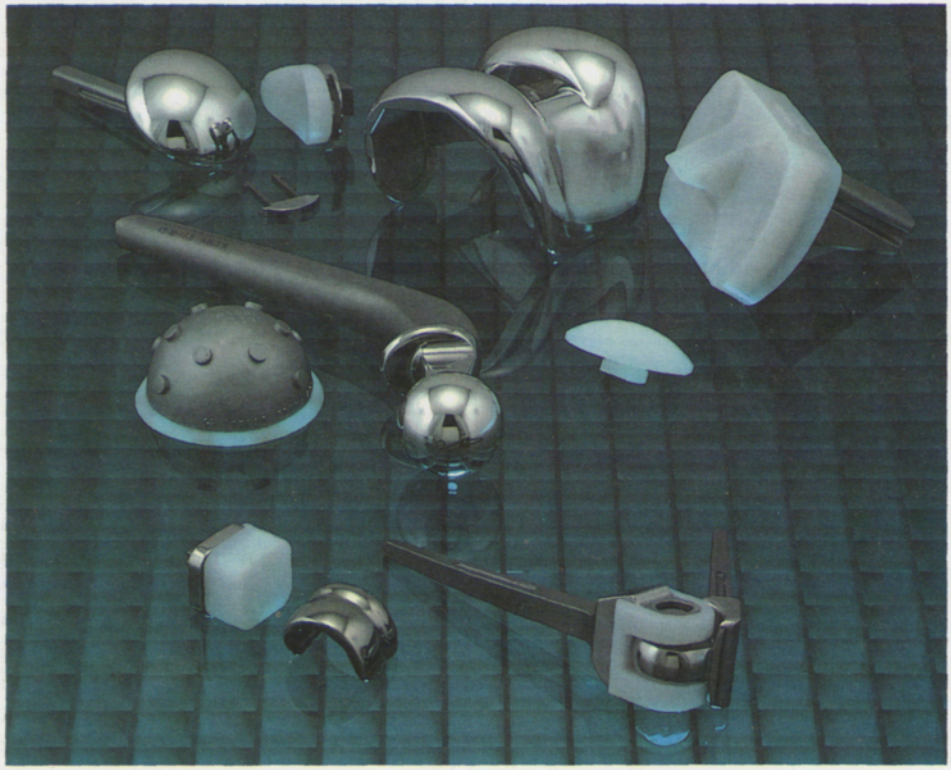

Figure 1. Typical total joint replacements, consisting of metal and polyethylene articulating surfaces. Clockwise from the upper left are shoulder, knee, elbow, great toe, and total hip replacements.

THE MECHANICS OF JOINT REPLACEMENT

Joints provide relative motion between bones and transfer loads. In many machines, moving parts and the movement of loads can be considered independently, but in human and animal joints the loads transferred across the joint and the kinematics of the joint are intimately coupled. If one is changed, the other will also change.

When prosthetic components are attached to bone, a new composite consisting of the bone, the implant, and the interface layer is formed. This structure must remain intact for a long time, it must be able to transmit loads from the joint to the supporting bone in a predictable, reliable way, and, ideally, it should produce stresses in the bone that are as close to normal as possible.

Approximating the normal stresses is important because bone has the property of remodeling according to the stresses applied to it. If the stresses in a particular region of the bone are drastically reduced because of the presence of the implant, the properties of the bone may change and its volume may be reduced in that region. Such changes in bone geometry and material properties may put the composite structure at risk and may make more difficult any revision surgery that becomes needed later on.

Components may be attached to bone in several ways. In one method, a layer of bone cement (polymethylmethacrylate) is used to fill the space between the prosthesis and the bone. Bone cement has the same chemistry as Plexiglas and is polymerized in situ. It is not an adhesive; good fixation of the device with respect to the bone requires mechanical interlock between the cement and the device and between the cement and the bone.

A second method is to fix the device to the bone by using some means of biologic fixation. The most common procedure is to apply a porous layer to the part of the prosthesis surface where fixation is desired; if contact occurs between the porous layer and the bone and if the relative motion between the layer and the bone is small enough, bone tissue can grow into the porous layer. This provides both fixation and load transfer from the device to the bone.

A third technique is to simply press fit the device into the bone without cement or biologic fixation. In such a case the prosthesis must closely match a cavity in the bone that has been prepared by the surgeon, and it must be designed so that load transfer from the device to the bone can be achieved without undue relative motion.

CURRENT GOALS IN THE CORNELL PROGRAM

The extraordinary success rate of total joint replacement today is due to improvements that have been made in functional design, in the methods used for fixation, and in the metals and polymers used in the components of the prostheses. But further improvements need to be made.

The Program in Biomechanical Engineering that is carried out by Cornell and the Hospital for Special Surgery has two specific goals at the present time: (1) to improve the fixation of femoral components for total hip

"These replacements are remarkably successful . . . because of advances made during the past two decades through collaboration between surgeons and engineers."

replacement, and (2) to design polyethylene components so as to minimize the surface damage that occurs in the long term.

Because the femoral component for total hip replacement is not a surface replacement, joint loads are transferred to the femur in a way that is quite different from what occurs normally. The load on the femoral head is large—about three times body weight during normal gait—and is transferred through the fixation stem and interface layer to the inside surface of the medullary cavity. The best configuration for the fixation stem and the best means for fixing the stem to the bone are still matters of controversy. A thorough understanding of the composite structure and the role that the interface characteristics play in load transfer is essential for the evaluation and development of new design concepts.

Damage to the articulating surfaces has been identified as possibly the most important long-term problem in total joint arthroplasty today. Debris that is released from the surface as a result of abrasion, pitting, and delamination migrates to surrounding tissue, and when sufficient particles have accumulated, biological reactions are triggered. These reactions release agents that can attack the bone near the implant. Infection and loosening of the device that occur long after a joint has been implanted have been associated with these reactions to accumulated debris.

A troubling observation, based on analysis of retrieved prostheses, is that surface damage increases with time and with the activity of the patient. This problem is intensified by the fact that improvements in fixation and function have meant that total joint replacements are being used more vigorously over longer periods of time. It is essential, therefore, that we determine the mechanisms responsible for the generation of the debris, and find materials and designs that minimize them.

PROBLEMS IN ANALYZING BONE-PROSTHESIS STRUCTURE

Analysis of the prosthetic and bone structures in total joint replacements presents formidable challenges.

First, the problems are highly nonlinear. For example, when bone cement is used in the operating room, there is little if any chemical adhesion between the device and the cement or between the cement and the bone. Interface strength depends entirely upon mechanical interlock. Consequently, with a relatively smooth fixation stem, load can be transferred only by compression across the interface or by friction between the contacting surfaces; tensile loads cannot be transferred. What this means for the analyst is that a nonlinear contact problem must be solved to determine the regions of contact between prosthesis and cement, and the magnitudes of the contact stresses.

Similar situations occur if no cement is used. For example, when prostheses that have regions of porous coating for bone ingrowth are implanted, loads may be transmitted by compression or tension if bone ingrowth has occurred. In the absence of bone ingrowth, loads may be transmitted by compression and friction where the porous layer exists, provided that separation of the prosthesis and the bone has not occurred in that region. But the portion of the surface without porous coating is smooth, and only compressive contact forces can be transferred across the interface because the frictional force between the device and the bone will be very small. Therefore, to understand the mechanics of fixation without cement, the resulting nonlinear contact problem must be solved for a variety of interface conditions.

Figure 2

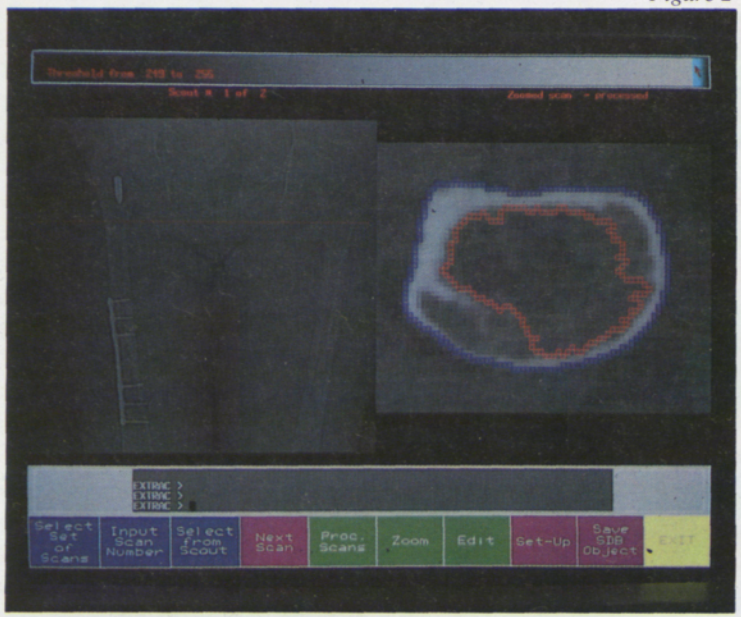

Figure 3

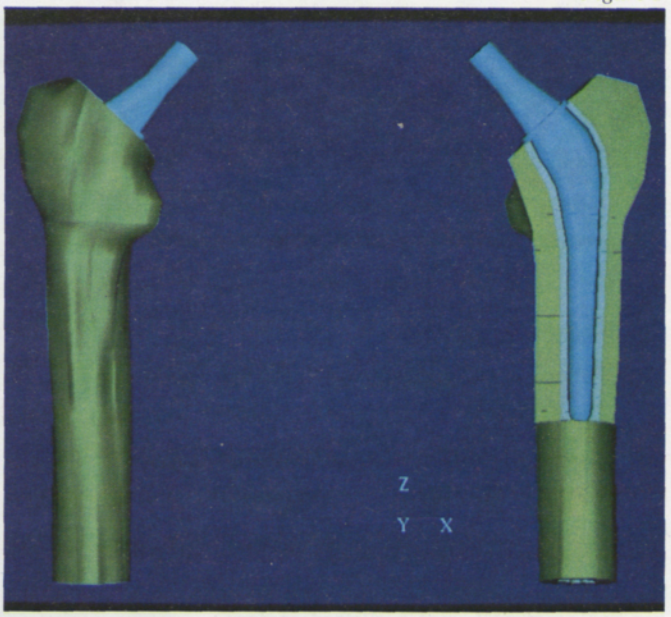

Figure 4

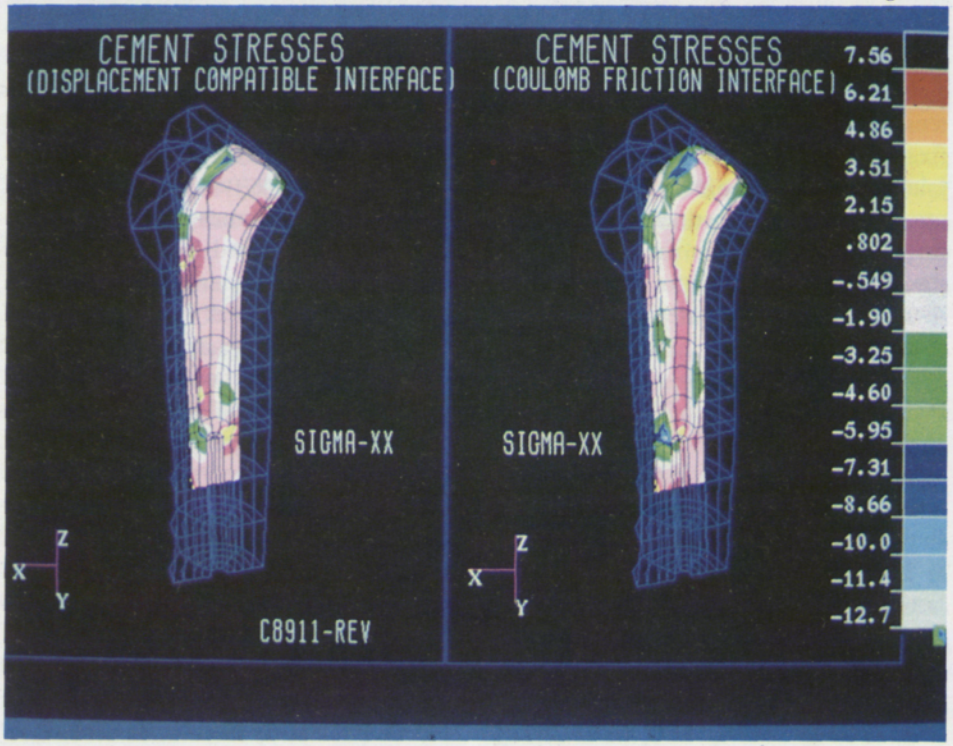

Figure 2. Computer imaging of a femur. Geometry and material properties are determined from clinical CT scans. The red horizontal line on the scout view at left defines the location of the cross section shown on the right. The red and blue contours on the cross section are the inner and outer boundaries of the bone.

Figure 3. The geometry of implant and interface layer for the proximal femur with a prosthesis in place. The interface layer (in this case bone cement) is seen as the thin white region.

These images were created with commercially available software; with interactive software developed at Cornell, the implant may be positioned with respect to the bone. This section view is for visualization only; a three-dimensional model is used for the structural analysis.

Figure 4. Modeled stresses in a cemented femur implant. The stresses are much higher when realistic interface characteristics are modeled at the stem-cement interface (right) than when the cement is considered to be perfectly bonded. The high stresses shown in proximal cement are hoop stresses; this is consistent with observed cement cracking and failure.

Nonlinear contact also occurs between the metal and the polyethylene components of a total joint replacement. As the load changes between nonconforming surfaces, so does the area of contact, and as a result, those stresses in the polyethylene component that are associated with surface damage are not directly proportional to changes in loading across the joint. Furthermore, the stress-deformation relationship for polyethylene is also nonlinear.

To add to the complexity of the problem, the material properties of a polyethylene component are changed when the component is sterilized by radiation and undergo further changes after implantation due to the chemical environment of the body and the loading on the joint during normal function.

These changes occur nonuniformly throughout the volume of the component. For example, the degradation of material properties that is the result of radiation or oxidative processes is greatest at the surface, but changes in material properties that are the result of loading are greatest at some distance beneath the articulating surface for components, such as total knee replacements, where the contact is nonconforming.

The analysis of prosthesis fixation also requires accurate representations of both the complex geometry of the bone and its material properties. A bone (the structure) consists of two types of bone tissue (the material). Cortical or compact bone, found in the shafts of long bones such as the femur, is the most dense bone tissue. Cancellous or trabecular bone, found at the ends of the bones near the joints, is much less dense than cortical bone and is itself a structure, consisting of small plates and beams organized to transfer load efficiently from joint surfaces and from muscle and ligament attachments to the more dense cortical bone.

The material properties of both cortical and cancellous bone tissue vary from point to point in a bone such as the femur. The elastic modulus is related to approximately the cube of the apparent density of the tissue. Consequently, within the complex geometrical shape of a bone there are wide variations in elastic modulus throughout the volume.

HOW WE CUSTOM DESIGN BONE-IMPLANT SYSTEMS

We determine the geometry and material properties of bones using clinical data and software that has been developed in our computational laboratory.

A program called EXTRACT is used to determine the inner and outer geometry of the patient's bone, and the distribution of material properties within the bone, from computerized tomography (CT) scans of a patient or of a bone specimen (Figure 2).

Images showing the geometry and material properties of an implant and the interface layer between the implant and the bone (Figure 3) are created using commercially available software for generating a finite-element mesh. This is translated to our graphics data base and, using interactive graphics, is combined with an image of the bone in a three-dimensional representation. The device is positioned with respect to the bone, and when this is achieved satisfactorily, the commands necessary to create a consistent finite-element mesh of the bone are automatically generated in the software. The material properties of each element in the finite-element mesh of the bone are then assigned. This is done by means of a program called PSORT, which uses the material-property distributions determined in EXTRACT. Finite-element models of polyethylene components that are loaded by contact with metal components are developed with use of conventional procedures and commercially available software.

The resulting nonlinear structural models are very large and computationally expensive. We use a finite-element analysis program, GNOME, which was developed by structural engineering specialists in Cornell's School of Civil and Environmental Engineering, and we use the Cornell supercomputer facility to do the computation. GNOME enables us to model the variety of conditions that can occur at the interfaces between the structural components of a total joint replacement.

UNDERSTANDING AND PREDICTING THE BEHAVIOR OF IMPLANTS

These computing capabilities have enabled us to determine characteristics of bone-implant systems that now make it possible to explain clinical observations and predict the behavior of new implant designs.

Consider, for example, an uncemented femoral component of a total hip replacement. Previously it was not possible to predict where the initial contact between the device and the bone occurs, or how that contact changes when a load is transferred across the hip joint. Our results have shown that these situations can be quite different. Now it is possible to include this important information as part of the design process.

When a femoral component is cemented, we can realistically model the cement-device interface as a no-tension bond with coulomb friction when the surfaces are in contact and there is compression across the interface. And we can predict where the interface will separate and where it will be in contact after the joint is loaded. The stresses in the cement are quite different when the bonding is considered to be perfect and when realistic conditions are modeled (Figure 4). The results of our studies have explained why certain devices loosen less frequently than others, and our capabilities are now being

used to design the next generation of cemented implants.

Through the use of our software and the supercomputer, we have also gained new understanding of the mechanisms of damage and debris generation in polyethylene components for total joint replacements.

For example, in studies of total knee replacements, our analyses indicate several conditions that are consistent with damage observed in polyethylene components retrieved during revision surgery. The modeling shows large tensile stresses at the edge of tibial components that are thin and have poor conformity with the mating metal component; retrieved components frequently have cracks in this region. Another prediction is that large maximum shear stresses occur beneath the surface under the area of contact; this is consistent with the delamination and pitting that has been observed in retrieved polyethylene components.

This ability to model the contact between metal and polyethylene components provides a powerful design tool. It is being used, along with studies of material behavior, to design polyethylene components with decreased risk of surface damage. This, in turn, decreases the risk of long-term problems such as infection and loosening.

But although we have made considerable progress in understanding and predicting the behavior of bone-implant systems, there is still much to be done. As I have mentioned, bone remodels in the presence of an implant, altering properties and geometry as the loads on the bone change with time. To completely understand the long-term performance of total joint replacements, our analyses will have to incorporate these future changes in the bone, in addition to conditions at the bone-device interface at the time of implantation.

Such analyses will require many iterations of what is already an expensive computational process. Large numbers of iterations with expensive structural analyses at each step will also be necessary for determining optimal designs of bone-implant systems. Consequently, the simulation of bone remodeling and the optimal design of implant systems may be feasible only if parallel computational procedures (in which several parts of a computation are carried out simultaneously on a supercomputer) are implemented to make the calculations possible in a reasonable amount of time.

The implications for our research program are clear. In order to continue improving our understanding of the mechanics of bone-implant systems and realize further improvements in prosthesis design, we will increasingly depend on the availability of large, fast computers and on collaborations with organizations such as the Cornell Theory Center.

Donald L. Bartel holds a joint appointment as a professor in the Sibley School of Mechanical and Aerospace Engineering at Cornell and as a senior scientist in the Department of Biomechanics of the Hospital for Special Surgery in New York City. This hospital is the orthopaedic affiliate of Cornell's Medical College.

Bartel has been affiliated with the hospital since 1976, when he served as a visiting scientist there. In 1977 he became director of the Cornell–Hospital for Special Surgery Program in Biomechanical Engineering. He has also worked in the area of animal orthopaedics in cooperative programs with the New York State College of Veterinary Medicine at Cornell.

He joined the Cornell faculty in 1969 after receiving a Ph.D. from the University of Iowa. He earned B.S. and M.S. degrees from the University of Illinois at Urbana and taught at Black Hawk Junior College in Moline, Illinois, for two years before beginning his doctoral studies in mechanics and hydraulics. In 1976–77 he was a Guggenheim fellow and visiting scientist in the Department of Orthopaedics at the Mayo Clinic.

MOLECULAR SIMULATION USING SUPERCOMPUTERS:

Techniques for Predicting Fluid Properties

by Keith E. Gubbins and John M. Walsh

Statistical mechanics provides exact equations for the prediction of the properties of fluids and solids. But unfortunately, these equations can be solved analytically in only a few rather simple cases, such as an ideal gas, a real gas at pressures up to a few tens of bars, a gas thinly adsorbed on a solid, or the thermodynamic properties of a perfectly crystalline solid. For many problems of practical interest, one must resort to approximations of uncertain accuracy in order to obtain a solution of the equations, and for other problems no approximations have yet been found.

An alternative approach is to use molecular simulation, in which the statistical mechanical equations are solved for the model system of interest by numerical methods using a powerful computer. Before the late 1970s, very few university researchers in the United States had access to sufficiently powerful machines, but as supercomputers and powerful workstations have become available in the past few years, there has been a rapid expansion in the use of molecular simulation. Both academic and industrial chemical engineers are finding applications in a wide range of scientific and technological problems.

THE TWO COMMON METHODS FOR MOLECULAR SIMULATION

Two methods are in common use—the Monte Carlo (MC) and the molecular dynamics (MD) techniques (Figure 1). In both cases, the computer must be provided with a molecular model, including an equation for the intermolecular forces. Also needed is information about the initial state of the molecules and details of the geometry of any surfaces.

The Monte Carlo (MC) method makes use of a random-number generator to move the molecules randomly. The various molecular arrangements that are generated are accepted or rejected by means of an algorithm that determines whether or not they appear with the correct probabilities. As statistical mechanics tells us, the probability of a particular arrangement, at a fixed temperature and density, is proportional to $\exp(-U/kT)$, where U is the total energy of the collection of molecules, k is the Boltzmann constant, and T is the temperature. After a long series of acceptable arrangements is generated, one can average over them to obtain the various equilibrium properties of the system of molecules.

In the molecular dynamics (MD) method, the molecules are allowed to move naturally under the influence of their own intermolecular forces. The positions and velocities of each molecule are followed in time by solving Newton's equation of motion (force equals mass times acceleration, a second-order differential equation) using standard numerical methods. The macroscopic properties are calculated by averaging the appropriate function of molecular positions and velocities over time.

These two techniques have several features in common. Provided that the simulation runs are carried on long enough, and that the number of molecules is sufficiently large, we should get highly accurate results for a precisely defined model system. In practice, the results are limited by the speed and storage capacity of current supercomputers. Typically, the number of molecules in the simulation sample can range up to a few thousand or tens of thousands, and the real time simulated in MD is of the order of a nanosecond. In order to minimize boundary effects in such small samples, it is customary to use periodic-boundary conditions—that is, the sample is surrounded on all sides by replicas of itself, so that when a molecule moves

Figure 1

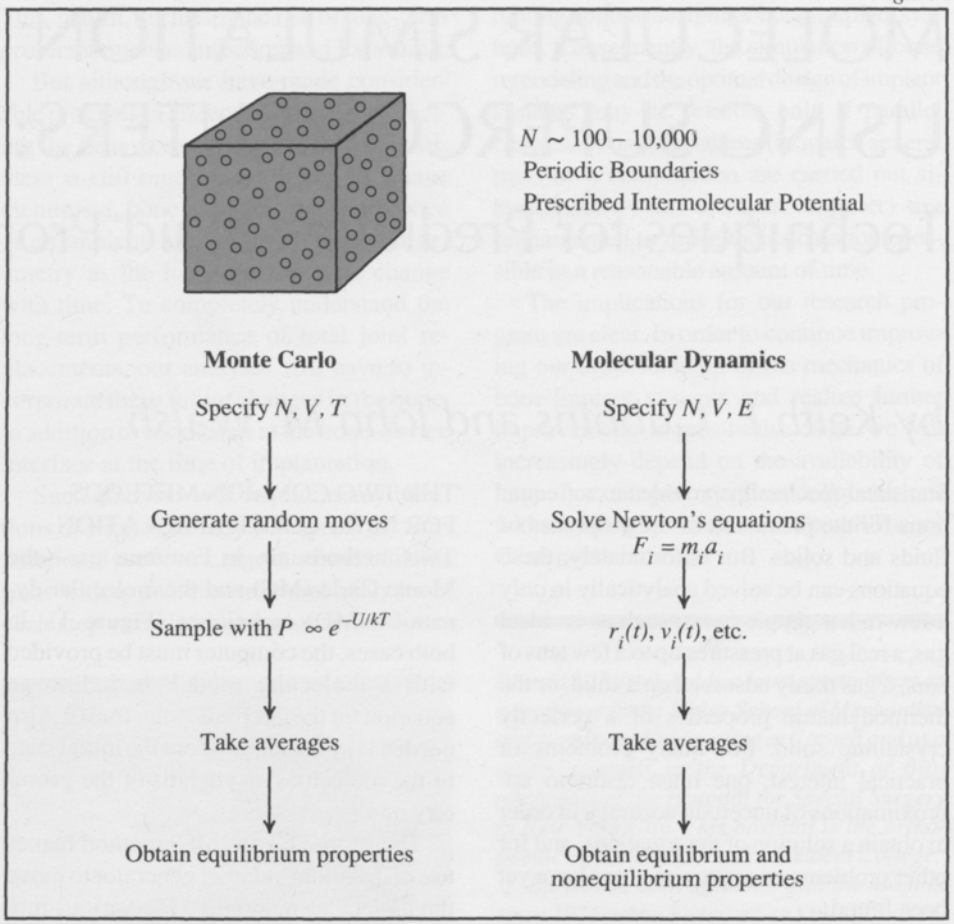

Figure 1. Two methods of molecular simulation. Typically, both treat a sample of N *molecules in a box of volume* V *(shown here as a cube).*

In the Monte Carlo method it is common, but not necessary, to choose N, V, *and temperature* T *as the independent variables, and to keep these fixed during the simulation. Molecules are moved randomly, generating a new molecular arrangement with the intermolecular potential energy* U. *These new arrangements are accepted or rejected in such a way that those accepted occur with the probability distribution that is required by the laws of statistical mechanics.*

In molecular dynamics the energy E, *rather than the temperature* T, *is fixed. The molecular positions* r_i *and the velocities* v_i *(and also orientations and angular velocities) for each molecule* i *are followed in time.*

(This figure originally appeared in the Summer 1988 issue of this magazine.)

through a boundary and so out of the sample, it is automatically replaced by a molecule moving into the sample through the opposite face of the box. (Anyone who has played Pacman, Asteroids, or similar video games is familiar with this periodic-boundaries trick.) Although molecular simulation can be successfully applied to a wide range of problems, difficulties can arise with some applications because of storage or speed limitations. Examples are ionic fluids (plasmas, electrolytes, etc.), in which the range of the intermolecular forces is very large, necessitating a large number of molecules; substances very near critical points and some surface phenomena, in which long-range fluctuations occur; and long-time phenomena.

There are also some significant differences between the MC and MD methods. MC is easy to program and can be easily adapted to different sets of conditions, such as mixture studies at constant pressure or adsorption at constant chemical potential. MD is more difficult to program, and since energy must be conserved, it is less easily adapted to different conditions. However, MD has two important advantages over MC: it can be used to study time-dependent phenomena and transport processes, and the molecular motions can be observed and photographed easily using computer graphics.

At Cornell an active program in which these techniques are applied to problems of interest in chemical engineering has been in progress since 1976. The applications have included studies of fluid droplets, fluids in porous materials, phase equilibria in liquid mixtures, ionic and associating liquids, liquid crystals, colloids and surfactants, and a variety of surface phenomena.

Calculations are carried out at the Cornell National Supercomputer Facility or at one of the other national supercomputer centers. (A typical MC or MD run takes a few hours or more on the Cornell supercomputer.) Advanced computer-graphics methods are used to observe molecular motions, behavior near surfaces, polymerization, and other phenomena. The potential of molecular simulation as a tool has expanded rapidly with improvements in speed and availability of supercomputers, and these trends are expected to continue for the next decade.

MONTE CARLO SIMULATION FOR STUDIES OF COMPLEX FLUIDS

In simple fluids the intermolecular forces include strong repulsions at short intermolecular distances (because of electron overlap) and weak attractive forces at larger separations. These weak attractive forces are van der Waals (also called dispersion or London forces) and multipole forces. Examples of such fluids are simple hydrocarbons (such as methane and benzene), carbon dioxide, nitrogen, and oxygen, that have intermolecular energies of the order of 1 kilojoule (kJ) per mole. Accurate statistical mechanical theories and semiempirical equations of state are available for such fluids, and chemical process equipment for handling them can be designed with confidence.

Complex fluids, though, cannot be represented so easily because of the presence of strong attractive forces that are highly directional. These forces, mostly electrostatic in nature, give rise to aggregates including dimers, trimers, and larger oligomeric species, and in some cases, to branched or network structures. Water is the most familiar of these complex, or associating, fluids. Its high boiling point, high dielectric constant, and strong solvent power all derive from the strong associative forces between its molecules.

Many other fluids, including the alcohols, organic acids, and amines, are also complex by virtue of molecular association. At high enough concentrations in water, long-chain fatty acids form droplike aggregates called micelles. Among the many other complex compounds in aqueous solution are the proteins and their building blocks, the amino acids. The binding sites of proteins consist of groups of atoms with strong, associative interactions, and in addition, proteins have many intramolecular interactions which give them a folded structure that exposes the active binding sites.

The associative interactions of water, alcohols, acids, amines, and proteins are referred to as hydrogen bonds. In other cases the interaction may involve weak chemical reaction or charge transfer between two molecules of different species. (Charge transfer occurs between many aromatic species—for example, between trinitrobenzene and mesitylene.)

These associative cohesive energies are in the range of 10 to 50 kJ per mole—up to fifty times greater than the energies of physical interactions in simple fluids, but weaker than most chemical bonding energies, which are typically 300 to 500 kJ per mole. The lifetime of an associated complex is roughly between 10 picoseconds (10×10^{-12} second) and 1 microsecond (10^{-6} second)—relatively long on a molecular time scale, but relatively short on a macroscopic time scale. Thus, the aggregates are not nearly as stable as distinct chemical species, but are easily observed by a variety of spectroscopic methods.

From the standpoint of statistical mechanics, complex fluids are a major chal-

"The potential of molecular simulation as a tool has expanded rapidly with improvements in speed and availability of supercomputers. . . ."

Figure 2a

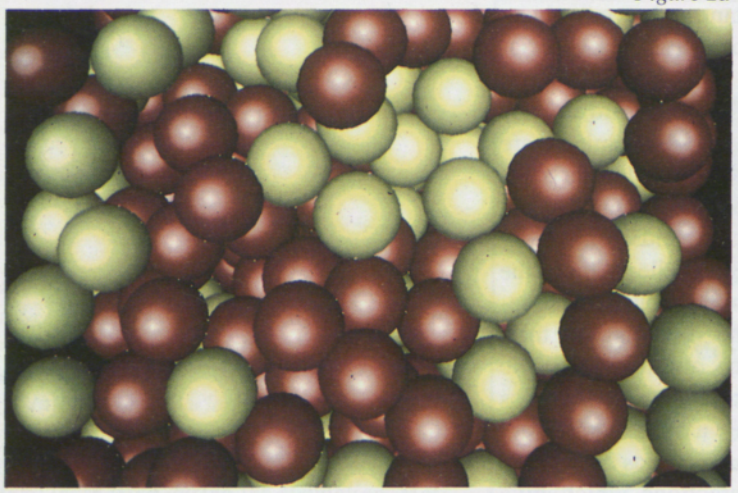

Figure 2b

Figure 2. "Snapshots" of a hydrogen-bonding fluid studied with use of the Monte Carlo (MC) simulation.

In Figure 2a the molecules that are hydrogen-bonded to their neighbors are shown in red. The monomers (molecules that are not hydrogen-bonded) are shown in green. During a simulation, hydrogen bonds are continually forming and breaking. Since each molecule has two hydrogen-bonding sites, it is possible for long winding chains of hydrogen-bonded molecules to form.

Figure 2b shows the same molecular configuration, but with the molecular diameters reduced to one-fifth their normal size. A red bond has been drawn between hydrogen-bonded molecules. To more clearly show the longer chains, bonds between dimers are not shown.

lenge. In simple fluids, attractive interactions are treated accurately as a weak perturbation. In complex fluids, the associative forces are too strong to be treated as a perturbation and are too weak to be treated as a permanent bonding force that might lead to stable chemical species.

The goal of our work is to develop a first-principles approach to the statistical mechanics of associating fluids. In a first-principles approach, the intermolecular forces are assigned, usually on the basis of ab initio quantum calculations. Statistical mechanics and computer simulation are then used to predict the liquid structure, equation of state, concentrations of monomeric and associated species, and other thermodynamic and transport properties.

We have carried out Monte Carlo computer simulation studies of molecules that have idealized association sites. The molecules are spherical and have one or more small spherical association sites. A molecule with two association sites corresponds to an alcohol that can form dimers, trimers, and long chains of associated molecules.

In Figure 2 we show "snapshots" of such a fluid, obtained by simulation. Images such as these are very useful in developing a mental picture, on a molecular scale, of the organization and structure of an associating fluid.

Such simulations are particularly helpful in developing and testing new statistical mechanical theories for complex fluids. Since the theory and simulation results are for the same molecular model, their comparison gives a direct and unambiguous test of the approximations in the theory itself. Recently, such tests have shown that a new theory of ours for the thermodynamic properties of associating fluids is highly accurate.

In order to use the theory to predict the behavior of actual complex fluids, suitable intermolecular-force models are needed. One of the mixtures we have been interested in is that of methanol with water; this is of importance in the gas industry, which uses methanol to inhibit the formation of gas hydrates in pipelines. In their pure states, both methanol and water have strong association interactions. Methanol has two association sites and water has four (Figure 3). In addition, there is a cross interaction between the two compounds, since methanol and water can associate with each other. Figure 4 shows the pressure-composition diagram for this mixture, along with the theoretical results. While there is good agreement between the measured properties and the theory, it should be noted

Figure 3

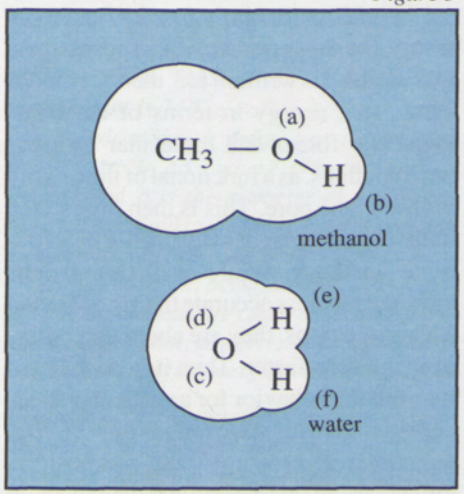

Figure 3. Models of methanol and water molecules shown with their hydrogen-bonding sites. Methanol has two sites (a, b) and water has four (c, d, e, f). In a mixture of methanol and water there is cross interaction between the sites on methanol with those on water.

Figure 4. Pressure versus composition for the mixture methanol/water at T = 338 K. The theory shows good agreement with the experimental results.

The phase envelope extends across the entire range of composition. Above this envelope (higher pressures) the mixture exists as a liquid; below, the mixture is a gas. At any point within the envelope there will be gas in equilibrium with liquid.

A particular point (a) with overall composition of roughly 0.5 mole fraction of methanol is shown as an example. The liquid composition is indicated on the abscissa as b, and the gas composition in equilibrium with this liquid is indicated as c. For this point, the gas phase is richer in methanol than is the liquid phase.

Figure 4

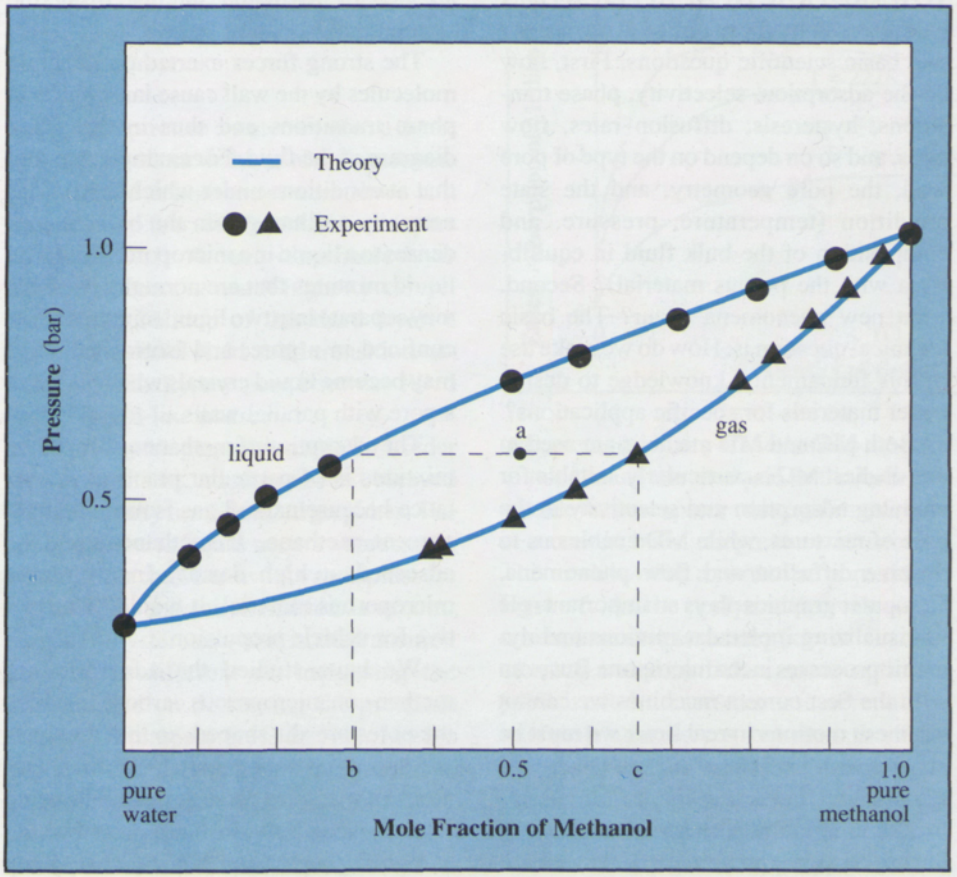

that some spectroscopic or other data are needed to develop the equation for the cross-intermolecular interaction. Nevertheless, the good agreement between theory and measured properties is encouraging, and suggests that in the future it will be possible to predict accurately the properties of associated fluids.

FLUID BEHAVIOR IN SMALL PORES

In microporous materials—in which pore size is below 20–30 angstroms (Å)—adsorbed fluids show unusual and interesting properties that are important in many industrial and natural processes. Such materials include silica gel, zeolites, porous oxides, and pillared clays.

The properties of interest include preferential adsorption of certain fluid components, chemisorption at particular sites, hysteresis effects, and a variety of unusual phase transitions, including capillary condensation, wetting and prewetting phenomena, layering transitions, and two-dimensional solid melting. For very small pores, the behavior becomes characteristic

"If methane could be adsorbed at high density in a suitable microporous material, it would be attractive for vehicle propulsion."

of one-dimensional (cyclindrical geometry, no phase transitions) or two-dimensional (parallel wall geometry) systems.

An understanding of these and related phenomena is needed for dealing with industrial applications such as ultrafiltration, catalysis, drying, chromatography, ion exchange, and the use of adsorbents for separation and purification, and for understanding such processes as frost heaving and the behavior of fuel gases in coal and other deposits. These phenomena are also important in many biological applications.

The design of industrial processes involving porous materials is almost entirely empirical at the present time, and in many cases the structure of the porous material (pore sizes and shapes, interconnectivity, porosity, etc.) is poorly characterized. Such theory as is used is generally based on hydrodynamic or thermodynamic (Kelvin, Laplace, etc.) equations; and this approach is known to fail for small pores. It is desirable to replace these empirical approaches with ones that are molecular in nature. By combining soundly based molecular theory and computer simulation with appropriate experiments, it should be possible to develop a detailed understanding of pore-fluid systems at the molecular level, and from this to design optimal advanced materials for specific processes.

Some progress toward this end has been made over the past few years. One advance is the development of theories and computer simulation methods that provide a detailed molecular picture of the behavior of fluids inside micropores. Another is the development of ways of preparing materials. Techniques such as track etching, sol-gel methods, and electrochemical processing are becoming available for the preparation of well characterized porous materials under controlled conditions.

SCIENTIFIC STUDY WITH A VIEW TOWARD PRACTICAL APPLICATION

Our research has been aimed at answering two basic scientific questions. First, how do the adsorption, selectivity, phase transitions, hysteresis, diffusion rates, flow rates, and so on depend on the type of pore wall, the pore geometry, and the state condition (temperature, pressure, and composition of the bulk fluid in equilibrium with the porous material)? Second, what new phenomena occur? The basic technical question is: How do we make use of this fundamental knowledge to design better materials for specific applications?

Both MC and MD methods are used in our studies. MC is particularly suitable for studying adsorption and selectivity in the case of mixtures, while MD enables us to observe diffusion and flow phenomena. Computer graphics plays an important role in visualizing molecular motions and dynamic processes in the micropore. But even with the best current machines we cannot see these motions in real time; we must be content with "still shots" or "movies" made a frame at a time.

The simulations are complemented by the use of approximate statistical mechanical theories, particularly density functional theory. In this approach, an approximate expression is written for the thermodynamic free energy in terms of the intermolecular forces and molecular distribution functions, as a functional of the density profile in the pore. This is then minimized with respect to the density profile by variational methods. While such calculations are generally less accurate than the MD and MC simulations, they are about two orders of magnitude faster. Thus it is possible to map out the behavior for a particular fluid-pore system over wide ranges of pore size, temperature, pressure, and composition quickly using this theory, and then focus on an area of particular interest using the simulations.

The strong forces exerted on the fluid molecules by the wall cause large shifts in phase transitions and thus in the phase diagram of the fluid. For example, we find that at conditions under which the fluid is normally a dilute gas in the bulk, it condenses to a liquid in a micropore. Similarly, liquid mixtures that are normally miscible may separate into two liquid mixtures when confined in a pore; and isotropic liquids may become liquid crystals when placed in a pore with parallel walls.

The adsorption of methane and methane mixtures is of particular practical importance because natural gas is more than 90 percent methane. If methane could be adsorbed at high density in a suitable microporous material, it would be attractive for vehicle propulsion.

We have studied the adsorption of methane on microporous carbons in which the pores are slit-shaped, so that the walls are approximately parallel. At low temperatures (Figure 5), a series of layering transitions occur at low gas pressures. At some low gas pressure there is a sharp jump

Figure 5

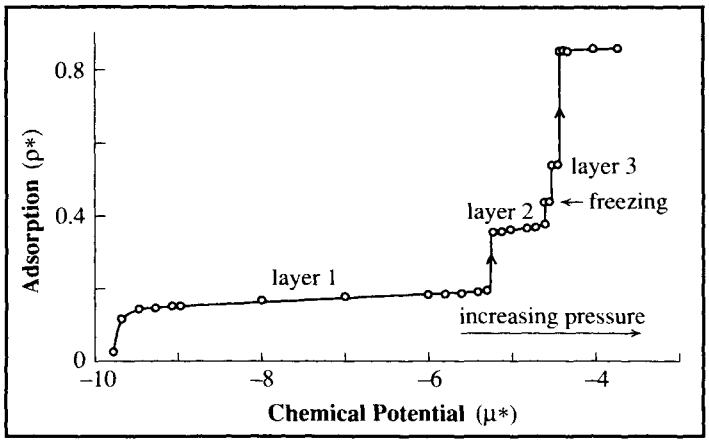

Figure 5. Adsorption of methane in a slit-shaped carbon pore at low temperature, from MC simulation. The pore is 38.2 Å wide. The temperature is 74 K.

The adsorption is defined as the average density ($\rho^* = \rho\sigma^3$, where ρ is the number density and σ is the diameter of a methane molecule) of fluid in the pore. Several layering transitions, as well as a two-dimensional freezing transition, occur during adsorption.

The simulations are carried out at constant chemical potential; however, the horizontal axis can be thought of as one of increasing pressure.

Figure 6

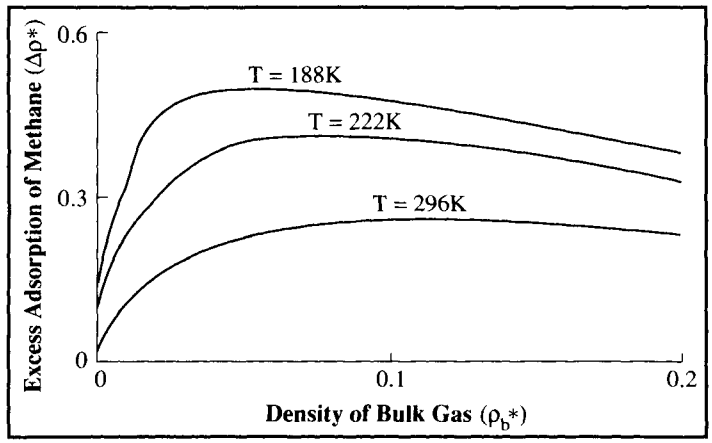

Figure 6. Excess adsorption of methane in a slit-shaped carbon pore at several average temperatures above the critical temperature. This pore is 18 Å wide.

Excess adsorption is defined as the average density in the pore minus the density of the bulk gas outside the pore.

in the adsorption to a state in which a dense monolayer of methane molecules covers the wall. At a higher pressure there is a second jump to a state in which two layers cover the wall. A jump to a three-layer covering occurs at a still higher pressure. During the buildup of this third layer, a two-dimensional fluid-solid transition occurs. And finally, the pore becomes filled with a liquid-like phase.

These layering transitions are first-order phase transitions, and have been observed experimentally for exfoliated graphites. The condensation to liquid occurs at pressures much lower than the usual vapor pressure of methane, and this transition is accompanied by hysteresis—that is, the transition pressure is different on increasing the pressure and on decreasing the pressure. The critical temperature is decreased by the action of the pore walls.

At temperatures above the critical temperature of the methane, these phase transitions are not seen, but the excess adsorption (the average density of methane in the pore minus that of the methane in the bulk gas outside the pore) passes through a maximum at a certain bulk gas pressure or density. This is shown for a particular pore size in Figure 6. As the pore size decreases, this maximum excess adsorption at first increases, and then below some optimum pore size it decreases because of repulsive intermolecular forces between the fluid molecules and the wall. Thus it is possible to determine both an optimum gas pressure and an optimum pore size for the storage of methane at any given temperature.

For gas mixtures, it is separation of the components via adsorption that is often of interest. In general, the pore walls have a greater attraction for one of the components of the mixture than for the others, and will preferentially adsorb that component. The selectivity, S, for a component, A, with respect to another component, B, varies roughly as the ratio of Boltzmann factors, $\exp(-\beta v_A)/\exp(-\beta v_B)$, where v_i is the fluid-wall potential and $\beta = 1/kT$. Thus, such adsorption processes can be made highly selective with only a small difference in wall forces, $(v_B - v_A)$.

Figure 7

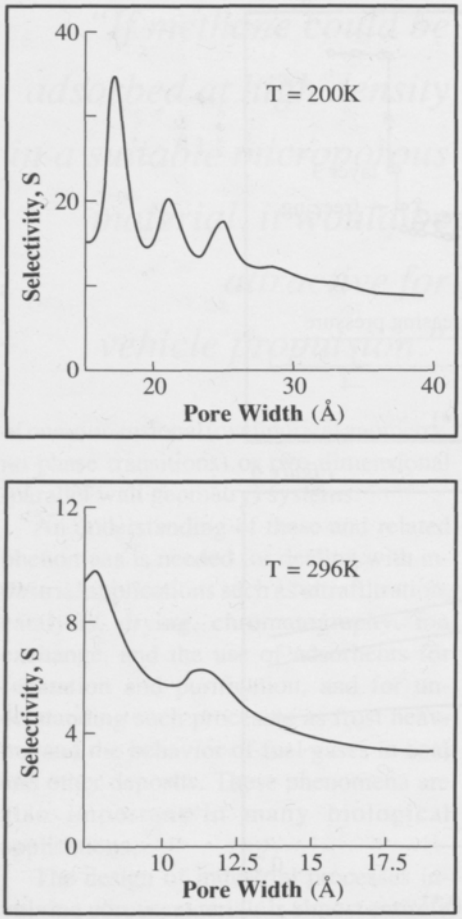

Figure 7. Simulation results illustrating how small pores in a solid can selectively adsorb one gas in a mixture. Here the bulk mixture consists of methane (at a mole fraction of 90 percent) and ethane, and the slit-shaped pores are in carbon. The preferential adsorption of ethane is given for two different temperatures at a pressure of 18.5 bar. Selectivity $S = (x_E/x_M)_{pore} \div (x_E x_M)_{bulk}$, *where x is the mole fraction and M and E represent methane and ethane.*

The oscillations are due to a packing effect. Because the fluid molecules have hard repulsive cores, a small decrease in pore size can suddenly squeeze out a whole layer of molecules, leading to a sharp change in selectivity.

This is illustrated in Figure 7 for a mixture of methane and ethane (two similar and inert molecules) in a carbon slit-shaped pore. Very large selectivities (the ratio of mole fractions of ethane to methane in the pore, divided by the same ratio for the bulk gas in equilibrium with the pore) are found even for this molecularly simple system, especially for small pores and low temperatures. For example, at pore sizes of about 18 Å, the fluid in the pore has an ethane concentration about thirty times higher than in the bulk gas when the temperature is 200 K, but when the temperature is only 120 K, selectivities of several hundred are obtained.

This work on simple fluids in carbons is now being extended to studies of more complex fluids such as water, aqueous solutions, and liquid crystals, and to other porous ceramic materials, including silicas and other oxides.

Keith E. Gubbins is the Thomas R. Briggs Professor of Engineering in Cornell's School of Chemical Engineering. He joined the school in 1976 and recently completed a term as its director. Gubbins earned his doctorate at the University of London in 1962 and subsequently held postdoctoral and faculty positions at the University of Florida. He has held visiting professorships at Imperial College, London, Oxford University, and the Universities of Guelph, Kent, and California at Berkeley. He is a member of the National Academy of Engineering, a former Guggenheim fellow, and a recipient of the Alpha Chi Sigma Research Award of the American Institute of Chemical Engineers.

John Walsh is working with Gubbins as a postdoctoral associate. After receiving the B.S. degree in chemical engineering from the University of Maine, he was employed as a process engineer at Westvaco, Inc., in Maryland, where he developed a latex-coated printing paper, and subsequently he earned the M.S. degree at the Institute of Paper Chemistry. He studied at Johns Hopkins University for the Ph.D. in chemical engineering, granted in 1989.

Below: Walsh and Gubbins

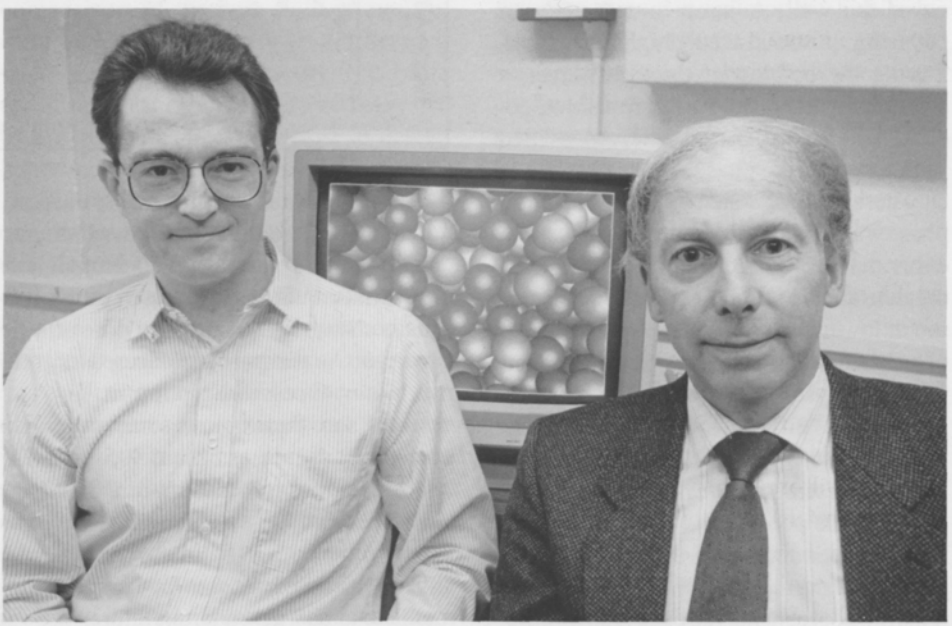

COMPUTER MODELING IN RESEARCH ON GENETICALLY MODIFIED BACTERIA

by Michael L. Shuler

Perhaps no other development in the last twenty years will have a greater impact on people than the invention of genetic engineering. Our health, our longevity, our environment, our wealth as a nation, our food supply, and our understanding of our human roots will all be positively affected by the consequences of genetic engineering.

A requirement for the realization of the vast potential of genetic engineering is that cells receiving new information must be able to stably express that information for extended periods of time. This article describes how complex models of cellular populations can be used to increase the utility of genetically engineering cells.

THE BASICS OF GENETIC ENGINEERING

We must first explore a few concepts and definitions.

The basic unit of genetics is the *gene*—a segment of an organism's DNA. Genes are "written" in the universal language of genetics: all organisms—bacteria, plants, fungi, and animals—use the same language, which consists of four "letters" that make up three-letter "words".

The function of the gene is to encode information for the production of a protein. Most biological reactions are mediated by biological catalysts, called *enzymes*, which are primarily proteins. Even a simple bacterium may have the ability to make almost two thousand different enzymes.

Some proteins are rare and in the past could be obtained only from human cadavers or other equally difficult sources. But with the advent of genetic engineering, we can take genes for rare but important enzymes and insert them into fast-growing, easily cultured cells such as some bacteria. These cells can then make large amounts of the desired protein at an affordable cost. In other cases, these genetically modified cells can be used as catalysts to make nonprotein chemicals, or as tools to degrade hazardous wastes.

The process of genetic engineering involves the insertion of a gene (often a rare gene) into a larger piece of DNA that is called a *vector*. With recombinant DNA technology, this process can be carried out in a test tube. Then the vector can be introduced into easily grown host cells, where the desired gene can be rapidly increased in number. Under the correct conditions, we can activate the genes through the use of a *promoter*, so that large amounts of the desired protein, called the *target protein*, are made. An inducible promoter is like an on/off switch that can be activated by adding or removing a small amount of a nutrient or other chemical.

The most commonly used vectors are *plasmids*—extrachromosomal, self-replicating pieces of DNA. Plasmids may be present in high or low *copy number*s (which refer to the number of plasmids per cell), as determined by the type of replication machinery encoded on the plasmid. Plasmids often have copy numbers greater than 30.

The most commonly used plasmids are a high-copy-number type with an origin of replication that is designated ColE1.

E. COLI AS HOST CELL FOR INDUSTRIAL PROCESSES

For many industrial processes, the host cell of choice is the simple bacterium *Escherichia coli* (often shortened to *E. coli*) that is used as the host cell for many industrial processes. This organism grows quickly on inexpensive nutrients and its genetics are well understood.

There is, however, an important constraint in the use of a plasmid *E. coli* sys-

"This article describes how complex models of cellular populations can be used to increase the utility of genetically engineering cells."

tem. This is *genetic instability*. When many gene copies and a strong promoter are present, over 20 percent of a cell's resources can be directed toward production of a target protein, but the remaining 80 percent is directed toward normal growth. And if a cell can rid itself of plasmids, or if it can inactivate the expression of genes for the target protein, then it can devote 100 percent of its resources to growth. Consequently, cells that produce less product grow more quickly, and in a few generations can completely dominate the bacterial population. Such an event is a manifestation of genetic instability.

Genetic instability can result from: (1) *segregational instability*, or missegregation of plasmids at cell division so as to give rise to a plasmid-free cell; (2) *structural instability*, or structural alteration of the plasmid to prevent formation of the desired protein; (3) *host mutation*, referring to chromosomal mutations that reduce or eliminate expression of the desired gene (for example, by excluding the entry of an inducer into the cell); and (4) *growth-rate-dependent instability*, or the overgrowth of the productive population by faster-growing cells that lack the plasmid and do not produce the target plasmid-encoded protein. Mechanism (4) becomes operable only if at least one cell in the population is altered by mechanisms (1), (2), or (3).

If the instability is due to rapid generation of plasmid-free cells, mechanism (1)—segregational instability—would be the dominant mechanism. If, on the other hand, the generation of a plasmid-free cell were an extremely rare event, but once such a cell was formed it had a very significant growth-rate advantage, mechanism (4)—growth-rate-dependent instability—would be the dominant type. It is these two mechanisms that I consider in this article.

UNDERSTANDING PLASMID ACTIVITY IN THE CELL

When there is a loss of plasmids, or when their structure or expression is modified in some cells, there is a change in *metabolic burden*, and the result is a population of cells with mixed capabilities. The direct experimental determination of the properties and frequency of subgroups within mixed populations is extremely difficult. Most experiments only generate population-averaged parameters. Even in the best of circumstances, the population can usually be subdivided only into plasmid-free and plasmid-containing cells. The plasmid-containing cells, then, are usually treated as a homogeneous population.

Such a treatment is crude and often misleading. Population-averaged values of the plasmid-containing cell fraction are inadequate to predict productivity and rates of generation of plasmid-free cells. Productivity is a nonlinear and saturable function of plasmid copy number; a cell with one hundred fifty plasmids may make less than twice the plasmid-encoded protein of a cell with seventy-five plasmids. Further, the probability of generating a plasmid-free cell is much greater when there are two plasmids in the cell than when there are twenty.

Thus, insight into the population dynamics of plasmid-containing cells depends on knowledge of (1) the distribution of copy numbers within a population, and (2) the relationship of each cell with a particular copy number to its growth rate, plasmid-encoded protein synthesis rate, and probability of generating a plasmid-free cell.

MATHEMATICAL MODELING IN STUDIES OF CELLULAR DYNAMICS

Mathematical models can serve as important tools in relating individual cellular

Figure 1

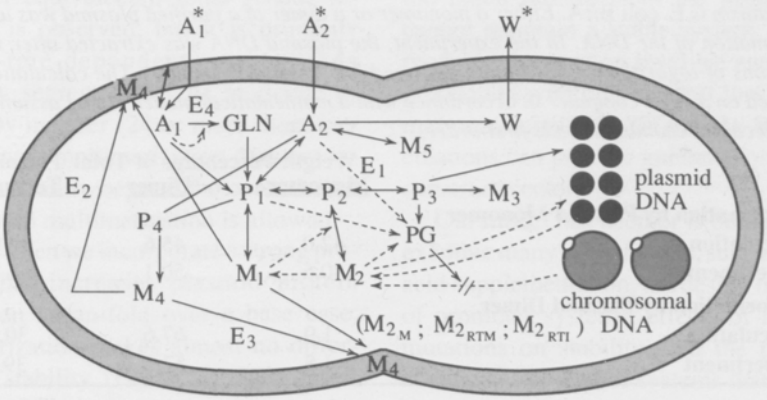

A_1 = ammonium ion
A_2 = glucose (and associated compounds in the cell)
W = waste products (CO_2, H_2O, and acetate) formed from energy metabolism during aerobic growth
P_1 = amino acids
P_2 = ribonucleotides
P_3 = deoxyribonucleotides
P_4 = cell envelope precursors
M_1 = protein (both cytoplasmic and envelope)
$M_{2_{RTI}}$ = immature "stable" RNA
$M_{2_{RTM}}$ = mature "stable" RNA
M_{2_M} = messenger RNA
M_3 = DNA
M_4 = nonprotein part of cell envelope
M_5 = glycogen
PG = a nucleotide with a regulatory function
E_1 = glutamine synthetase
E_2, E_3 = molecules involved in directing cross-wall formation and cell-envelope synthesis
GLN = glutamine

Figure 1. An idealized sketch of a model of E. coli *growing in a medium of glucose and ammonium salts, with glucose or ammonia as the limiting nutrient.*

At the time shown, the cell has just completed a round of DNA replication and initiated cross-wall formation and a new round of DNA replication.

Solid lines indicate the flow of material, and dashed lines indicate the flow of information. An asterisk indicates that the material is present in the external environment.

dynamics to population behavior. Models that take into account both the highly complex and structured nature of individual cells and the distributive nature of properties in a population are called *structured and segregated*. Such models can be cast in the form of population-balance equations, but that approach leads to integral-differential equations that become intractable at even modest levels of structure.

We have circumvented this problem by writing highly structured models for individual cells (see Figure 1) and then constructing models of populations using a finite representation technique. In this technique the population is divided into subgroups, with each subgroup represented by a model of an individual cell. All the cells within a subgroup are presumed to be identical. This approach can relate the kinetics of individual cells to population-averaged values.

THE MODEL FOR ONE TYPE OF GENETIC INSTABILITY

Although this modeling framework can be used to probe any of the causes of genetic instability, I will concentrate here on plasmid *multimerization*. In some cases host-cell enzymes will cause the fusion of single plasmids (monomers) into double plasmids (dimers), or dimers into four-monomer complexes (tetramers). Since such multimerization decreases the number of replicating units to be distributed to daughter cells at division, it could be an important factor in generating plasmid-free cells. (The mechanism involved would be the one I have called plasmid missegregation.)

The basic Cornell model for an individual *E. coli* cell with a high-number, ColE1-type plasmid has twenty-eight ordinary, but nonlinear, coupled differential equations. Each equation is a transient mass balance on a cellular component; this approach treats the cell as a chemical reactor and applies the principles of chemical reaction engineering. These equations are integrated forward in time. A number of conditional equations describing cell geometry and tracking DNA replication are included.

To construct a population model, we approximate a population by a finite representation technique. It is thought that with cells containing high-copy-number plasmids, the division of plasmids among progeny is done randomly according to a

Some results of the study are shown in Table I and Figures 2 and 3.

The Table I data indicate that the mathematical model satisfactorily predicts experimental results under conditions of first-order intermolecular recombination.

Figures 2 and 3 are examples showing how the model can be used to predict genetic instability under other conditions. Such predictions could influence the design of genetic experiments.

Figure 2 shows that neither the predicted plasmid stability nor the production of plasmid-encoded protein are affected by multimerization, even at high promotor strength. In this simulation, the average copy number was 48 and the promoter strength was set at 7. (A promoter strength of 1 corresponds to the strength of the so-called lac *promoter, which is one of those that have been studied best.) The simulation is for a continuous culture with a mean residence time of one hour (which is the time required for one generation).*

Figure 3 shows the total production of target protein in continuous culture at three promoter strengths. The area under each curve corresponds to the total amount of target protein made by the system. Because of genetic instability, an intermediate value of promoter strength will maximize total production over a "long" run.

Table I. **A Comparison of Modeling and Experiment**

The organism is E. coli B/rA. *Either a monomer or a dimer of a purified plasmid was used for transformation of the DNA. In the experiment, the plasmid DNA was extracted after seventy generations of logarithmic growth and analyzed for size heterogeneity. The calculation was performed on a supercomputer in accordance with a mathematical model. It was assumed that intermolecular recombination is first-order.*

	Weight Percentage of Total Plasmid		
	Monomer	Dimer	Tetramer
Transformation by Plasmid Monomer			
Calculation	42.0	45.6	12.0
Experiment	40.6	50.1	6.5
Transformation by Plasmid Dimer			
Calculation	1.9	67.6	30.5
Experiment	1.8	57.3	39.9

binomial distribution. In our plasmid-free cell population model, the progeny of cell division are made identical; and for plasmid-containing cells, we assume that all progeny are chemically identical except for plasmid content. Plasmid copy number is the master parameter for regrouping of all progeny from cell divisions. (Without regrouping, the size of the model population would increase without limit.) The population model we have used in the work I am discussing here contains 272 cell categories, with seventeen different groups of plasmid copy numbers and sixteen groups based on cell size (which is approximately the same as cell age).

To calculate the progress for many generations of a reactor with 272 complex cells is a formidable task. The supercomputer's speed and large memory are critical to the success of the calculation.

In the model, we have incorporated equations representing plasmid recombination pathways and mechanisms. A kinetic approach assuming a first-order recombination predicted experimental results satisfactorily (Table I). By including multimerization kinetics, the model shows

Figure 2

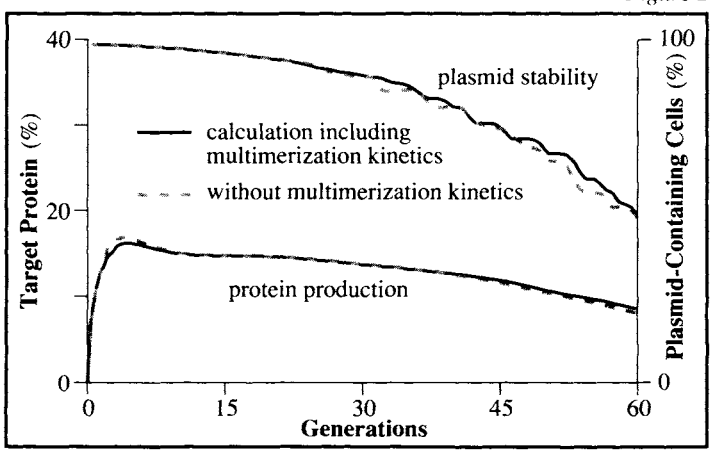

Figure 3

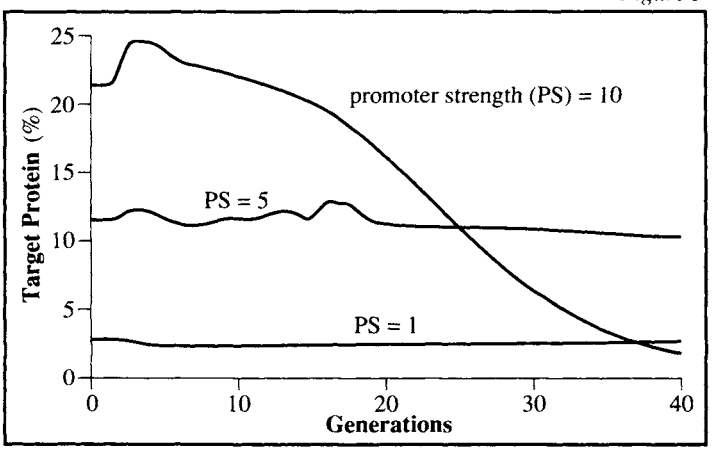

that if the plasmid copy number is low (12 monomer equivalents), some genetic instability is observed, but it is primarily growth-rate-dependent rather than primarily segregational. At moderate or high copy number (24 or more monomer equivalents), multimerization does not increase instability beyond the control case in which no multimerization is allowed.

Even when we incorporate a strong promoter that increases plasmid protein production seven-fold over a base case, multimerization makes almost no difference in stability (Figure 2). This result would be unexpected by most molecular biologists, and suggests that the use of certain mutants (for example, cells whose recombination pathways have been altered) is unnecessary.

Another example of our findings is a study of the effect of varying the strength of a promoter. (This is a parameter that can be physically manipulated.) If we try to make too much protein from the plasmid, we cannot maintain a stable system; but at a moderate production level we can sustain production with only modest loss of plasmid-containing cells (Figure 3). Such calculations can provide guidance on how to construct vectors.

Our model has been or is being used to examine many other factors, such as amino acid supplementation, the design of details of promoter systems, effects of host-cell mutations on stability, and the potential advantages of reactor systems that include cycling or have several stages.

Models are very helpful in research of this kind because they can be used to rapidly test hypotheses about cellular mechanisms and the effects of different molecular-level alterations of the cell or plasmid. Further, modeling can be used in the design of reactor configurations and operating strategies. Realistic models—which become more practical as our computational capabilities improve—will speed the realization of the great potential of genetic engineering.

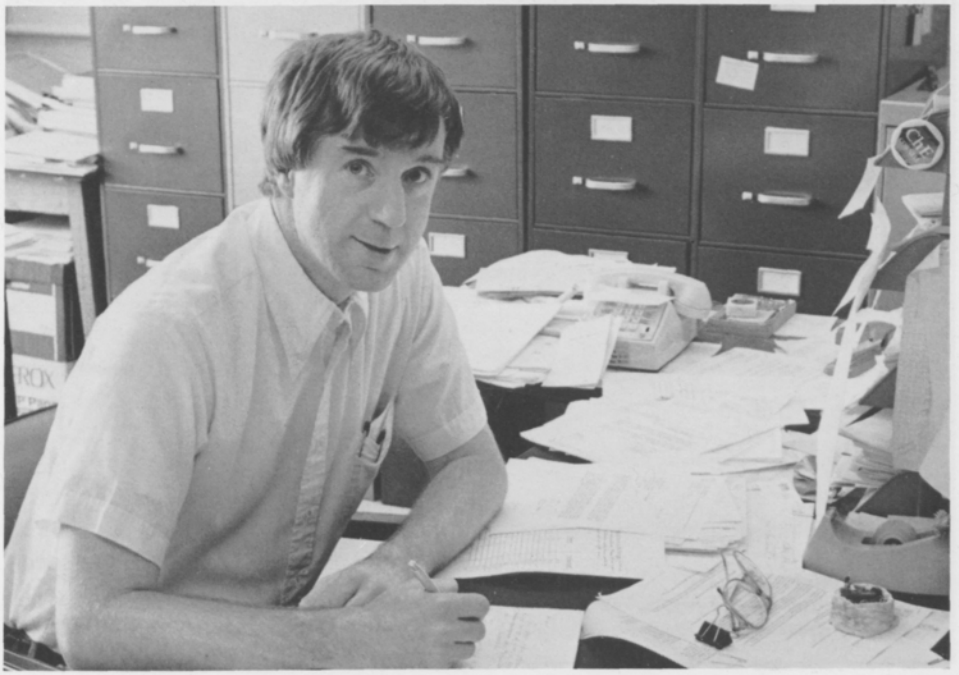

Michael L. Shuler joined Cornell's chemical engineering faculty in 1974, after earning the B.S. degree at Notre Dame University and a doctorate at the University of Minnesota.

His research involves considerable interdisciplinary collaboration. At Cornell he is a member of the graduate fields in food science and in microbiology, as well as in chemical engineering, and he has been active in the development of the Biotechnology Institute and Center.

Shuler, a full professor at Cornell, has held visiting appointments at several other universities. He was the founding editor-in-chief of Biotechnology Progress *and is currently on the editorial boards of three other journals.*

He has been honored with the 1986 Marvin J. Johnson Award of the Microbial and Biochemical Technology Division of the American Chemical Society, and with the 1989 Food, Pharmaceutical, and Bioengineering Award of the American Institute of Chemical Engineers. In 1989 he was elected to the National Academy of Engineering.

THE MICROSTRUCTURE OF MATERIALS:

Studies Using a New Kind of Electron Microscope and a Supercomputer

by John Silcox

The widespread use of electron microscopy in studies of the microstructure of materials relies quite heavily on the effective use of computers. As increased computational resources have become available, new applications have been found in electron microscopy.

At Cornell we have been working on expanding the applications of a new type of electron microscope, taking advantage of powerful computing capability. Specifically, we are studying materials at the forefront of current research: high-temperature superconductors and electronic materials in which thin layers of metal are grown on silicon.

The use of electron microscopy in conjunction with advanced computing technology is a particularly promising approach to microstructural studies. Our electron microscope is capable of higher spatial resolution than conventional instruments. Also, new contrast modes are feasible, and high-resolution chemical and electronic structure studies are possible.

Figure 1

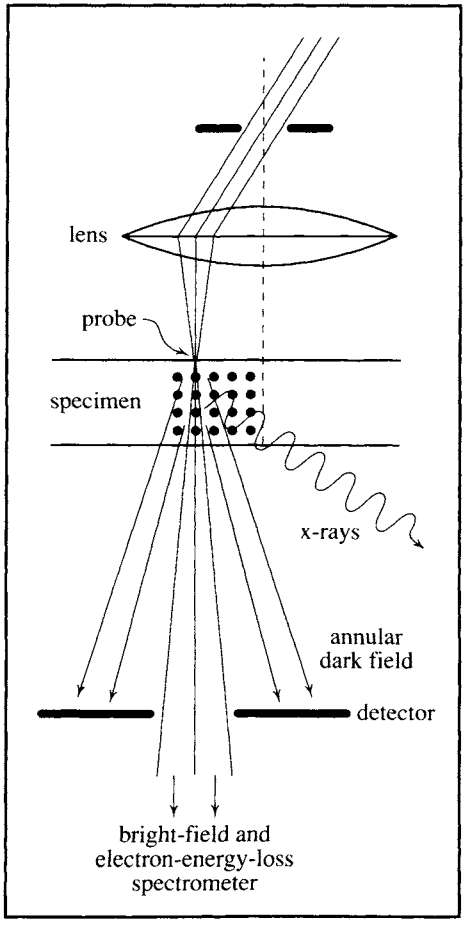

Figure 1. The instrumentation used to study the microstructure of materials. In a similar fashion to the way an optical lens can be used to form a fine point of light and move it, so an electron lens can form a fine electron point and move it around on the sample.

Typical signals recorded include the annular dark-field signal, from elastically scattered electrons; the energy-loss signal (obtained with use of the electron energy-loss spectrometer), from inelastically scattered electrons; and x-rays.

If the beam is raster scanned, the signal can be displayed on a TV screen, giving a high-magnification image of the sample.

OBTAINING MICROSTRUCTURAL AND CHEMICAL INFORMATION

In principle, our instrument operates in a simple fashion (see Figure 1). A very tiny spot of electrons is raster scanned over a small area of the specimen, electron scattering to large angles is measured for each position of the beam, and an image is made by synchronously displaying the results on a TV screen.

The electron beam is about 2 angstroms (Å) in diameter. (An angstrom is 10^{-10} meter or one-tenth of a nanometer; we call our electron beam a *nanoprobe*.) The specimen area is 200 Å by 200 Å. And since the TV screen is 20 centimeters in diameter, the magnification of the image is 10 million.

"As increased computational resources have become available, new applications have been found in electron microscopy."

Figure 2

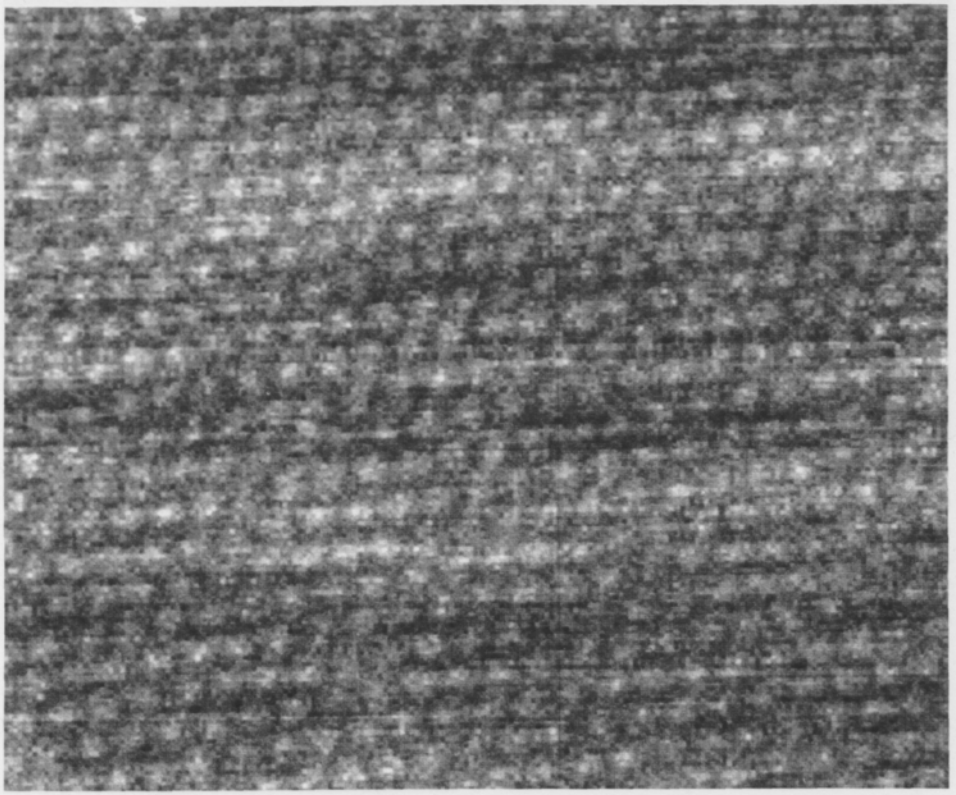

Figure 2. A large-angle scattering image showing a projection of silicon atoms down a (111) direction in which the atoms form columns that are 1.9 Å apart. This image was recorded by graduate student Peirong Xu.

If the specimen contains columns of atoms at a spacing close to the electron-spot size, then—as indicated in Figure 1—the electron scattering will vary according to whether the electron beam is centered on the atoms or between them, and the image will yield information about the atomic spacing. The scattering image shown in Figure 2, for example, is of a thin film of silicon oriented down a (111) axis in which the atom columns are 1.9 Å apart.

Another example of a scattering image is shown in Figure 3. This is for a high-critical-temperature (high-T_c) sample of the superconducting oxide $YBa_2Cu_3O_7$. In this case, differing intensities associated with differing atomic number Z are observed.

Other possible modes of use are indicated in Figure 1. For example, the electron spectrometer can be used to measure the number of electrons that lose energy to the sample. Since the energy loss is characteristic of the particular atoms that are irradiated and of the way these atoms are bonded to the neighboring atoms, these measurements can add chemical and electronic structural details to images of the type shown in Figure 2. Another possible use for nanoprobe chemical analysis would be to

Figure 3

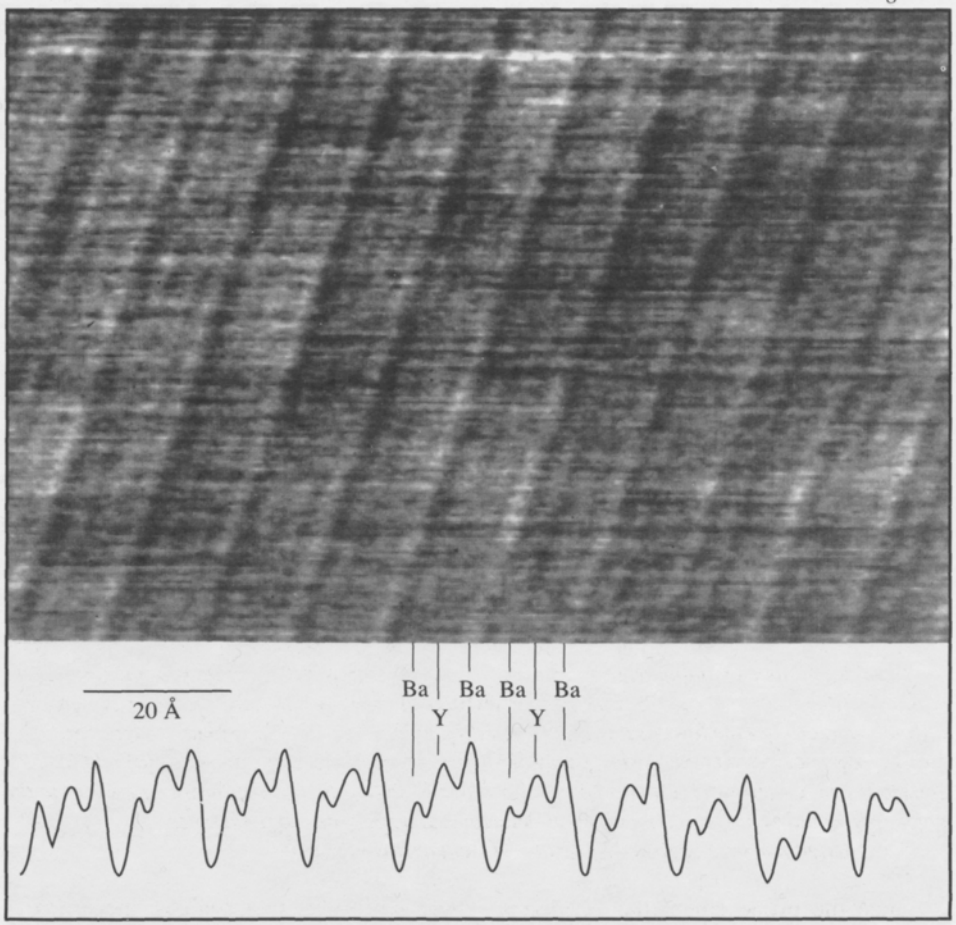

Figure 3. An image of the superconducting oxide $YBa_2Cu_3O_7$ recorded perpendicular to the c-axis. The contrast is due to the Y and Ba planes, as shown by the variation in intensity with position in the intensity line scan seen underneath the image.

This image was recorded by graduate student Don-Hyuk Shin in collaboration with Stephen Russek of Professor Robert A. Buhrman's research group.

"The image calculations are lengthy because of the large number of image points—more than ten thousand—that are needed to form the complete image. . ."

measure the x-rays emitted from the sample as a result of a stationary probe.

SUPERCOMPUTER SIMULATION FOR INTERPRETING THE IMAGES

To ensure that we understand these images, we are using supercomputer simulations to explore how different settings of the microscope (focus, objective aperture, and so forth) affect the images.

The simulation procedure can be divided into three parts. The first step is to model the probe using settings and known microscope parameters such as focus and aperture choices, and lens defects such as spherical aberration.

Figure 4

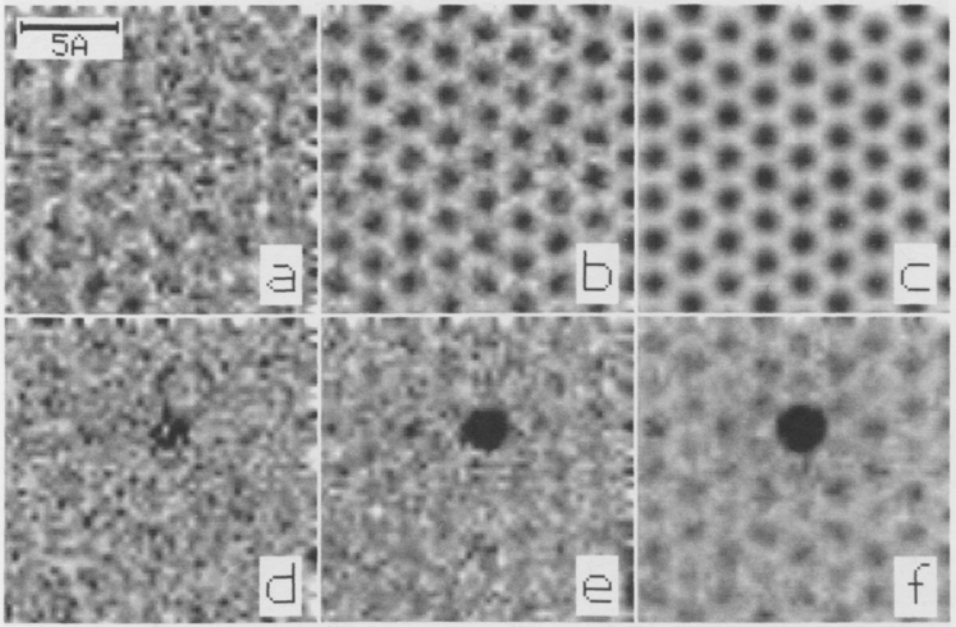

Figure 4. Simulated scanning transmission electron microscopy (STEM) images of a single gold atom on a film of silicon 94 Å thick. The upper set (a, b, c) shows just the silicon image as measured by one detector, and the lower set (d, e, f) shows the gold atom as seen by another detector.

The sequence reflects increasing signal. The levels are 10^3 electrons per Å^2 in (a) and (d); 10^4 electrons per Å^2 in (b) and (e); and 10^5 electrons per Å^2 in (c) and (f). Shot noise equivalent to the noise that would be produced by an ideal detector has been added to the images.

The simulations were executed by graduate student Russell Loane.

Once the probe enters the specimen, then—in the second phase of the simulation—the progress of the probe through the sample has to be calculated by solving the Schrödinger wave equation. The first step in obtaining a solution is to estimate the electrostatic potential of the sample, which is done by adding up the atomic potentials of all the atoms centered at particular sites. As the probe passes through the sample, two effects occur simultaneously: the phase of the electron wavefunction alters, and the electron wave undergoes diffraction. In the calculation, these are handled sequentially, but for only a small slice of the sample; the whole sample is dealt with by repeating the calculation for many slices; indeed, it is referred to as a *multislice calculation*.

The final step in the simulation is to calculate the progress of the scattered electrons from the exit surface to the detector. This yields one element in the image and has to be repeated for each step of the calculation to get a complete image.

The computer requirements for doing an effective job are substantial. The calculations require extensive use of Fourier transform techniques and matrix multiplication with arrays typically of size 256 x 256. The vector-processing capability of supercomputers is well suited for such a task. Over the past five years or so, we have used the IBM 3090 supercomputer in the Cornell Theory Center and the Convex C210 mini-supercomputer in the Materials Science Center.

Even with powerful computers like these, the computations take considerable time. The calculation of one image on the IBM 3090 has taken up to four hours, and a recent calculation of intensity in the detector plane took more than three hours on the Convex C210. The image calculations are lengthy because of the large number of image points—more than ten thousand—that are needed to form the complete image; by contrast, the simulation of a conventional microscope image requires only one calculation. In the case of our recent detector-plane calculations, the time required is lengthened because of some of the factors we are now including.

SIMULATION TO STUDY EFFECTS OF INSTRUMENTAL DETAILS

Figure 4 shows simulations obtained in a study of the effects of different detector geometries and different defocus (corrective) settings of the instrument.

The simulations pertain to a silicon (111) structure of the type shown in Figure 2,

Figure 5

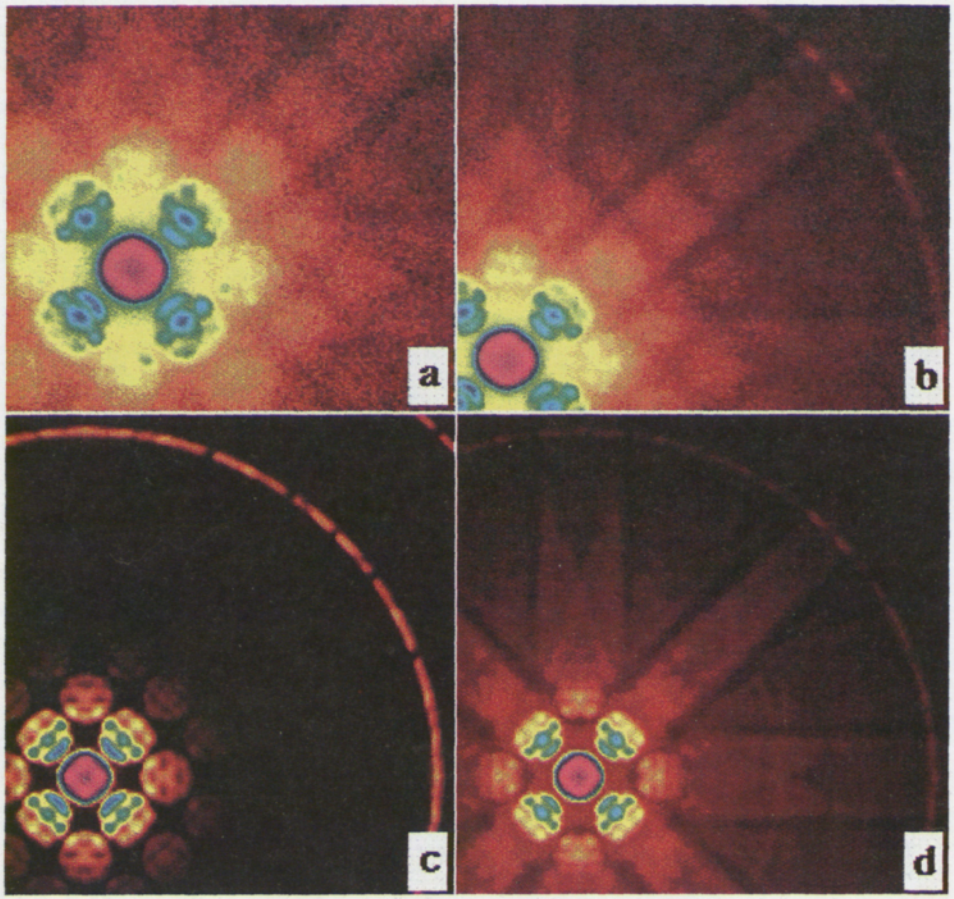

Figure 5. Experimental and simulated diffraction patterns.

Figures 5a and 5b are experimental patterns recorded by Russell Loane and Peirong Xu using a scanning transmission electron microscope (STEM) and a VAX 3200 workstation installed by Dr. Earl Kirkland.

Figure 5c is a simulation in which random displacements of the atoms (due to thermal vibrations) have not been considered.

Figure 5d shows a simulation in which thermal displacements have been taken into account in the calculations.

The simulations were carried out by Russell Loane.

Figure 6. Sketch showing atoms displaced from normal positions by thermal vibrations (the "frozen phonon" approximation).

with a gold atom added to the entrance surface.

These simulations show many of the qualitative effects that the experiments show. For example, the "atom" dots in the simulation do not change position with the focus or with sample thickness, and they do show *Z contrast*—that is, atoms with higher atomic number *Z* show more scattered intensity. In detail, however, the variations may not be simple, and these features need to be checked out.

One of the reasons the simulations may not be entirely accurate is that they were simulated with the atoms all located at the ideal position in the crystal structure. In reality, atoms at room temperature move because of thermal energy, and this effect was not taken into account in our standard multislice calculations. As illustrated in

Figure 6

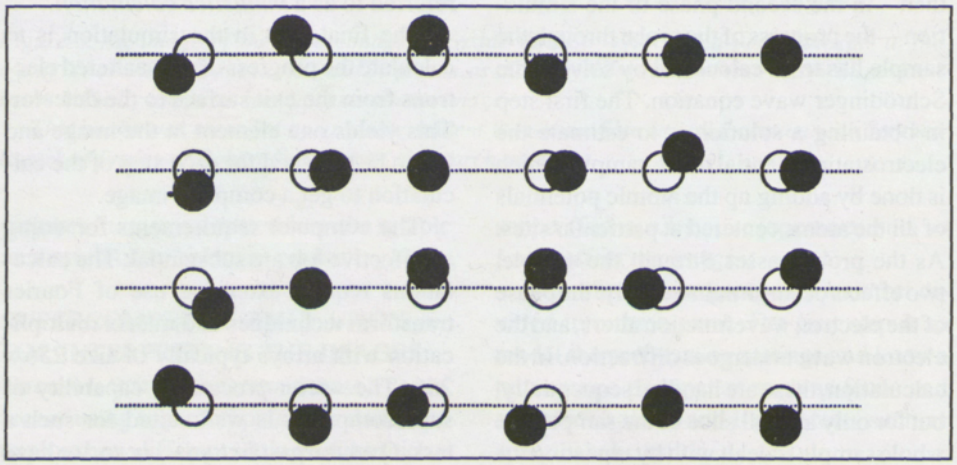

Figure 5, this effect may, however, be important for these images.

Figure 5 shows a comparison of experimental and simulated detector-plane intensity patterns—or convergent beam electron diffraction (CBED, as it is known in the trade). The experiments (Figures 5a and 5b) show a set of bands coming radially from the pattern center (Kikuchi bands) and a diffuse scattering intensity at intermediate angles—features that are not predicted by the standard simulation (Figure 5c). To include this effect in the simulations, probability theory and a random-number generator have been used to displace the atoms slightly from the equilibrium positions in accordance with Einstein's version of the theory of thermal vibrations.

Figure 6 illustrates the effect. After the initial CBED pattern is calculated, a new set of displacements is calculated to give a new displacement configuration, and a second CBED pattern is simulated and added to the first. Fortunately, only sixteen of these configurations need to be calculated to achieve a pattern (as in Figure 5d) that has acceptable features and small enough randomness.

The good agreement between the experiment (Figure 5a and b) and the simulation with the added displacements (Figure 5d) gives us confidence in a key assumption underlying the calculation: the "frozen phonon" approximation that says that the electron, which is traveling at one-half the speed of light, is scattered from the atom in a time significantly less than a vibration period. Elementary classical and quantum mechanical considerations suggested that this assumption was well satisfied, but it is comforting to see that the simulations do, indeed, hold up.

We can now predict CBED patterns at different temperatures. Next we need to extend the kind of work we have done with silicon, an element, to explore compounds (such as indium phosphide, of interest in semiconductor electronics). Also, we plan to enlarge the usefulness of simulations by settling questions about characteristics such as contrast origin and depth of focus. The group carrying out this work has included graduate students Russell Loane, Don-Hyuk Shin, and Peirong Xu; Earl J. Kirkland, a senior research associate; and Malcolm Thomas, a research support specialist, who kept the microscope operating.

One thing is clear. Without the supercomputer at Cornell, it is extremely unlikely that we would have embarked on this work. State-of-the-art facilities not only help research programs; often they open up new possibilities and approaches.

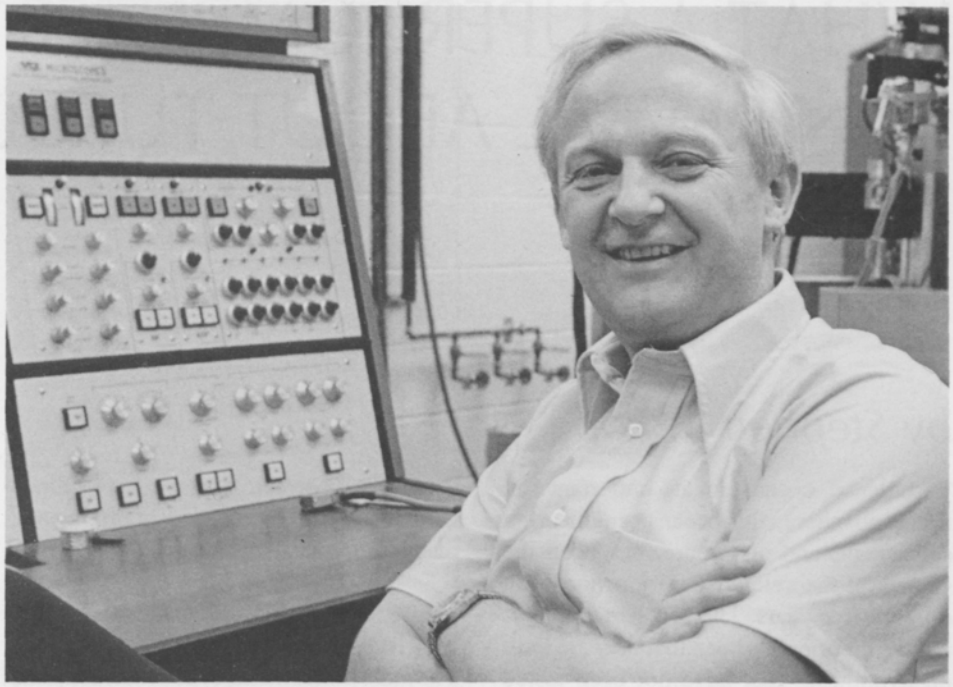

John Silcox, the David E. Burr Professor of Engineering in the School of Applied and Engineering Physics, is currently director of the Materials Science Center at Cornell. He has also served two terms as director of the school.

Silcox came to Cornell in 1961 after earning the B.Sc. degree from the University of Bristol, England, and the Ph.D. from Cambridge University. He has spent sabbatical leaves as a Guggenheim fellow in France and England, at Bell Laboratories, and at the national electron microscopy facility at Arizona State University.

He is a fellow of the American Physical Society and a member and past president of the Electron Microscopy Society of America. He has served on the Solid State Sciences Committee of the National Academy of Sciences/ National Research Council. Currently he is a member of the Materials Advisory Committee for the National Science Foundation, and of advisory committees to the national electron microscopy facilities at Argonne National Laboratory and at Arizona State University.

WHAT A SUPERCOMPUTER CAN REVEAL ABOUT TURBULENCE

by Stephen B. Pope

Turbulence, because of its importance in the atmosphere, the oceans, engineering equipment, and elsewhere, has been the subject of theoretical study for more than seventy-five years. The problem in applying the theories has been that they are built on hypotheses that have not been tested because of insuperable experimental difficulties. Now, however, it is possible not only to test these hypotheses, but to do much more: to answer longstanding questions about the basic physical processes of turbulence.

The key is the supercomputer. In our research at Cornell, we simulate surfaces under turbulent conditions using a supercomputer to do the calculations. We have found that some of the theoretical conjectures that have been generally accepted for years are incorrect. And we have gained fresh insights into processes of mixing and reaction in turbulent flows.

This article is based on a paper, "Stretching and Bending of Material Surfaces in Turbulence," that won the $25,000 first prize in the engineering division of the 1989 IBM 3090 Supercomputing Competition. In addition to Pope, the authors are two of his former graduate students—Pui-Kuen Yeung, now of the Department of Mechanical Engineering at Pennsylvania State University, and Sharath S. Girimaji of Analytical Services and Materials, Inc.

MATERIAL SURFACES IN TURBULENT MOVING FLUIDS

The most fundamental type of surface is the material surface, which, by definition, moves with the fluid. A material surface is defined by its initial conditions (such as a position on a specified plane at time $t=0$) and by the condition that every point on the surface moves with a velocity that is the same as the velocity of the fluid at that time and place. The significance of material surfaces is illustrated by two examples.

The first example (Figure 1) is the mixing of two bodies of water in a closed container; the material surface is the interface between them. Initially one of the bodies (A in the figure) contains a trace solute, and the other (B) is pure water. When the water is set in turbulent motion, the material surface is convected, stretched, and bent. In the first stages of mixing, the concentration is uniform everywhere except in the immediate vicinity of the material surface, where there is a thin diffusive layer. Locally, this thin layer behaves (to an excellent approximation) as if it were a plane layer experiencing a certain strain, and therefore the mixing process can be completely analyzed in terms of the statistics of straining on the material surface. (At later times the material surface folds over, and the analysis breaks down once the distance between folds is comparable to the thickness of the diffusion layer.)

The second example (Figure 2) is an idealization of a turbulent premixed flame, such as that in a spark-ignition automobile engine. Under appropriate conditions, there is a thin flame sheet that forms a connected but highly wrinkled surface separating the combustion reactants from the products. This flame surface is convected, bent, and strained by the turbulence, and propagates at a certain speed relative to the fluid. If this propagation speed is small enough, the flame surface behaves as a material surface. In this example, as with the two mixing bodies of water, the statistics of the straining on the material surface are significant. Also important in the flame example is the curvature of the surface, since this affects the propagation speed.

Figure 1

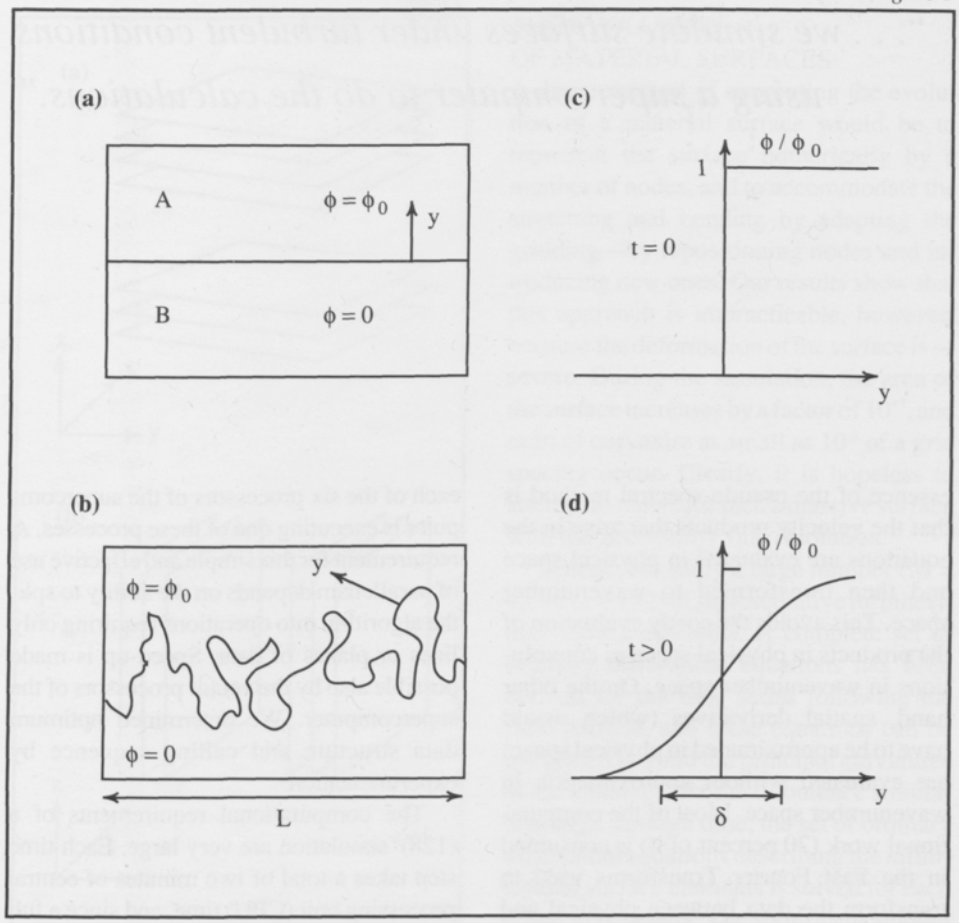

Figure 1. The effect of turbulence on the material surface between two bodies of water (A and B) in a closed vessel. Initially, at time t=0, A contains a trace solute of concentration $\phi = \phi_0$, while B is pure water ($\phi = 0$).

The sketch labeled (a) represents the material surface that is initially coincident with the interface between A and B; (b) represents the situation after the water has been set in turbulent motion (at time $t > 0$). Here the surface has become convected, stretched, and bent. The sketches labeled (c) and (d) are normalized concentration profiles normal to the surface. Note that $\delta << L$, which is the size of the vessel.

Figure 2. The surface between reactants (outside the shaded areas) and products (in the shaded areas) in a turbulent premixed flame. The wrinkled and deformed surface propagates at a speed w relative to the fluid; at sufficiently small w, it behaves as a material surface.

Figure 2

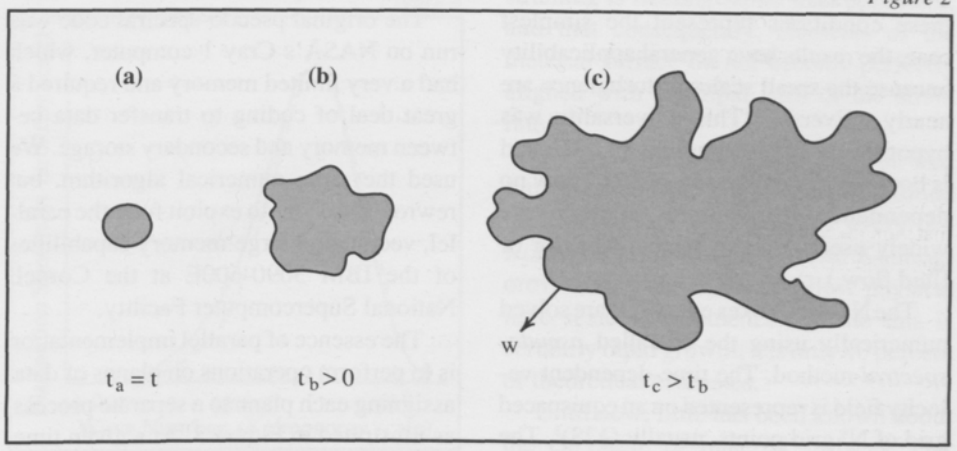

". . . we simulate surfaces under turbulent conditions using a supercomputer to do the calculations."

In our work, we use simulations of turbulence to study the processes that affect material surfaces such as these. In particular, we use the simulations to characterize the statistics of surface straining and curvature.

OUR METHOD FOR SIMULATING TURBULENCE

To create our simulations, we solve the governing equations of fluid motion—the Navier-Stokes equations—for the simplest possible turbulent flow: homogeneous, isotropic (the same in every direction), and statistically stationary. But even though these conditions represent the simplest case, the results have general applicability because the small scales of turbulence are nearly universal. (This universality was hypothesized by Kolmogorov in 1941, and is borne out by our results, which show no dependence on Reynolds number, the widely used indicator of the behavior of fluid flow.)

The Navier-Stokes equations are solved numerically using the so-called *pseudo-spectral* method. The time-dependent velocity field is represented on an equispaced grid of N^3 grid points, usually $(128)^3$. The essence of the pseudo-spectral method is that the velocity products that arise in the equations are evaluated in physical space and then transformed to wavenumber space. This avoids the costly evaluation of the products in physical space as convolutions in wavenumber space. On the other hand, spatial derivatives (which would have to be approximated in physical space) are evaluated without approximation in wavenumber space. Most of the computational work (70 percent of it) is consumed in the Fast Fourier Transforms used to transform the data between physical and wavenumber space.

The original pseudo-spectral code was run on NASA's Cray 1 computer, which had a very limited memory and required a great deal of coding to transfer data between memory and secondary storage. We used the same numerical algorithm, but rewrote the codes to exploit fully the parallel, vector, and large-memory capabilities of the IBM 3090-600E at the Cornell National Supercomputer Facility.

The essence of parallel implementation is to perform operations on planes of data, assigning each plane to a separate process, as illustrated in Figure 3. At a given time, each of the six processors of the supercomputer is executing one of these processes. A requirement for this simple and effective use of parallelism depends on the ability to split the algorithm into operations requiring only lines or planes of data. Speed-up is made possible also by the vector processors of the supercomputer. We determined optimum data structure and calling sequence by experimentation.

The computational requirements of a $(128)^3$ simulation are very large. Each time step takes a total of two minutes of central processing unit (CPU) time, and since a full run requires, typically, 2,400 time steps, the total CPU time required is about eighty hours. However, the turn-around time can be reduced to less than twenty hours through the use of parallelism.

The accuracy of the simulations is determined by the spatial and temporal resolution, which has been excellent for all the simulations we have performed. Figure 4, comparing computed and experimentally measured dissipation spectra, illustrates the veracity of the simulations. We have found that the simulated small scales have the same statistics as experimentally realized turbulence.

Figure 3

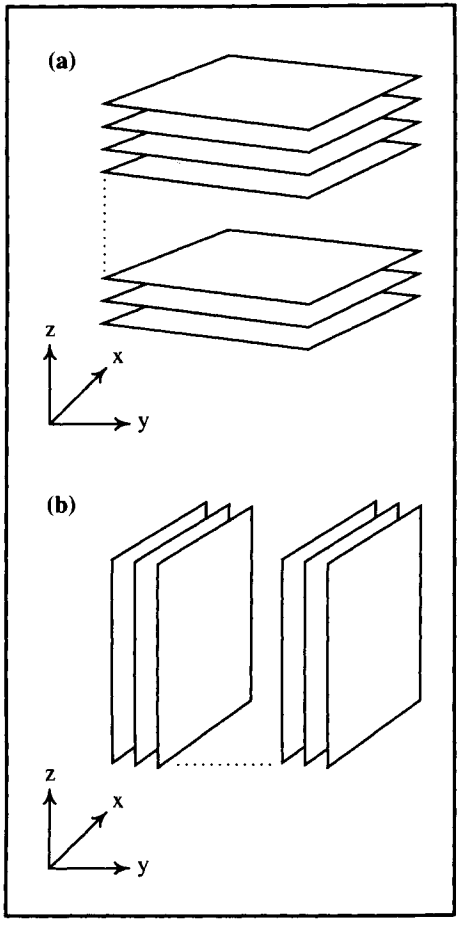

Figure 3. Sketch showing an N^3 grid of data as (a) N x-y planes and (b) N x-z planes. Each plane has N^2 nodes. In the simulation work discussed here, N = 128 and the grid had more than two million nodes.

Figure 4. Computed and experimentally measured dissipation spectra, demonstrating the accuracy of the simulations. The solid curve represents simulations; the dashed line represents experimental data of Comte-Bellot and Corrsin. Note that the spectrum quantity plotted in the figure is cubically proportional to the spectrum function; this accentuates the high-wavenumber (that is, small-scale) components of the velocity field.

THE EVOLUTION OF MATERIAL SURFACES

A direct method of computing the evolution of a material surface would be to represent the surface numerically by a number of nodes, and to accommodate the stretching and bending by adapting the gridding—by repositioning nodes and introducing new ones. Our results show that this approach is impracticable, however, because the deformation of the surface is so severe. During the simulation, the area of the surface increases by a factor of 10^{17}, and radii of curvature as small as 10^{-8} of a grid spacing occur. Clearly, it is hopeless to attempt to represent such a massive surface with the necessarily fine resolution.

Instead, we study a large number (M = 4,096 or 8,192) of representative infinitesimal surface elements. A complete set of ordinary differential equations has been derived for the time series following the fluid particle, and these equations can be integrated to yield the principal curvatures of the elements. As the turbulence simulation steps through time, the set of ordinary differential equations describing the infinitesimal surface elements is solved for each of the M elements. The significant amount of calculation that is needed is implemented on the supercomputer, exploiting the parallel processing capabilities in much the same way as in the pseudo-spectral code.

Figure 4

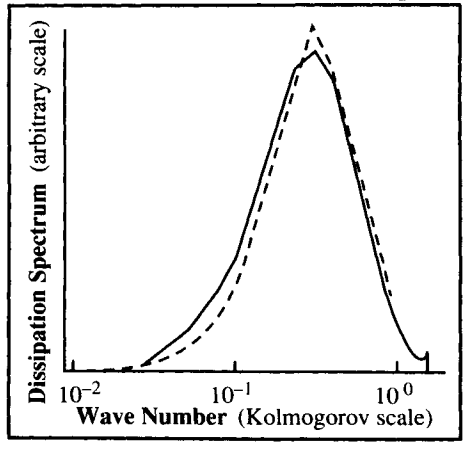

Analysis of our results shows that our method of tracking infinitesimal surface elements is sufficient for the accurate calculation of surface statistics.

WHAT WE HAVE DISCOVERED ABOUT TURBULENT SURFACES

In our research so far, we have obtained statistics characterizing the straining of materials surfaces, and also the curvature.

The straining on material surfaces was first and most comprehensively studied by G. K. Batchelor over thirty years ago. He introduced two conjectures: (1) straining is persistent (that is, the time scale of change of the strain rate is large compared to the time scale of strain itself); and (2) the material surface becomes aligned with the principal axes corresponding to the two greatest principal strain rates. These conjectures have been accepted in subsequent work.

As explained in our scientific papers, our research has shown that turbulent straining is fleeting rather than persistent, and that consequently, elements of the material surface do not become perfectly aligned with principal axes of the strain rate.

We have also determined, for the first time, the mean rate of stretching. We found that the surface area doubles every 2.5 Kolmogorov time scales. (The Kolmogorov time scale is the smallest physical time scale in turbulence.) While this is certainly rapid growth, it is only 40 percent of theoretical estimates.

Until now, little has been known about the curvature of material surfaces. Our

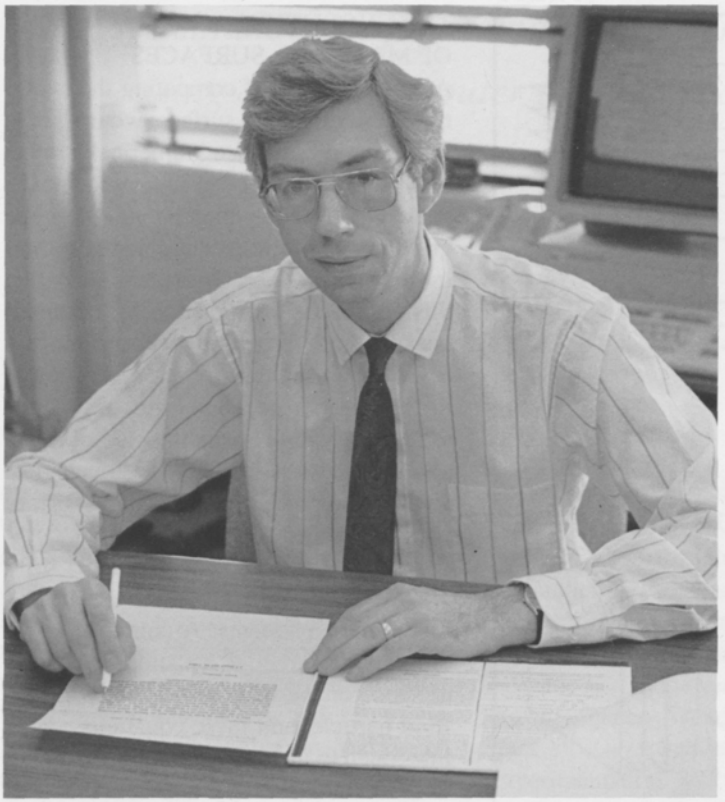

results show that under turbulent conditions, material surfaces become extremely contorted; they are strained and bent by small-scale motions. Contrary to what had been thought, very small curvatures arise—as small as 10^{-8} of the smallest turbulent scale (the Kolmogorov scale). Moreover, these highly curved elements are found to be almost perfectly cylindrical in shape, rather than spherical, as had been assumed.

THE NEW POSSIBILITIES IN RESEARCH ON TURBULENCE

The new quantitative information that our research has already revealed has theoretical and practical significance. Although the work done so far pertains to the simplest possible turbulent flow—homogeneous isotropic turbulence—the results have general applicability, since the behavior of the small-scale curvatures of the material surface is almost universal; it does not depend on the flow characteristics of the fluid as expressed by the Reynolds number.

Since the earliest work on turbulence almost a century ago, there has been no shortage of imaginative theories, but they have not all been soundly based because the underlying hypotheses and conjectures have been impossible to test. The work I have outlined here clearly demonstrates that supercomputers have changed the prospects. Researchers can study turbulence in terms of numerical simulation, using supercomputers to extract detailed information that can be used to test hypotheses and suggest new ones. Turbulence research is entering a new era.

Stephen B. Pope, a professor of mechanical and aerospace engineering, joined the Cornell faculty in 1982.

He studied at Imperial College, London, for the degrees of B.Sc. (1971), and Ph.D. (1976). He received the Unwin prize, awarded annually for the best Ph.D. thesis in the College of Engineering. In 1986 he was awarded a High Doctorate, D.Sc.(Eng.), by the University of London for "published work of high standing".

Before coming to Cornell, he served as a postdoctoral researcher at Imperial College, as a research fellow in aeronautics at the California Institute of Technology, and as a member of the mechanical engineering faculty at the Massachusetts Institute of Technology.

Pope has published some sixty research papers. This year he presented the invited plenary lecture on turbulent combustion at the 23rd International Combustion Symposium. He is a consultant to several industries.

He is a member of the Combusion Institute and the American Physical Society, an associate fellow of the American Institute of Aeronautics and Astronautics, and an overseas fellow of Churchill College, Cambridge University. He is an associate editor of Physics of Fluids A.

FACULTY PUBLICATIONS

Current research activities at the Cornell University College of Engineering are represented by the following publications and conference papers that appeared or were presented during the three-month period July through September 1990. (Earlier entries omitted from previous Quarterly *listings are included here with the year of publication in parentheses.) The names of Cornell personnel are in italics.*

■ AGRICULTURAL AND BIOLOGICAL ENGINEERING

Albright, L. D. 1990. *Environment control for animals and plants.* St. Joseph, MI: American Society of Agricultural Engineers.

Campbell, J. K. 1990. *Dibble sticks, donkeys, and diesels: Machines in crop production.* Manila, Philippines: International Rice Research Institute.

Chen, S., and *M. B. Timmons.* 1990. Size distribution of suspended solids in recirculating aquaculture systems. In *Proceedings, World Aquaculture '90,* p. 57. Baton Rouge, LA: World Aquaculture Society.

Choi, H.-L., *L. D. Albright,* and *M. B. Timmons.* 1990. An application of the k-e turbulence model to predict how a rectangular obstacle in a slot-ventilated enclosure affects air flow. *Transactions of the American Society of Agricultural Engineers* 33(1):274–81.

Datta, A. K. 1990*a*. Estimation of quality parameters in liquid food processing. Paper read at Annual Meeting, Institute of Food Technologists, 16–20 June 1990, in Anaheim, CA.

___. 1990*b*. Heat and mass transfer during microwave processing of food materials. *Chemical Engineering Progress* 86(6):47–53.

___. 1990*c*. Novel chemical and biological sensors for monitoring and control of food processing operations. *Journal of Food Engineering* 12:223–38.

___. 1990*d*. On the theoretical basis of the asymptotic semilogarithmic heat penetration curves used in food processing. *Journal of Food Engineering* 12:177–90.

Glass, R. J., S. Cann, J. King, N. Bailey, J.-Y. Parlange, and *T. S. Steenhuis.* 1990. Wetting front instability in unsaturated porous media: A three-dimensional study. *Transport in Porous Media Journal* 5:247–68.

Knowlton, K. F., R. E. Pitt, and *D. G. Fox.* 1990. *Value of reduced solubility of haycrop silage protein in dairy cattle rations.* Department of Agricultural and Biological Engineering report no. 90–2. Ithaca, NY: Cornell University.

Parlange, J.-Y., R. J. Glass, and *T. S. Steenhuis.* 1990. Application of scaling to the analysis of unstable flow phenomena. Chapter 5 in *Scaling of soil physics: Principles and applications,* ed. D. Hillel and D. E. Elrick, pp. 53–57. Madison, WI: Soil Science Society of America.

Reinemann, D. R., *J. Y. Parlange,* and *M. B. Timmons.* 1990. Theory of small diameter airlift pumps. *International Journal of Multiphase Flow* 16(1):113–22.

Sanford, W. E., R. J. Kopka, J. H. Peverly, T. S. Steenhuis, J. M. Surface, and M. J. Lavine. 1990. An investigation into the use of subsurface flow rock-reed filters for the treatment of leachate from a solid waste landfill. Paper read at Water Pollution Control Federation Specialty Conference: Water Quality and Management of Landfills, 15–18 July 1990, in Chicago, IL.

Timmons, M. B. 1990. Tunnel ventilation needs proper design procedures. *Poultry Digest* 49(5):22–30.

Timmons, M. B., R. W. Bottcher, and S. E. Scheideler. 1990. *Economic analysis of broiler housing options for heat stress relief.* American Society of Agricultural Engineers paper no. 90–4005. St. Joseph, MI: ASAE.

■ APPLIED AND ENGINEERING PHYSICS

Bilderback, D. H., D. J. Thiel, A. Lewis, and E. Stern. 1990. Microscience opportunities with x-ray beams funneled through x-ray "light pipes". Paper read at 15th International Union of Crystallography, 19–28 July 1990, in Bordeaux, France.

Chambliss, D. D., and *T. N. Rhodin.* 1990. Electronic and atomic structure of the Cu/Si(111) quasi-5x5 overlayer. *Physical Review B* 42:1674–83.

Fleischmann, H. H., W. Podulka, and *S. Jones.* 1990. *TSX—A potential experiment on tilt stabilization of FRX-rings using large-orbit ion rings.* In *Proceedings, 11th U.S.–Japan Workshop on Compact Toroids,* ed. D. C. Barnes et al., p. 125. Report no. LA-11808-C. Los Alamos, NM: Los Alamos National Laboratory.

Kirkland, E. J. 1990. An image and spectrum acquisition system for a VG HB501 STEM using a color graphics workstation. *Ultramicroscopy* 32:349–64.

Russek, S. E., D. K. Lathrop, B. H. Moeckly, R. A. Buhrman, D. H. Shin, and *J. Silcox.* 1990. Scaling behavior of $YBa_2Cu_3O_{7-\delta}$ thin-film weak links. *Applied Physics Letters* 57:1155–57.

Sahlin, P. A., W. Pierce, H. Biglari, H. H. Fleischmann, and S. C. Jardin. 1990. Numerical drift orbit calculations for force-free spheromak configurations. *Physics of Fluids B* 2(3):554–60.

Shin, D. H., J. Silcox, S. E. Russek, D. K. Lathrop, B. Moeckly, and *R. A. Buhrman.* 1990. Clean grain boundaries and weak links in high T_c superconducting $YBa_2Cu_3O_{7-x}$ thin films. *Applied Physics Letters* 57:508–10.

Thomas, J., and *W. W. Webb.* 1990. Fluorescence photobleaching recovery: A probe of membrane dynamics. In *Non-invasive techniques in cell biology,* ed. S. Grinstein and K. Foskett, pp. 129–52. New York: John Wiley–Liss.

■ CHEMICAL ENGINEERING

Chapman, W. G., K. E. Gubbins, G. Jackson, and *M. Radosz.* 1990. New reference equation of state for associating liquids. *I & EC Research* 29:1709–21.

de Miguel, E., L. F. Rull, M. Chalam, and *K. E. Gubbins.* 1990. Computer simulation of liqued crystals: Gay-Gerne model. Paper read at 1st Liquid Matter Conference, European Physical Society, 7–11 July 1990, in Lyon, France.

Gubbins, K. E. 1990*a*. Behavior of fluids in micropores. Paper read at Fluid Physics Summer School, Aguadulce, 6 August 1990, in Almeria, Spain.

___. 1990*b*. Molecular adsorption in micropores. *Chemical Engineering Progress* 86:42–44.

___. 1990*c*. Statistical mechanical treatment of inhomogeneous fluids: Simulation and density functional theory. Paper read at Fluid Physics Summer School, Aguadulce, 6 August 1990, in Almeria, Spain.

Harriott, P. 1990. A simple model for SO_2 removal in the duct injection process. *Journal of the Air and Waste Management Association* 40:998–1003.

Kim, B.-G., and *M. L. Shuler.* 1990. A structured, segregated model for genetically modified *E. coli* cells and its use for prediction of plasmid stability. *Biotechnology and Bioengineering* 36:581–92.

Lackney, V. K., R. M. Spanswick, T. J. Hirasuna, and *M. L. Shuler.* 1990. PEG-enhanced, electric field-induced fusion of tonoplast and plasmalemma of grape protoplasts. *Plant Cell, Tissue, and Organ Culture* 23:107–14.

Lion, L. W., M. L. Shuler, and *W. C. Ghiorse.* 1990. Characterization of biofilm interactions with toxic trace metals: Consequences for metal removal and the biophase. Paper read at American Society of Civil Engineers National Conference on Environmental Engineering, 9–11 July 1990, in Washington, DC.

Matsumoto, M., and K. E. Gubbins. 1990. Hydrogen bonding in liquid methanol. *Journal of Chemical Physics* 93:1981–94.

McCabe, W. L., *J. C. Smith,* and *P. Harriott.* (1989.) *Operasi teknik kimia* (Unit operations of chemical engineering), 4th ed., vol. 2, Ir. E. Jasjfi, translator. Jakarta, Indonesia: Penerbit Erlangga.

Patel, S. K., and *C. Cohen.* 1990*a*. Effect of pendant chains on the physical properties of PDMS networks. Paper read at 33rd International Union of Pure and Applied Chemistry (IUPAC) International Symposium on Macromolecules, 8–13 July 1990, in Montreal, Canada.

___. 1990*b*. Structural effects on the swelling and the dynamic light scattering of gels. *Polymer Preprints* 31(2):124–25.

Peterson, B. K., G. S. Heffelfinger, K. E. Gubbins, and *F. van Swol.* 1990. Layering transitions in cylindrical pores. *Journal of Chemical Physics* 93:679–85.

Shah, N. N., M. E. Pozo de Fernández, J. A. Zollweg, and *W. B. Streett.* 1990. Vapor-liquid equilibrium in the system carbon dioxide + 2,2-dimethylpropane form 262 to 424 K at pressures to 8.4 MPa. *Journal of Chemical and Engineering Data* 35:278–83.

Shaqfeh, E. S. G., and *D. L. Koch.* 1990. Orientational dispersion of fibers in extensional flows. *Physics of Fluids A* 2:1077–93.

Steinmeyer, D. E., and *M. L. Shuler.* 1990. Mathematical modeling and simulations of membrane bioreactor extractive fermentations. *Biotechnology Progress* 6(5):362–69.

Tan, Z., and *K. E. Gubbins.* 1990. Adsorption in carbon micropores at supercritical temperatures. *Journal of Physical Chemistry* 94:6060-61.

Walsh, J., and *K. E. Gubbins.* 1990. Associating fluids: Theory, simulation, application. Paper read at 11th International Union of Pure and Applied Chemistry (IUPAC) Conference on Chemical Thermodynamics, 23 August – 3 September 1990, in Como, Italy.

Wickham, T. J., R. R. Granados, H. A. Wood, D. A. Hammer, and *M. L. Shuler.* 1990. General analysis of receptor-mediated viral attachment to cell surfaces. *Biophysics Journal* 58:1501–16.

■ CIVIL AND ENVIRONMENTAL ENGINEERING

Bhaskaran, S., and *M. A. Turnquist.* 1990. Multiobjective transportation considerations in multiple facility locations. *Transportation Research A* 24(2):139–48.

Bisogni, J. J., Jr., R. I. Dick, K. C. Hover, B. B. Bierck, and *K. Natesaiyer.* 1990. Properties of sludge inceinerator ash-cement mixture. In *Environmental Engineering: Proceedings, ASCE 1990 Specialty Conference,* ed. C. R. O'Melia, pp. 683–90. New York: American Society of Civil Engineers.

Deierlein, G. G., T. M. Sheikh, J. A. Yura, and J. O. Jirsa. 1990. Design of beam-column connections for composite framed structures. In *Proceedings, International Association of Bridge and Structural Engineers (IABSE) Symposium: Mixed Structures Including New Materials,* pp. 311–16. Zurich, Switzerland: IABSE.

Hsieh, K. M., L. W. Lion, and *M. L. Shuler.* 1990. Production of extracellular and cell-associated biopolymers by *Pseudomonas atlantica. Biotechnology Letters* 12:449–54.

Lee, J.-H., and *W. D. Philpot.* 1990. A spectral-textural classifier for digital imagery. In *Remote sensing for the nineties: Proceedings of IGARSS '90 (International Geoscience and Remote Sensing Symposium),* ed. R. Mills, pp. 2005–08. New York: Institute of Electrical and Electronics Engineers.

McLean, D. I., L. Phan, H. S. Leu, and *R. N. White.* 1990. Punching shear behavior of lightweight concrete slabs and shells. *ACI Structural Journal* 87:386–92.

Pessiki, S. P., C. H. Conley, P. Gergely, and *R. N. White.* 1990. *Seismic behavior of lightly reinforced concrete column and beam-column joint details.* NCEER report no. 90–0014. Buffalo, NY: National Center for Earthquake Engineering Research.

Philpot, W. D. 1990. Extraction of target-specific reflectance from remote observations. In *Proceedings, Ocean Optics X,* pp. 101–12. SPIE Proceedings Series, vol. 1302. Bellingham, WA: International Society for Optical Engineering.

Philpot, W. D., and *A. Vodacek.* 1990. Remote fluorescence spectroscopy for detection of organic substances in water. In *Remote sensing for the nineties: Proceedings of IGARSS '90 (International Geoscience and Remote Sensing Symposium),* ed. R. Mills, pp. 2181–84. New York: Institute of Electrical and Electronics Engineers.

Sansalone, M., and N. J. Carino. 1990. Finite element studies of the impact-echo response of layered plates containing flaws. In *International advances in nondestructive testing,* ed. W. McGonnagle, pp. 313–36. New York: Gordon and Breach.

Schuler, R. E. 1990. Municipal solid waste: Crisis or opportunity? *Engineering: Cornell Quarterly* 24(4):4–10.

Turnquist, M. A., and J. A. Werk. 1990. Interactive modeling for multiobjective scheduling and routing of radioactive waste shipments. In *Proceedings, Packaging and Transportation of Radioactive Materials (PATRAM '89) conference,* vol. 2, pp. 582–89. Washington, DC: U.S. Department of Energy.

Wu, J.-K., and *P. L.-F. Liu.* 1990. Harbour excitations by incident wave groups. *Journal of Fluid Mechanics* 217:595–613.

Yoon, S. B., and *P. L.-F. Liu.* 1990. Effects of opposing waves on momentum jets. *ASCE Journal of Waterway, Port, Coastal, and Ocean Engineering* 116:545–57.

■ COMPUTER SCIENCE

Birman, K. P., and *R. Cooper*. 1990. *The ISIS Project: Real experience with a fault tolerant programming system*. Department of Computer Science report no. 90–1138. Ithaca, NY: Cornell University.

Birman, K. P., and T. A. Joseph. 1990. Communication support for reliable distributed computing. In *Fault-tolerant distributed computing*, ed. B. Simons and A. Spector, pp. 124–37. Lecture Notes in Computer Science, vol. 448. New York: Springer-Verlag.

Hartmanis, J. 1990. Computational complexity. In *Strategic directions in computing research*, ed. P. Wegner, pp. 21–23. New York: ACM Press.

Hartmanis, J., and L. Hemachandra. 1990. Robust machines accept easy sets. *Theoretical Computer Science* 74:217–25.

Makpangou, M., and *K. P. Birman*. 1990. *Designing application software in wide area network settings*. Department of Computer Science report no. 90–1165. Ithaca, NY: Cornell University.

■ ELECTRICAL ENGINEERING

Anantharam, V. 1990*a*. Controlled hydrodynamics for decentralized trunk reservation based control of circuit switched networks with dynamic routing. In *Proceedings, 1990 Bilkent Conference on Communications, Control and Signal Processing*, ed. E. Arikan, pp. 128–34. Amsterdam, The Netherlands: Elsevier.

___. 1990*b*. A hydrodynamic limit for a lattice caricature of dynamic routing in circuit switched networks. In *Proceedings, 9th International Conference on Analysis and Optimization of Systems*, ed. A. Bensoussan and J. Lions, pp. 937–46. New York: Springer-Verlag.

Anantharam, V., and *M. Benchekroun*. 1990. A technique for determining the sojourn time of typical customers in large systems of interacting queues. In *Proceedings, 24th Conference on Information Sciences and Systems*, ed. B. Liu and J. B. Thomas, pp. 491–96. Princeton, NJ: Princeton University.

Anantharam, V., and P. Tsoucas. 1990. Stochastic concavity of throughput in series of queues with finite buffers. *Advances in Applied Probability* 22:761–63.

Azari, N. G., and *S.-Y. Lee*. 1990. Parallelizing particle-in-cell simulation on multiprocessors. In *Proceedings, 1990 International Conference on Parallel Processing*, vol. 3, no. 352–53. University Park, PA: Pennsylvania State University Press.

Bar, J. E., and *J. P. Krusius*. 1990. Simulation of ultrafast carrier relaxation processes in pulse/probe and dual pulse correlation probing of InGaAs type narrow band gap semiconductors. In *Ultrafast laser probe phenomena in bulk and microstructure semiconductors III*, ed. R. A. Alfano, pp. 162–69. SPIE Proceedings Series, vol. 1282. Bellingham, WA: International Society for Optical Engineering.

Berger, T., and *Z. Ye*. 1990*a*. Cardinality of phase transition of Ising models on closed Cayley trees. *Physica A* 166:549–74.

___. 1990*b*. ε-entropy and critical distortion of random fields. *IEEE Transactions on Information Theory* 36:717–25.

___. 1990*c*. Entropic aspects of random fields on trees. *IEEE Transactions on Information Theory* 36:1006–18.

Brent, R. P., *F. T. Luk*, and C. J. Anfinson. 1990. Checksum schemes for fault tolerant systolic computing. In *Mathematics in signal processing II*, ed. J. G. McWhirter, pp. 791–804. Oxford, England: Clarendon Press.

Butler, J. M., C. B. Wharton, and *S. Furukawa*. 1990. Dependence of relativistic backward-wave oscillator properties on effective beam-gamma. *IEEE Transactions on Plasma Science* 18:490–96.

Chen, L. Y., and *N. C. MacDonald*. 1990. Multilevel microdynamical devices. Paper read at American Vacuum Society meeting, 23–27 October 1989, in Boston, MA.

Cheng, L. K., W. R. Bosenberg, and *C. L. Tang*. 1990. Growth and characterization of nonlinear optical crystals suitable for frequency-conversion. *Progress in Crystal Growth and Characterization* 20:9–57.

Dalman, G. C. 1990. New waveguide-to-coplanar waveguide transition for centimeter and millimeter wave applications. *Electronic Letters* 26:830–31.

Delchamps, D. F. 1990*a*. Observability and observers for linear systems with quantized outputs. In *Proceedings, 24th Conference on Information Sciences and Systems*, ed. B. Liu and J. B. Thomas, pp. 104–08. Princeton, NJ: Princeton University.

___. 1990*b*. Stabilizing a linear system with quantized state feedback. *IEEE Transactions on Automatic Control* 35:916–24.

Eastman, L. F. 1990. Progress in high frequency heterojunction field effect transistors. In *Proceedings, 20th European Solid State Device Research Conference (ESSDERC '90)*, ed. W. Eccleston and P. J. Rosser, pp. 619–24. New York: American Institute of Physics.

Graude, W. J., J. Johnson, and *C. L. Tang*. 1990. Characterization of etch rate and anisotropy in the temperature-controlled chemically assisted ion-beam etching of GaAs. *Journal of Vacuum Science and Technology B* 8:1075–79.

Johnson, S., and *N. C. MacDonald*. 1990. A program for Monte Carlo simulation of electron energy loss in nanostructures. *Journal of Vacuum Science and Technology B* 7:1513.

Kendall, K., S. Kurtz, *R. Lane, R. Bosenberg, C. L. Tang*, et al. 1990. Non-critically phase-matched second-harmonic generation by ß-$Gd_2(MO_4)_3$ in the mid-infrared. Paper read at International Symposium on the Application of Ferroelectrics, 6–8 June 1990, at Urbana, IL.

Knudsen, D. J., M. C. Kelley, G. D. Earle, J. F. Vickrey, and M. Boehm. 1990. Distinguishing Alfvén waves from quasi-static field structures associated with the discrete aurora: Sounding rocket and Hilat satellite measurements. *Geophysical Research Letters* 17(7):921–24.

Krusius, J. P. 1990. Packaging architecture considerations of high density multi-chip electronic packages via system optimization. *Journal of Electronic Packaging* 112:267–71.

Loh, W. H., A. T. Schremer, and *C. L. Tang*. 1990. Hysteresis and multistable behavior in a polarization self-modulated external ring cavity semiconductor laser. *Electronics Letters* 26:1666–68.

MacDonald, N. C., L. Y. Chen, J. J. Yao, Z. L. Zhang, J. A. McMillan, D. C. Thomas, and *K. R. Haselton*. (1989.) Selective chemical vapor deposition of tungsten for microelectromechanical structures. *Sensors and Actuators* 20:123–33.

McMillan, J. A., S. Johnson, and *N. C. MacDonald*. (1989.) Simulation of electron beam exposure of submicron patterns. *Journal of Vacuum Science and Technology B* 7:1540.

Offsey, S. D., W. J. Schaff, L. F. Lester, and *L. F. Eastman*. 1990. Single and multiple quantum well strained layer InGaAs-GaAs-AlGaAs lasers grown by molecular beam epitaxy. In *Extended abstracts of solid state devices and materials*, ed. N. Mikoshiba, pp. 545–48. Tokyo, Japan: Japan Society of Applied Physics.

Onn, R., A. Steinhardt, and *A. Bojanczyk*. 1990. The hyperbolic SVD and applications. In *Proceedings, IEEE Signal Processing Conference on the Singular Value Decomposition*, pp. 211–13. Kingston, RI: University of Rhode Island.

Pence, W. E., and *J. P. Krusius*. 1990. Package thermal resistance: Geometrical effects in conventional and hybrid packages. *IEEE Transactions on Components, Hybrids, and Manufacturing Technology* 13(2):245–51.

Perera, A. M., and *J. P. Krusius*. 1990. System 9: A new positive tone novalac-based high resolution electron beam resist. In *Electron-beam, x-ray, and ion-beam technology: Submicrometer lithographies IX*, ed. D. J. Resnick, pp. 297–304. SPIE Proceedings Series, vol. 1263. Bellingham, WA: International Society for Optical Engineering.

Plimpton, S. J., and *E. D. Wolf*. 1990. Effect of intercratonic potential in simulated grain-boundary and bulk diffusion: A molecular-dynamics study. *Physical Review B* 41:2712–21.

Ralph, S. E., and *G. J. Wolga*. 1990. Field-induced nonequilibrium carrier distributions in GaAs probed by electronic Raman scattering. *Physical Review B* 42:1353–63.

Röttger, J., M. T. Rietveld, C. LaHoz, *T. Hall, M. C. Kelley*, and *W. E. Swartz*. 1990. Polar mesosphere summer echoes observed with the EISCAT 933-MHz radar and the CUPRI 46.9-MHz radar, their similarity to 224-MHz radar echoes, and their relation to turbulence and electron density profiles. *Radio Science* 25(4):671–87.

Sahr, J. D., W. E. Swartz, D. T. Farley, and *J. F. Providakes*. 1990. Summary of CUPRI observations from the ERRRIS 2 campaign. Paper read at 1990 URSI convention, 20–30 August 1990, in Prague, Czechoslovakia.

Sanford, C. A., and *N. C. MacDonald*. (1989*a*.) Electron optical characteristics of negative electron affinity cathodes. *Journal of Vacuum Science and Technology B* 6:2005.

___. (1989*b*.) High speed E-beam testing using GaAs negative electron affinity photocathodes. Paper read at 2nd European Conference on Electron and Optical Beam Testing of Integrated Circuits, 1–4 October 1989, in Duisburg, Germany.

___. (1989*c*.) Laser pulsed GaAs cathodes for electron microscopy. *Journal of Vacuum Science and Technology B* 7:1903.

___. 1990. Electron emission properties of laser pulsed GaAs negative electron affinity photocathodes. Paper read at 34th International Symposium on Electron, Ion, and Photon Beams, 30 May–2 June 1990, in San Antonio, TX.

Schremer, A. T., W. H. Loh, and *C. L. Tang*. 1990. Polarization self-modulation in external-cavity-semiconductor lasers. Paper read at Conference on Lasers and Electro-Optics (CLEO), May 1990, in Anaheim, CA.

Spallas, J. P., S. C. Arney, C. C. Cheng, and *N. C. MacDonald*. (1989.) Self-aligned silicon-strip field emitter array. Paper read at 2nd International Conference on Vacuum Microelectronics, 24–26 July 1989, in Bath, England.

Spallas, J. P., C. Cheng, S. C. Arney, and *N. C. MacDonald*. (1989.) Microfabrication of wedge-shaped silicon field emitting cathode arrays using high temperature lateral oxidation. Paper read at 2nd International Conference on Vacuum Microelectronics, 24–26 July 1989, in Bath, England.

Swartz, W. E., and *D. T. Farley*. 1990. Doppler and interferometer radar measurements of sub-kilometer turbulent structure in the equatorial electrojet. Paper read at 23rd General Assembly, URSI, 27 August–6 September 1990, in Prague, Czechoslovakia.

Ukachi, T., R. J. Lane, W. R. Bosenberg, and *C. L. Tang*. 1990. Measurement of noncritically phase-matched second-harmonic generation in a LiB_3O_5 crystal. *Applied Physics Letters* 7:980–82.

Wharton, C. B. 1990. X-band tandem oscillator-amplifier. Paper read at Institute of Electrical and Electronics Engineers International Conference on Plasma Science, 21–23 May 1990, in Oakland, CA.

Wharton, C. B., and *J. M. Butler*. 1990. Relativistic O-type oscillator-amplifier systems. In *Intense microwave and particle beams*, pp. 23–35. SPIE Proceedings Series, vol. 1226. Bellingham, WA: International Society for Optical Engineering.

Wharton, C. B., J. M. Butler, S. Furukawa, and *G. Barreto*. 1990. High power microwave oscillator-amplifier systems. In *Proceedings, 1990 International Conference on High Power Beams at Novosibirsk*, pp. 48–58. Moscow: USSR Academy of Sciences.

Won, Y. H., K. Yamasaki, T. Daniels-Race, P. J. Tasker, W. J. Schaff, and *L. F. Eastman*. 1990. A high voltage-gain GaAs vertical field-effect transistor with an InGaAs/GaAs planar-doped barrier launcher. *IEEE Electron Device Letters* 11:376–78.

■ GEOLOGICAL SCIENCES

Bloom, A. L., and *A. N. Fox*. 1990. Landsat thematic mapper (TM) images of the Andes as a classroom tool. *Journal of Geological Education* 38(4):323–29.

Cathles, L. M. 1990. Scales and effects of fluid flow in the upper crust. *Science* 248:323–29.

Chaimov, T., M. Barazangi, J. Best, D. Al-Saad, T. Sawaf, A. Youssef, and A. Gebran. 1990. Mesozoic and Cenozoic deformation inferred from seismic stratigraphy in the southwestern Palmyride fold belt of central Syria. In *Expanded abstracts of the Tectonical Program, 60th Annual International Meeting, Society of Exploration Geophysicists*, vol. 1, pp. 191–94. Tulsa, OK: SEG.

Fielding, E., B. Isacks, and *M. Barazangi*. 1990. Topographic expression of active faults in central Asia and topographic relief effects on Lg propagation. In *Proceedings, 12th Annual DARPA/GL Seismic Research Symposium*, ed. J. Lewkowicz and J. McPhetres, pp. 257–63. Hanscom AFB, MA: Geophysics Laboratory.

Flemings, P. B., and T. E. Jordan. 1990. Stratigraphic modeling of foreland basins: Interpreting thrust deformation and lithosphere rheology. *Geology* 18:430–34.

Gephart, J. W. 1990*a*. FMSI: A FORTRAN program for inverting fault/slickenside and earthquake focal mechanism data to obtain the regional stress tensor. *Computers and Geosciences* 6:953–89.

___. 1990*b*. Stress and the direction of slip on fault planes. *Tectonics* 9:845–58.

Hearn, T., N. Beghoul, and *M. Barazangi*. 1990. First tomographic study of western U.S. completed. *EOS: Transactions of the American Geophysical Union* 71:1083.

Huang, J., and *D. L. Turcotte*. 1990*a*. Evidence for chaotic fault interactions in the seismicity of the San Andreas fault and Nankai trough. *Nature* 348:234–36.

___. 1990*b*. Fractal image analysis: Application to the topography of Oregon and synthetic images. *Journal of the Optical Society of America A* 7:1124–30.

Kay, R. W. 1990*a*. The changing slab component in central Aleutian magmas. Paper read at V. M. Goldschmidt Conference, 2–4 May 1990, in Baltimore, MD.

___. 1990*b*. Subduction zone fluids: Facts and fiction. Paper read at V. M. Goldschmidt Conference, 2–4 May 1990, in Baltimore, MD.

___. 1990*c*. Western Aleutian high magnesium andesites: Evidence for storage of crustal components in the back-arc mantle. Paper read at V. M. Goldschmidt Conference, 2–4 May 1990, in Baltimore, MD.

Kay, S. M., R. W. Kay, G. P. Citron, and M. R. Perfit. 1990. Calc-alkaline plutonism in the intra-oceanic Aleutian arc, Alaska. In *Geological Society of America*, Special Paper no. 241, pp. 233–55. Boulder, CO: GSA.

Ramdani, M., B. Tadili, and *M. Barazangi*. 1990. Seismotectonics of Morocco: Active deformation of the Rif and Atlas intracontinental mountain belts. Paper read at Conference on Regional Seismological Assembly in Africa, 22–29 August 1990, in Nairobi, Kenya.

Tadili, B., M. Ramdani, I. Dafali, A. Aboudi, J.-P. Kueffer, M. Kasmi, *G. Hade*, and *M. Barazangi*. 1990. Seismological networks in Morocco. Paper read at Conference on Regional Seismological Assembly in Africa, 22–29 August 1990, in Nairobi, Kenya.

Turcotte, D. L. 1990. On the role of laminar and turbulent flow in buoyancy driven magma fractures. In *Magma transport and storage*, ed. M. P. Ryan, pp. 103–11. New York: John Wiley.

Turcotte, D. L., H. Ockendon, J. R. Ockendon, and S. J. Cowley. 1990. A mathematical model of vulcanian eruptions. *Geophysical Journal International* 103:211–17.

Vevoort, J. D. 1990. Genetic relationships between ultramafic sills and tholeiitic basalts in the wawa greenstone belt of NE Minnesota, USA. Paper read at 3rd International Archean Symposium, 17–21 September 1990, in Perth, Australia.

Vervoort, J. D., and *W. M. White*. 1990. Pb and Nd isotopic study of the footwall rocks of the Noranda Cu-Zn sulfide deposits, Quebec. Paper read at 7th International Conference on Geochronology, Cosmoschronology, and Isotope Geology, 24–29 September 1990, in Canberra, Australia.

■ MATERIALS SCIENCE AND ENGINEERING

Angelopoulos, E., C. K. Ober, and *E. J. Kramer.* 1990. Melt diffusion in model LC polymers. Paper read at 200th American Chemical Society National Meeting, 26–31 August 1990, in Washington, DC.

Argon, A. S., R. E. Cohen, O. S. Gebizlioglu, H. R. Brown, and *E. J. Kramer.* 1990. A new mechanism of toughening glassy polymers. 2. Theoretical approach. *Macromolecules* 23(17):3975–82.

Barclay, G. G., S. G. McNamee, and *C. K. Ober.* 1990. Mechanical and magnetic orientation of liquid crystalline epoxy networks. Paper read at 200th American Chemical Society National Meeting, 26–31 August 1990, in Washington, DC.

Barclay, G. G., C. K. Ober, K. Papathomas, and D. Wang. 1990. Liquid crystalline epoxy networks. Paper read at 200th American Chemical Society National Meeting, 26–31 August 1990, in Washington, DC.

Dieckmann, R. 1990. Non-stoichiometric oxides: Point defects, transport properties, and kinetics of solid state reactions. Paper read at Pennsylvania State University Department of Materials Science and Engineering Seminar, 17 October 1990, in University Park, PA.

Duclos, S. J., Y. K. Vohra, and *A. L. Ruoff.* 1990. Experimental study of the crystal stability and equation of state of Si to 248 GPa. *Physical Review B* 41(17):12021–28.

Gall, T. P., R. C. Lasky, and *E. J. Kramer.* 1990. Case II diffusion: Effect of solvent molecule size. *Polymer* 31:1491–99.

Hong, Q. Z., J. G. Zhu, W. Xia, and *J. W. Mayer.* 1990. Ge transport and epitaxy in the amorphous-Ge/Pd_2Si/[111]Si system. In *Layered structures: Heteroepitaxy, supperlattices, strain, and metastability,* ed. B. W. Dodson et al., p. 313. Materials Research Society Symposium Proceedings, vol. 160. Pittsburgh, PA: MRS.

Martin, H., and *C. K. Ober.* 1990. Organometal polymer precursors to glass-ceramic composites. Paper read at 200th American Chemical Society National Meeting, 26–31 August 1990, in Washington, DC.

Mates, T., and *C. K. Ober.* 1990. New thermotropic polyesters from distyrylbenzene bisphenols. *Journal of Polymer Science Letters* 28:331–39.

Miller, P., and *E. J. Kramer.* 1990. Environmental shear deformation zones and crazes in crosslinked polystyrene and poly(*para*-methylstyrene). *Journal of Materials Science* 25:1751–61.

Norton, M. G., and *C. B. Carter.* 1990. Interfaces in structural ceramics. *MRS Bulletin* 15(10)51–59.

Norton, M. G., S. McKernan, and *C. B. Carter.* 1990. Direct observation of grain orientation in $YBa_2Cu_3O_{7-\delta}$ thin films. *Philosophical Magazine Letters* 62(2):77–82.

Norton, M. G., L. A. Tietz, C. B. Carter, S. E. Russek, B. H. Moeckly, and *R. A. Buhrman.* 1990. Grain boundaries in $YBa_2Cu_3O_{7-\delta}$ thin films. In *Materials Research Society Symposium Proceedings,* vol. 169, pp. 513–16. Pittsburgh, PA: MRS.

Ober, C. K., S. McNamee, A. Delvin, and R. Colby. 1990. Chemical heterogeneity in LC polyesters. In *Liquid-crystalline polymers,* ed. R. A. Weiss and *C. K. Ober,* pp. 220–40. American Chemical Society Symposium Series, no. 435. Washington, DC: ACS.

Ober, C. K., and R. A. Weiss. 1990. Current topics in liquid-crystalline polymers. In *Liquid-crystalline polymers,* ed. R. A. Weiss and *C. K. Ober,* pp. 1–16. American Chemical Society Symposium Series, no. 435. Washington, DC: ACS.

Ognjanovic, R., C.-Y. Hui, and *E. J. Kramer.* 1990. The study of polystyrene surface swelling by quartz crystal microbalance and Rutherford backscattering techniques. *Journal of Materials Science* 25:514–18.

Paik, K. W., and *A. L. Ruoff.* 1990. Adhesion enhancement of thin copper film on polyimide modified by oxygen reactive ion beam etching. *Journal of Adhesion Science and Technology* 4(6):465–74.

Russek, S. E., B. H. Moeckly, R. A. Buhrman, J. T. McWhirter, A. J. Sievers, M. G. Norton, L. A. Tietz, and *C. B. Carter.* 1990. Pulsed laser deposition of high-T_c superconducting thin films. In *Materials Research Society Symposium Proceedings,* vol. 169, pp. 455–58. Pittsburgh, PA: MRS.

Shull, K. R., E. J. Kramer, and L. J. Fetters. 1990. Effect of number of arms on diffusion of star polymers. *Nature* 345(6278):790–91.

Tadayan, B., S. Tadayan, J. G. Zhu, M. G. Spencer, G. L. Harris, J. Griffin, and *L. F. Eastman.* 1990. Growth of indium doped GaAs by migration-enhanced epitaxy at the extremely low substrate temperature of 120°C. *Journal of Vacuum Science Technology B* 8:131.

Tead, S. F., W. E. Vanderlinde, G. Marra, A. L. Ruoff, E. J. Kramer, and F. D. Egitto. 1990. Polymer diffusion as a probe of damage in ion or plasma etching. *Journal of Applied Physics* 68(6):2972–82.

Theodore, N. D., P. Mei, *C. B. Carter,* C. Palmstrøm, S. A. Schwarz, J. P. Harbison, and L. T. Florez. 1990. Behavior of dopant-related defects in AlGaAs superlattices. In *Impurities, defects, and diffusion in semiconductors: Bulk and layered structures,* ed D. J. Wolford, J. Bernholc, and E. E. Haller, pp. 709–14. Materials Research Society Symposium Proceedings, vol. 163. Pittsburgh, PA: MRS.

Vohra, Y. K., H. Xia, H. Luo, and *A. L. Ruoff.* 1990. Optical properties of diamond at pressures of the center of Earth. *Applied Physics Letters* 57(10):1007–09.

Weiss, R. A., and *C. K. Ober,* eds. 1990. *Liquid-crystalline polymers.* American Chemical Society Symposium Series, no. 435. Washington, DC: ACS.

Zhu, J. G. 1990. TEM study of epitactically grown GaAs/$Sc_xEr_{1-x}As$/GaAs heterostructures. In *Proceedings, 12th International Congress on Electron Microscopy,* vol. 4, pp. 586–87. San Francisco, CA: San Francisco Press.

Zhu, J. G., S. McKernan, C. J. Palmstrøm, and *C. B. Carter.* 1990. High-resolution imaging of CoGa/GaAs and ErAs/GaAs interface. In *Atomic scale structure of interfaces,* ed. R. D. Bringans, R. M. Feenstra, and J. M. Gibson, pp. 89-94. Materials Research Society Symposium Proceedings, vol. 159. Pittsburgh, PA: MRS.

Zhu, J. G., C. J. Palmstrøm, S. Mounier, and *C. B. Carter.* 1990. Characterization of ErAs/GaAs and GaAs/ErAs/GaAs structures. In *Layered structures: Heteroepitaxy, supperlattices, strain, and metastability,* ed B. W. Dodson, et al., pp. 325–30. Materials Research Society Symposium Proceedings, vol. 160. Pittsburgh, PA: MRS.

■ MECHANICAL AND AEROSPACE ENGINEERING

Gouldin, F. C. 1990. Combustion simulation: A new tool for the design of waste incinerators. *Engineering: Cornell Quarterly* 24(4):20–28.

Kumar, A., P. K. Goenka, and *J. F. Booker.* 1990. Modal analysis of elastohydrodynamic lubrication: A connecting rod application. *Journal of Tribology* 112:524–34.

Louge, M., D. J. Lischer, and *H. Chang.* 1990. Measurements of voidage near the wall of a circulating fluidized bed river. *Powder Technology* 62:269–76.

Ramesh, P. S., and *K. E. Torrance.* 1990. Stability of boiling in porous media. *International Journal of Heat and Mass Transfer* 33(9):1895–1990.

Shapiro, V., and D. L. Vossler. 1990. *B-rep->CSG conversion I: Construction and optimization of CSG representations.* Sibley School of Mechanical and Aerospace Engineering technical report CPA89–3a. Ithaca, NY: Cornell University.

Veeravalli, S., and *Z. Warhaft.* 1990. Thermal dispersion from a line source in the shearless turbulence mixing layer. *Journal of Fluid Mechanics* 216:35–70.

■ OPERATIONS RESEARCH AND INDUSTRIAL ENGINEERING

Bechhofer, R. E., C. W. Dunnett, D. M. Goldsman, and M. Hartmann. 1990. A comparison of the performances of procedures for selecting the normal population having the largest mean when the populations have a common unknown variance. *Communications in Statistics: Simulation and Computation* 19(3):971–1006.

Billera, L. J., P. Filliman, and *B. Sturmfels.* 1990. Constructions and complexity of secondary polytopes. *Advances in Mathematics* 83:155–79.

Goldsman, D., M. Meheton, and *L. Schruben.* 1990. Properties of standardized time series weighted area variance estimators. *Managment Science* 36(5):602–12.

Goldsman, D., and *L. Schruben*. 1990. New confidence interval estimators using standardized time series. *Managment Science* 36(3):393–97.

Jackson, P. L., J. A. Muckstadt, and C. V. Jones. 1990. Cosmos: A framework for a computer-aided logistics system. *Journal of Manufacturing Operations Management* 2:222–48.

Jennison, C., and *B. W. Turnbull*. 1990. Statistical approaches to interim monitoring of medical trials: A review and commentary. *Statistical Science* 5:299–317.

Ruppert, D. 1990. Review of "Regression analysis with applications" by G. B. Wetherill. *Metrika* 37:382–84.

Ruppert, D., and D. Simpson. 1990. Comment on "Unmasking multivariate outliers and leverage points" by P. Rousseeuw and B. van Zomeren. *Journal of the American Statistical Association* 85:644–46.

Schruben, L. 1990. SIGMA: A graphical simulation system. San Francisco, CA: Scientific.

Todd, M. J., and Y. Ye. 1990. A centered projective algorithm for linear programming. *Mathematics of Operations Research* 15:508–29.

Turnbull, B. W., E. J. Iwano, W. S. Burnett, H. L. Howe, and *L. C. Clark*. 1990. Monitoring for clusters of disease: Application to leukemia incidence in upstate New York. *American Journal of Epidemiology* 132(1):136–43.

■ PLASMA STUDIES

Coleman, M. D., D. A. Hammer, B. R. Kusse, D. D. Meyerhofer, J. J. Moschella, G. D. Rondeau, C. K. Struckman, and *R. N. Sudan*. (1989.) Light ion diode research for inertial confinement fusion. In *Plasma physics and controlled nuclear fusion research 1988,* vol. 3, pp. 147–51. Vienna: International Atomic Energy Agency.

Ronchi, C., R. N. Sudan, and P. L. Similon. 1990. Effect of short-scale turbulence on kilometer wavelength irregularities in the equatorial electrojet. *Journal of Geophysical Research A* 95(1):189–200.

Similon, P. L., and *R. N. Sudan*. 1990. Plasma turbulence. *Annual Review of Fluid Mechanics* 22:317–47.

■ THEORETICAL AND APPLIED MECHANICS

Bergmann, V., and *S. Mukherjee*. 1990. A hybrid strain finite element for plates and shells. *International Journal for Numerical Methods in Engineering* 30:233–57.

Burns, J. A. 1990*a*. Dusty planetary rings. Paper read at Communications on Space Research conference, 25 June–5 July 1990, in The Hague, The Netherlands.

___. 1990*b*. Physical processes on circumplanetary dust. Paper read at International Astronomy Union Colloquium 126: Origin and Evolution of Interplanetary Dust, 27–30 August 1990, in Kyoto, Japan.

___. 1990*c*. Planetary rings. In *The new solar system,* 3rd ed., ed. J. K. Beatty and A. Chaiken, pp. 153–70. Cambridge, MA: Sky Publishing.

Coppola, V. T., and *R. H. Rand*. 1990. Averaging using elliptic functions: Approximation of limit cycles. *Acta Mechanica* 81:125–42.

Holmes, P. 1990*a*. The tale of a vibrating string and a degenerate Hamiltonian system. Paper read at 11th Dundee Conference on Ordinary and Partial Differential Equations, 3–6 July 1990, in Dundee, Scotland.

___. 1990*b*. Poincaré, celestial mechanics, dynamical systems theory, and "chaos". *Physics Reports* 193(3):137–63.

Jenkins, J. T., and *E. Askari*. 1990. Boundary conditions for rapid granular flows: Phase interfaces. *Journal of Fluid Mechanics* 223:497–508.

Kinsey, R. J., D. L. Mingori, and *R. H. Rand*. 1990. Spinup through resonance of rotating unbalanced systems with limited torque. In *Proceedings, American Institute of Aeronautics and Astronautics (AIAA)/ American Astronautical Society (AAS) Astrodynamics Conference,* pp. 805–13. New York: AIAA.

Ognjanovic, R., C.-Y. Hui, and *E. J. Kramer*. 1990. The study of polystyrene surface swelling by quartz crystal microbalance and Rutherford backscattering techniques. *Journal of Materials Science* 25:514–18.

Polse, K., J. W. Chandler, J. P. Hughes, *J. T. Jenkins,* D. R. Korb, G. W. Mertz, and M. F. Refojo. 1990. *Contact lens use under adverse conditions: Applications in military aviation*. Washington, DC: National Academy Press.

Szen, A. J., and *P. Holmes*. 1990. Nonlinear stability and bifurcation in Hamiltonian systems with symmetry. In *Mathematics of nonlinear science,* ed. M. Berger, pp. 33–62. Contemporary Mathematics, vol. 108. Providence, RI: American Mathematical Society.

■ OTHER

Ditz, D. W. 1990. Biological monitoring of airborne pollution. *Engineering: Cornell Quarterly* 24(4):29–33.

Harrison, E. Z. 1990*a*. Getting out the word on waste. *Engineering: Cornell Quarterly* 24(4):11–14.

___. 1990*b*. Plastics in the waste stream: Special properties, special problems. *Engineering: Cornell Quarterly* 24(4):38–42.

Martin, J. H., Jr. 1990. The sewage sludge story. *Engineering: Cornell Quarterly* 24(4):34–37.

Raymond, L. S., Jr. 1990. Ethics in siting landfills: A case study of a host-community benefits program. *Engineering: Cornell Quarterly* 24(4):15–19.

Rooks, M. J., H. V. Roussell, and L. M. Johnson. 1990. Polyimide optical waveguides fabricated with electron-beam lithography. *Applied Optics* 29:3880–82.

ENGINEERING
Cornell Quarterly

Published by the College of Engineering
Cornell University

Editor: Gladys McConkey

Associate Editor and Illustrator: David Price

Assistant Editor: Lindy Costello

Circulation Manager: Susan Drew

Printing: Davis Press
Worcester, Massachusetts

Photography credits:
Harvey Ferdschneider: 28
Timothy Hursley: inside back cover
Peter Morenus, Jr.: 1(Sudan and Longcope), 20
Jon Reis: front cover (top row center), 1(Silcox), 53
David Ruether: 1(Burns, Bartel, Walsh and Gubbins, Shuler, Pope), 3, 4, 13(top), 34, 42, 47, 58

Opposite: The new Engineering and Theory Center Building.

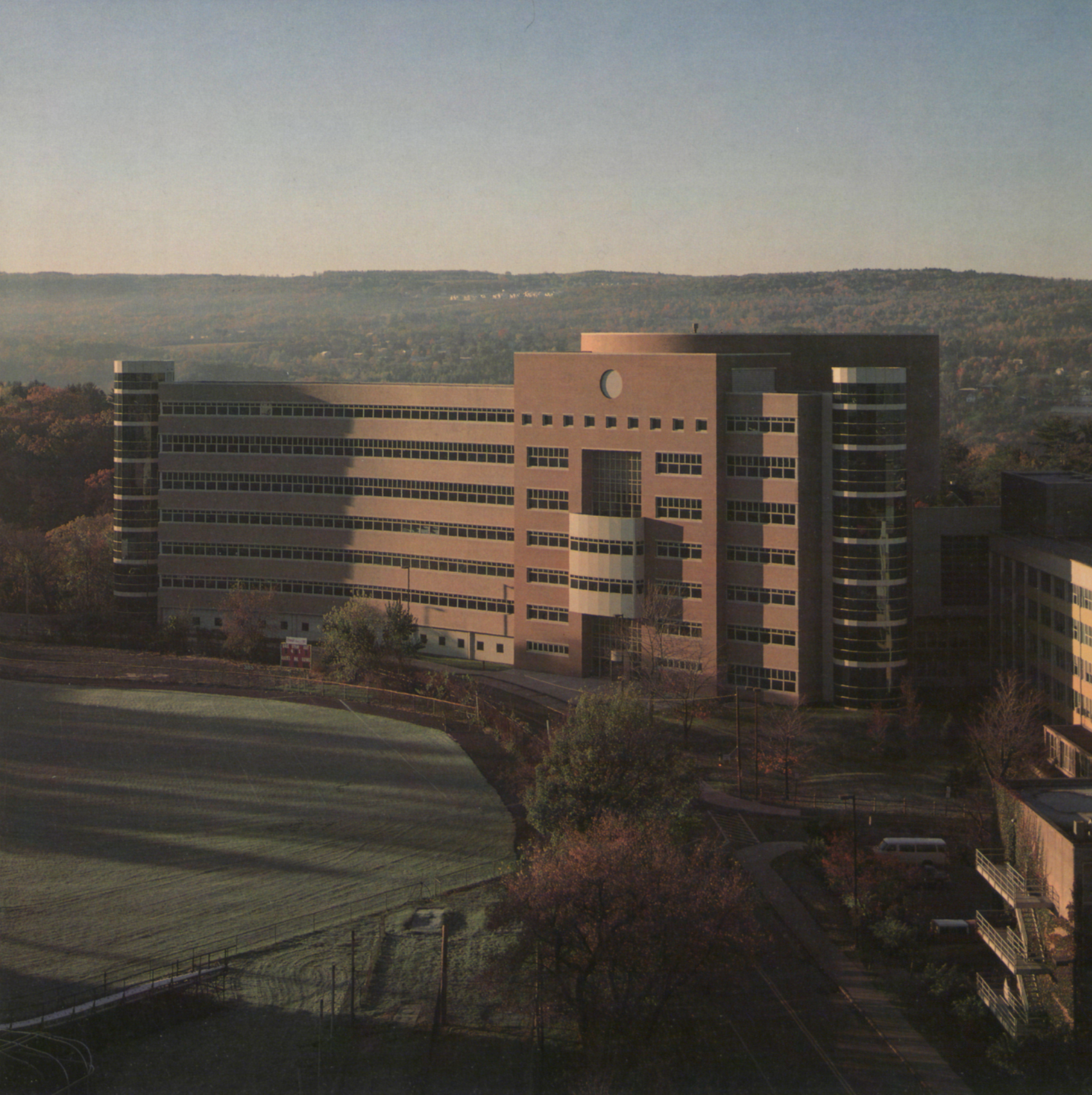

ENGINEERING
Cornell Quarterly
Carpenter Hall, Ithaca, N.Y. 14853

Address Correction Requested

Nonprofit Organization
U.S. Postage
PAID
Worcester, MA
Permit No. 114